

UNIVERZITET U BEOGRADU  
TEHNOLOŠKO-METALURŠKI FAKULTET

**SINTEZA, STRUKTURA I SOLVATOHROMIZAM NOVIH  
5-(4-SUPSTITUISANIH FENILAZO)-4-(4-SUPSTITUISANIH FENIL)-  
-6-HIDROKSI-3-CIJANO-2-PIRIDONA**

Doktorska disertacija  
Mr ADEL. S. ALIMMARI

Beograd, 2012

UNIVERSITY OF BELGRADE  
FACULTY OF TECHNOLOGY AND METALLURGY

**SYNTHESIS, STRUCTURE AND SOLVATOCHROMISM OF NEW  
5-(4-SUBSTITUTED PHENYLAZO)-4-(4-SUBSTITUTED PHENYL)-  
-6-HYDROXY-3-CYANO-2-PYRIDONES**

Doctoral dissertation  
Mr ADEL. S. ALIMMARI

Belgrade, 2012

UNIVERSITY OF BELGRADE  
FACULTY OF TECHNOLOGY AND METALLURGY

Final Examining Committee

---

Dr Gordana Ušćumlić, full professor of TMF, Thesis Supervisor

---

Dr Dušan Mijin, full professor of TMF

---

Dr Nataša Valentić, assistant professor of TMF

---

Dr Vesna Vitnik, scientific adviser of IHTM, university of Belgrade

Candidate

---

Mr Adel. S. Alimmari

## CONTENTS

<b>ABSTRACT</b> .....	1
<b>ABSTRACT IN SERBIAN</b> .....	2
<b>1. INTRODUCTION</b> .....	3
<b>2. THEORETICAL PART</b> .....	5
2.1. SYNTHESIS, STRUCTURE AND PROPERTIES OF AZO PYRIDONE DYES .....	5
2.1.1. General synthesis .....	6
2.1.1.1. Monoazo dyes .....	7
2.1.1.2. Disazo dyes .....	18
2.1.1.3. Trisazo dyes .....	22
2.1.2. Properties of azo pyridone dyes.....	23
2.1.3. Azo – hydrazone tautomerism of azo pyridone dyes .....	24
2.1.3.1. UV spectroscopic study of tautomerism .....	27
2.1.3.2. NMR spectroscopic study of tautomerism.....	29
2.1.3.3. Analysis of solvent influence on azo – hydrazone tautomerism using <i>ab initio</i> quantum chemical calculations.....	31
2.2. CORRELATION ANALYSIS IN ORGANIC CHEMISTRY .....	33
2.2.1. Substitution effects and linear free energy relationships.....	33
2.2.2. The Hammett equation and its extension.....	38
2.2.3. Separation of electronic effects.....	47
2.3. SOLVENT EFFECTS .....	51
2.3.1. Solvent effects on the keto / enol equilibria.....	53
2.3.2. Solvent effects on the other tautomeric equilibria.....	54
2.3.3. Solvent effects on the rates of homogenous chemical reactions.....	55
2.3.3.1. The Grunwald – Winstein equation .....	56
2.3.4. Koppel – Palm solvatochromic treatment.....	58
2.3.5. Kamlet – Taft solvatochromic treatment .....	58
2.3.6. Correlation analysis of solvent effects by means of substituent constants.....	60

<b>3. EXPERIMENTAL PART .....</b>	<b>61</b>
3.1. PREPARATION OF 5-ARYLAZO-6-HYDROXY-4-PHENYL-3-CYANO-2-PYRIDONE DYES (A1–A12) .....	61
3.2. PREPARATION OF 5-ARYLAZO-6-HYDROXY-4-(4-METHOXYPHENYL)-3-CYANO-2- PYRIDONE DYES (A13–A23).....	65
3.3. PREPARATION OF 5-ARYLAZO-6-HYDROXY-4-(4-NITROPHENYL)-3-CYANO-2- PYRIDONE DYES (A24–A33).....	69
<b>4. RESULTATES AND DISCUSSION.....</b>	<b>73</b>
4.1. SOLVENT AND STRUCTURAL EFFECTS ON THE UV-VIS ABSORPTION SPECTRA OF 5- -ARYLAZO-6-HYDROXY-4-PHENYL-3-CYANO-2-PYRIDONE DYES .....	73
4.1.1. Spectral characteristics and tautomerism.....	73
4.1.2. Solvent effects on the azo–hydrazone tautomerism.....	74
4.1.3. Substituent effects on the azo–hydrazone tautomerism.....	82
4.1.4. Quantum chemical calculations .....	84
4.2. SOLVENT AND STRUCTURAL EFFECTS ON THE UV-VIS ABSORPTION SPECTRA OF 5- -ARYLAZO-6-HYDOXY-4-(4-METHOXYPHENYL)-3-CYANO-2-PYRIDONE DYES .....	85
4.2.1. Spectral characteristics of arylazo pyridone dyes.....	87
4.2.2. Solvent effects on the UV-vis absorption spectra.....	87
4.2.3. Absorption maxima of hydrazone form as a function of dispersive interaction.....	92
4.2.4. Variation of absorption maxima with $E_T^N$ .....	94
4.2.5. Correlation with multiparameter solvent polarity scales .....	95
4.2.6. Substituents effects on the UV-vis absorption spectra .....	102
4.3. SOLVENT AND STRUCTURAL EFFECTS ON THE UV-VIS ABSORPTION SPECTRA OF 5- ARYLAZO-6-HYDOXY-4-(4-NITROPHENYL)-3-CYANO-2-PYRIDONE DYES.....	104
4.3.1. Spectral characteristics and solvatochromism .....	105
<b>5. CONCLUSIONS.....</b>	<b>115</b>
<b>6. REFERENCES .....</b>	<b>117</b>
<b>7. APPENDIX.....</b>	<b>125</b>

## LIST OF SCHEMES

Scheme 2.1. Preparation of the arylazo pyridone dyes from pyridone .....	6
Scheme 2.2. Preparation of the arylazo pyridone dyes from arylazo intermediate .....	7
Scheme 2.3. Disperse dyes with pyridone moiety substituted by Me or Ph group in position 4 and with OH or C <sub>6</sub> H <sub>5</sub> NH in position 6.....	10
Scheme 2.4. The equilibrium between hydrazone form and azo form .....	27
Scheme 2.5. The equilibrium between azo (34a) and hydrozone (34b) tautomeric forms of 1-phenylazo-4-naftol.....	31
Scheme 2.6. Inductive effect of -N <sup>+</sup> Me <sub>3</sub> substituent.....	35
Scheme 2.7. Resonance effect .....	37
Scheme 2.8. Influence charge at the starred carbon.....	43
Scheme 2.9. Duality of substituent constants .....	44
Scheme 2.10. Ionization of p-substituted phenols .....	48
Scheme 2.11. Resonance in p-nitrophenolate .....	48
Scheme 2.12. Heterolysis reaction of p-substituted phenyldimethyl chloromethanes .....	48
Scheme 2.13. Resonance in p-aminobenzyl cation.....	49
Scheme 2.14. Resonance effect at meta-position.....	50
Scheme 2.15. Keto – enol tautomeric form .....	53
Scheme 2.16. Lactam – lactim tautomeric forms .....	54
Scheme 4.1. The equilibrium between azo form (A) and hydrazone form (B) of 5-aryldazo-6-hydroxy-4-phenyl-3-cyano-2-pyridones (X = H (A1), OH (A2), OCH <sub>3</sub> (A3), CH <sub>3</sub> (A4), Cl (A5), Br (A6), I (A7), F(A8), CN (A9), COOH (A10), COCH <sub>3</sub> (A11), NO <sub>2</sub> (A12))......	74
Scheme 4.2. The equilibrium between azo form (A) and hydrazone form (B) of 5-aryldazo-6-hydroxy-4-(4-methoxyphenyl)-3-cyano-2-pyridone dyes (X = H (A13), F (A14), Cl (A15), Br (A16), I (A17), OH (A18), CH <sub>3</sub> (A19), OCH <sub>3</sub> (A20), COCH <sub>3</sub> (A21), CN (A22), NO <sub>2</sub> (A23)). Resonance effect of electron-accepting (structure C) and electron-donating (structure D) substituents of the arylazo component on the hydrazone tautome .....	86

Scheme 4.3. The equilibrium between azo form (**A**) and hydrazone form (**B**) of 5-aryazo-6-hydroxy-4-(4-nitrophenyl)-3-cyano-2-pyridone dyes: R = H (**A24**), 4-F (**A25**), 3-Cl (**A26**), 4-Br (**A27**), 4-I (**A28**), 4-CN (**A29**), 4-COCH<sub>3</sub> (**A30**), 4-CH<sub>3</sub> (**A31**), 4-NO<sub>2</sub> (**A32**), 4-OH (**A33**).....105

## LIST OF TABLES

Table 2.1. Absorption spectral data for the dye (33) ( $\lambda_{\max}/\text{nm}$ ; $\epsilon_{\max}/10^4 \text{ M}^{-1} \text{ cm}^{-1}$ ).....	27
Table 2.2. Values of the energies of the H (hydrazo) and A (azo) forms (HF/6-31G level) in different solvents calculated according to the Onsager model .....	7
Table 2.3. $\sigma$ values for several commonly encountered substituents.....	42
Table 2.4. Inductive and resonance values .....	50
Table 2.5. Dielectric constant of some common solvents .....	53
Table 2.6. Selected values of Kamlet-Taft parameters .....	59
Table 4.1. Absorption maxima of the hydrazone tautomer (B) of arylazo pyridone dyes (A1– A12) in protic solvents.....	76
Table 4.2. Absorption maxima of hydrazone tautomer (B) of arylazo pyridone dyes (A1– A12) in aprotic solvents.....	77
Table 4.3. Solvent parameters.....	79
Table 4.4. Regression fits to the solvatochromic parameters .....	80
Table 4.5. Percentage contribution of the solvatochromic parameters.....	82
Table 4.6. The relative energies and the statistical Boltzmann distribution weighted values of the most stable azo-hydrazone tautomers of dye A1.....	84
Table 4.7. The absorption frequencies of the investigated compounds (A13–A23) in selected solvents.....	89
Table 4.8. The physical parameters of the solvents .....	91
Table 4.9. The results of the correlation between $\nu_{\max}$ and the solvent dispersive function $f(n)$ .....	93
Table 4.10. Regression fits to the solvatochromic parameters (Eq. 4.1) .....	96
Table 4.11. Percentage contribution of solvatochromic parameters (Eq. 4.1).....	97
Table 4.12. Regression fits to solvatochromic parameters (Eq. 4.5) .....	98
Table 4.13. Percentage contribution of solvatochromic parameters (Eq. 4.5).....	99
Table 4.14. The absorption frequencies of the investigated compounds (A24–A33) in selected solvents.....	108
Table 4.15. Regression fits to the solvatochromic parameters (Eq. 4.1) .....	109
Table 4.16. Percentage contribution of solvatochromic parameters (Eq. 4.1).....	110

Table 4.17. Regression fits to solvatochromic parameters (Eq. 4.5) .....	111
Table 4.18. Percentage contribution of solvatochromic parameters (Eq. 4.5).....	112

## LIST OF FIGURES

Figure 2.1. Disperse dyes obtained from (disulfoanilino)dihalotriazines.....	9
Figure 2.2. Disperse dyes prepared from phthalimidyl and pyridone moieties .....	10
Figure 2.3. Azo dyes prepared from 3-cyano-4-hydroxy-2-phenyl-2-pyridone ( <b>4</b> ) and 3-cyano-6-hydroxy-4-phenyl-2-pyridone ( <b>5</b> ).....	11
Figure 2.4. Cyanodimethyl(phenylhydrazono)pyridinethione ( <b>6</b> ) and its chloropyridine derivative ( <b>7</b> ).....	11
Figure 2.5. Yellow reactive azo dyes obtained from cyanuric fluoride.....	12
Figure 2.6. Basic azo pyridone dyes used to dye acrylic fibbers .....	13
Figure 2.7. Cyano hydroxy pyridone dyes for liquid-crystal displays.....	14
Figure 2.8. Pyridone azo dyes used in the production of colored plastics.....	14
Figure 2.9. Azo dyes used in jet and hot-melt printing.....	15
Figure 2.10. Yellow dyes derived from 1-substituted 3-cyano-6-hydroxy-4-methyl-2-pyridones which are used in inks for thermal-transfer recording .....	15
Figure 2.11. Azo pyridone dyes used in a thermal-transfer printing material .....	16
Azo pyridone dyes from 6-hydroxy-2-pyridone and isoxazole ( <b>16</b> ), 1,2,4-triazole ( <b>17</b> ) or pyrazole ( <b>18</b> ).....	17
Figure 2.13. 5-(4-Arylazophenyl)azo-3-cyano-6-hydroxy-4-methyl-2-pyridones .....	18
Figure 2.14. Reactive disazo pyridone dyes .....	19
Figure 2.15. Disazo pyridone dyes used in phase change inks.....	19
Figure 2.16. Disazo dyes obtained from bispyridone derivative .....	20
Figure 2.17. Disazo yellow pyridone dyes used in the production of colored plastics.....	20
Figure 2.18. Disazo dyes from substituted 6-hydroxy-2-pyridones ( <b>24</b> ) and 4-methyl-3-cyano-6-hydroxy-2-pyridones ( <b>25</b> ) which are used as electrophotographic photoconductors .....	21
Figure 2.19. Trisazo pyridone dyes used to dye nylon 6 .....	22
Figure 2.20. Azopyridone moieties used for the synthesis of trisazo colorants .....	23
Figure 2.21. Azo pyridone dyes with good photostability.....	24
Figure 2.22. Azo (A) - hydrazone (H) tautomerism .....	25

Figure 2.23. Structure of C.I. Disperse Yellow 119 ( <b>30</b> ), D.I. Disperse Yellow 211 ( <b>31</b> ) and C.I. Disperse Yellow 114 ( <b>32</b> ) .....	26
Figure 2.24. The chemical structure of the azo dye synthesized from 1-ethyl-3-cyano-6-hydroxy-4-methyl-5-amino-2-pyridone.....	28
Figure 2.25. Absorption spectra of dye 33 in different solvents: (1. Acetone, 2. Ethanol, 3. Chloroform, 4. DMSO, 5. DMF) .....	28
Figure 2.26. Absorption of dye <b>33</b> in different volume ratios (a. $\frac{1}{4}$ ; b. $\frac{3}{2}$ ; c. $\frac{7}{3}$ ; d. $\frac{4}{1}$ ) of chloroform / DMSO .....	29
Figure 2.27. The chemical structures of the azo pyridone dyes investigated by Q. Peng at al.....	29
Figure 2.28. The $^{13}\text{C}$ NMR spectra of azo pyridone dyes (Figure 2.27, substituent 4'-SO <sub>3</sub> K) (at 90 °C). (A) in DMSO-d <sub>6</sub> ; (B) 20ml piperidine was added to (A); (C) Na <sub>2</sub> CO <sub>3</sub> was added to (A) .....	30
Figure 2.29. The most stable azo ( <b>A</b> ) and hydrazone ( <b>B</b> ) tautomer optimized structures of dye <b>A1</b> , at B3LYP/6-31G(d) level of theory .....	33
Figure 2.30. Hammett plot for the hydrolysis of ethyl benzoates.....	40
Figure 2.31. Hammett plots for phenylacetic acid and benzoic acid ionization in ethenol.....	47
Figure 2.32. One dimensional Gibbs energy diagram for a chemical reaction in three different solvents I, II and III.....	56
Figure 4.1. Absorption spectra of dyes <b>A1–A12</b> in methanol .....	75
Figure 4.2. Absorption spectra of dyes <b>A1–A12</b> in dimethyl sulfoxide .....	75
Figure 4.3. Resonance effect of electron-accepting (structure <b>C</b> ) and electron-donating (structure <b>D</b> ) substituents of the arylazo component on the hydrazone tautomer.....	81
Figure 4.4. Relationship between $\nu_{\text{max}}$ and $\sigma_{\text{p}^+}$ for arylazo pyridone dyes <b>A1–A12</b> in methanol.....	83
Figure 4.5. The most stable hydrazone tautomer ( <b>a</b> ) and some other azo-hydrazone tautomers of 5-phenylazo-6-hydroxy-4-phenyl-3-cyano-2-pyridone. (The geometries correspond to the energy minimum in vacuo). .....	85
Figure 4.6. The UV-vis absorption spectra of 5-arylazo-6-hydroxy-4-(4-methoxyphenyl)-3-cyano-2-pyridone dyes in ethanol (a) and dimethyl sulfoxide (b).....	90
Figure 4.7. The correlation of $\nu_{\text{max}}$ of the dye <b>A18</b> with $E_{\text{T}}^{\text{N}}$ (excluded ethanol).....	94

Figure 4.8. Experimental versus calculated values of $\nu_{\max}$ from Eq. 4.1 (A) and Eq. 4.5 (B) .....	101
Figure 4.9. Relationship between $\nu_{\max}$ and $\sigma_{p+}$ for arylazo pyridone dyes in ethanol (excluding <b>A14</b> and <b>A19</b> ).....	104
Figure 4.10. UV-vis absorption spectra of azo dyes in different solvents (ethanol, ethyl acetate, dimethylformamide) .....	106
Figure 4.11. The plot of $\nu_{\max}$ calculated against $\nu_{\max}$ observed for Kamlet-Taft (I) and Catalan (II) equation in different solvents .....	113

## ABSTRACT

Three series of some novel arylazo pyridone dyes, 5-arylazo-6-hydroxy-4-phenyl-3-cyano-2-pyridone dyes, 5-arylazo-6-hydroxy-4-(4-methoxyphenyl)-3-cyano-2-pyridone dyes and 5-arylazo-6-hydroxy-4-(4-nitrophenyl)-3-cyano-2-pyridone dyes have been synthesized. The structure of the dyes was confirmed by UV-Vis, FTIR,  $^1\text{H}$  NMR and  $^{13}\text{C}$  NMR spectroscopy and elemental analysis. The solvatochromic behavior of the dyes was evaluated with respect to their visible absorption properties in various solvents. The azo-hydrazone tautomeric equilibration was found to depend on the substituents as well as on the solvent. These dyes exist in the hydrazone form in the solid state and in solvent  $\text{DMSO}-d_6$  and there was an equilibrium between hydrazone form and azo form in the different solvents.

The Kamlet-Taft and Catalan parameters were used for describing the solute-solvent interactions and solvatochromic shifts of the visible absorption band. It was found that the solute dipolarity / polarizability (especially polarizability by Catalan equation) play an important role in the description of the pronounced solvatochromism in the studied solutions.

The Catalan solvent scales were found to be more suitable for describing the solvatochromic shifts.

The geometry data of the investigated dyes were obtained using DFT quantum-chemical calculations. The obtained calculational results are in very good agreement with the experimental data.

*Keywords:* Arylazo pyridone dyes, Tautomerism, Solvent Effects, Substituent Effects, Solvatochromism

*Scientific field:* Chemistry

*Specific scientific field:* Organic Chemistry

## IZVOD

U okviru proučavanja strukture i karakteristika azo piridonskih boja, u čvrstom stanju i u rastvoru, su sintetisane tri nove serije arilazo piridonskih boja koje do sada nisu poznate u literaturi: 5-arilazo-6-hidroksi-4-fenil-6-cijano-2-piridonske boje, 5-arilazo-6-hidroksi-4-(4-metoksifenil)-6-cijano-2-piridonske boje i 5-arilazo-6-hidroksi-4-(4-nitrofenil)-6-cijano-2-piridonske boje. Sve azo boje su sintetisane diazotovanjem odgovarajućih 4-supstituisanih anilina i kuplovanjem dobijenih diazo soli sa odgovarajućim piridonima, prethodno dobijenim iz odgovarajućih etil-4-supstituisanih benzoilacetata i cijanoacetamida. Struktura sintetisanih azo boja je potvrđena na osnovu podataka iz UV-vis, FTIR,  $^1\text{H}$  NMR i  $^{13}\text{C}$  NMR spektara. Solvatohromna svojstva su određena u odnosu na njihovu apsorpciju u vidljivom delu UV-Vis spektra u različitim rastvaračima. Efekti polarnosti rastvarača, proton-donorske i proton-akceptorske karakteristike interakcije rastvarač-rastvorena supstanca su kvantitativno procenjene Kamlet-Taft-ovim i Catalan-ovim solvatohromnim modelima. Proučavanje uticaja supstituenata na arilazo komponenti na azo-hidrazon tautomeriju sintetisanih boja izvršeno je korelacijom UV-Vis apsorpcionih frekvenci Hammett-ovom jednačinom.

Azo boje sintetizovane u ovoj disertaciji mogu postojati u azo i hidrazon tautomernim oblicima. Na azo-hidrazon ravnotežu veliki uticaj imaju rastvarači i supstituenti prisutni u arilazo komponenti. Rezultati ostvareni u ovom radu ukazuju na dominantan hidrazonski tautomerni oblik, kako u čvrstom stanju tako i u rastvorima azo boja u rastvaračima različitih svojstava. Hidrazonska struktura proučavanih azo boja je potvrđena kvantno-hemijskim izračunavanjima korištenjem DFT/B3LYP metode.

*Ključne reči:* Arilazo piridonske boje, Tautomerija, Uticaj rastvarača, Uticaj supstituenata, Solvatohromizam.

*Naučna oblast:* Hemija

*Uža naučna oblast:* Organska hemija

## 1. INTRODUCTION

Azo compounds are very important in the field of dyes, pigments and advanced materials. Over 50% of all colorants are azo dyes and they are most widely used compounds in various areas, such as dyeing textile fibres, coloring of different materials, in biological-medical studies and advanced applications in organic synthesis. The success of azo colorants is in the simplicity of their synthesis, in almost innumerable possibilities presented by variation on the diazo compounds and coupling components, to the generally high molar extinction coefficient, as well as to the medium to high light and wet fastness properties. In recent years, azo dyes have attracted wide interest and found many uses in materials for optical applications and in analysis. Due to their properties, including optical storage capacity, optical switching, holography and non-linear optical properties, polymers with azo units represent promising candidates for photoactive materials.

Pyridone derivatives are heterocyclic intermediates for the preparation of azo dyes. The azo pyridone dyes give bright hues and are suitable for dyeing of polyester fabrics. The physico-chemical properties of arylazo pyridones are closely related to their tautomerism. Determination of azo-hydrazone tautomers in the solid state and in solution is quite interesting both from theoretical and practical standpoints, since the tautomers have different technical properties and dyeing performances. The UV-vis absorption spectroscopy is widely used method for investigation of the intermolecular interaction and solvatochromism. Several investigations on substituted arylazo pyridones, with respect to their visible absorption spectra in various solvents, have been carried out and reviewed. It has been concluded that the equilibrium between the two tautomers is influenced by the structure of the compounds and the solvent used. The introduction of the electron-attracting or electron-donating substituents into the *para* or *ortho* positions of the diazo components of an azo pyridone dye, resulted in additive or subtractive color shifts and fading rates, depending on the nature and the orientation of the substituents.

In this thesis three series of arylazo pyridone dyes, 5-arylazo-6-hydroxy-4-phenyl-3-cyano-2-pyridone dyes, 5-arylazo-6-hydroxy-4-(4-methoxyphenyl)-3-cyano-2-pyridone dyes and 5-arylazo-6-hydroxy-4-(4-nitrophenyl)-3-cyano-2-pyridone dyes have been synthesized. The structure of the dyes was confirmed by UV-vis, FTIR, <sup>1</sup>H NMR and

$^{13}\text{C}$  NMR spectroscopy and elemental analysis. The solvatochromic properties have been studied in a set of twenty solvents of different properties. Different solvent parameters, such as microscopic solvent polarity  $E_T^N$ , relative permittivity  $\epsilon_r$ , refractive index  $n$ , the Kamlet-Taft and the Catalan parameters were used for describing the solvent-solute interactions and the solvatochromic shifts of the UV-vis absorption band of the investigated arylazo dyes. For the quantitative assessment of the substituent effects, the simple Hammett equation was used.

The geometry data of the investigated dyes were obtained using DFT quantum-chemical calculations. The obtained results are in very good agreement with the experimental data.

## 2. THEORETICAL PART

### 2.1. Synthesis, structure and properties of azo pyridone dyes

Azo dyes are synthetic organic colorants bearing chromophoric azo group (-N=N-). On one side azo group is attached to an aromatic or heterocyclic nucleus and on the other, to an unsaturated molecule of the carbocyclic, heterocyclic, or aliphatic type [1]. IUPAC defines azo compounds as: "Derivatives of diazene (diimide), HN=NH, wherein both hydrogens are substituted by hydrocarbyl groups, e.g. PhN=NPh azobenzene or diphenyldiazene" [2].

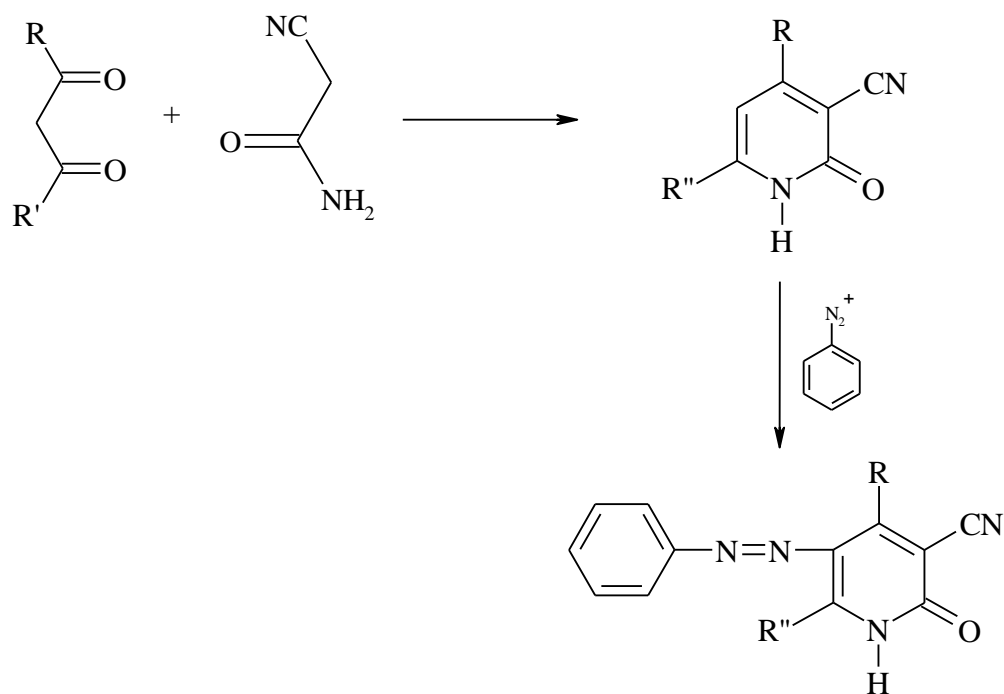
Azo group is not presented in natural dyes. Commercially, these colorants are the largest and most versatile class of organic dyestuffs. As published in Kirk-Othmer Encyclopedia of Chemical Technology [1] in 2003, there were more than 10,000 Colour Index (CI) generic names assigned to commercial colorants. Approximately 4,500 of them are in use, and over 50% of these belong to the azo compounds. Azo dyes can be divided according to the number of azo groups to monoazo, disazo, trisazo and polyazo, and also further subdivision can be achieved according to the solubility or according to the types of component used. The widest range of usage of azo dyes is because of number of variations in chemical structure and methods of application which are generally not complex. Cotton, paper, silk, leather, and wool can be dyed by azo dyes. Also, there are azo dyes for dyeing polyamides, polyesters, acrylics, polyolefins, viscose rayon, and cellulose acetate. They can be used for the coloring of paints, varnishes, plastics, printing inks, rubber, foods, drugs, and cosmetics. Azo colorants are also used in diazo printing and color photography. The shades of azo dyes cover the whole spectrum [1].

Among azo colorants arylazo pyridone dyes have become important in last several decades. The high molar extinction coefficient, and the medium to high light and wet fastness properties are very favourable [3]. They find application generally as disperse dyes. Disperse dyes are characterized by low aqueous solubility and are applied to hydrophobic fibers from an aqueous system, in which the dye is present in a highly dispersed state. The importance of disperse dyes increased in the 1970s and 1980s due to the use of polyester and nylon as the main synthetic fibers. Also, disperse dyes were used rapidly since 1970 in inks for the heat-transfer printing of polyester [1].

### 2.1.1. General synthesis

The main synthetic route for the preparation of azo dyes is coupling reaction between an aromatic diazo compound and a coupling component. Of all dyes manufactured, about 60% are produced by this reaction [1]. The success of azo colorants is due to the simplicity of their synthesis by diazotization and azo coupling, and to the almost innumerable possibilities presented by variation on the diazo compounds and coupling components [3]. All coupling components used to prepare azo dyes have the common feature of an active hydrogen atom bound to a carbon atom.

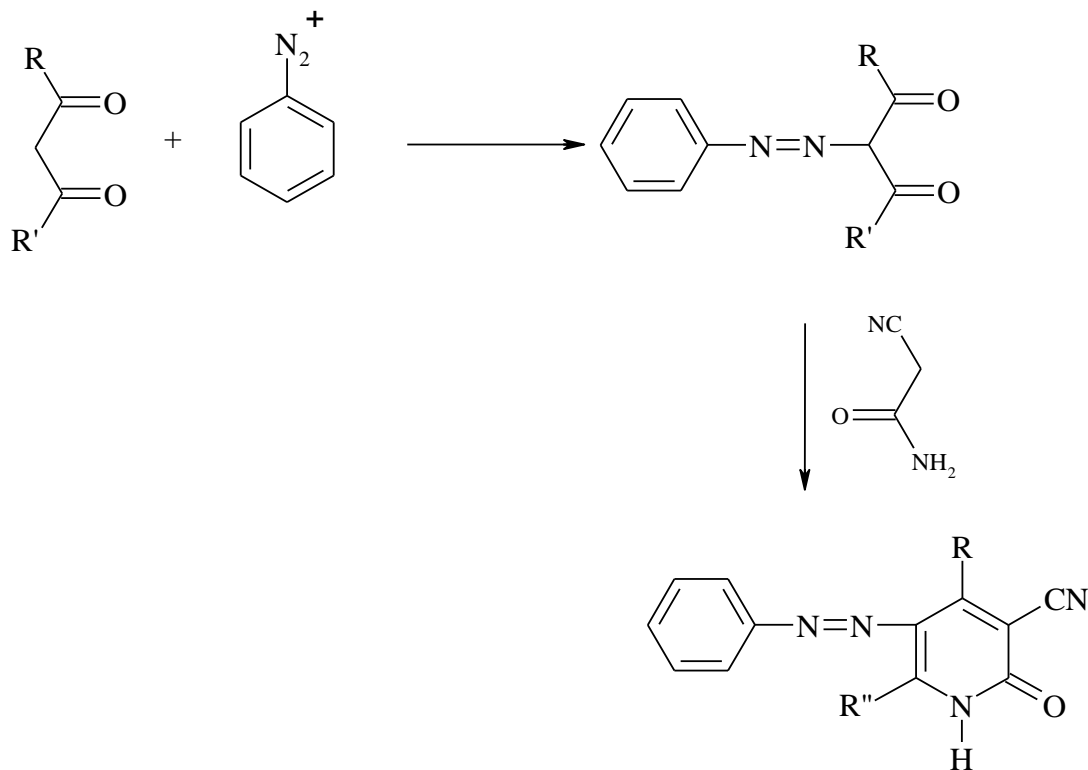
Generally, arylazo pyridone dyes can be prepared from pyridone moiety as a coupling component and various diazonium salts using well known reaction [3] (Scheme 2.1). R is usually methyl, R' ethoxy and R'' hydroxy group. Nitrogen can be substituted, while diazonium salts can be derived from different substituted anilines or other heterocyclic derivatives. Pyridones can be prepared using known procedures [4-7].



Scheme 2.1. Preparation of the arylazo pyridone dyes from pyridone.

Arylazo dyes containing pyridone ring can be also prepared from arylazo diketones or arylazo ketoesters (obtained by coupling  $\beta$ -diketones or  $\beta$ -ketoesters with

diazonium salts) by condensation with cyanoacetamide (Scheme 2.2) [8-10]. And here, R is usually methyl, R' ethoxy or methyl and R'' hydroxy or methyl group.



Scheme 2.2. Preparation of the arylazo pyridone dyes from arylazo intermediate.

Lately, a novel protocol for the rapid synthesis of pyridone colorants under controlled microwave irradiation in a dedicated reactor is described according to Scheme 2.2. Short reaction times, high isolated yields, and versatility for different substrates are the advantages of the reported method [11].

All other procedures are mostly variants given in Schemes 2.1 or 2.2, where different diazo salts and pyridones were used.

#### 2.1.1.1. Monoazo dyes

Disperse azo dyes useful for dyeing polyester fibers fast brilliant yellow shades were described in 1972 by Burkhard *et al.* These dyes were prepared by coupling diazotized anilines with 3-cyano-6-hydroxy-4-methyl-2-pyridones in HOAc at 0-5 °C and pH 4.5 [12]. Starting from different anilines disperse dyes were prepared and used in dyeing or printing polyester fibers with fast, yellow to greenish yellow shades [13]. In addition, disperse azo dyes were manufactured and used to dye synthetic fibers fast

greenish yellow to red shades, by further modification of amino component (e.g. 5-amino-4,6-dicyanoindan) [14]. Lightfast yellow shades were obtained by dyeing poly(ethylene terephthalate) (PET) fibers with azo dyes where molecules like decyl 4-aminobenzoate was diazotized and coupled with 3-cyano-6-hydroxy-4-methyl-2-pyridone [15]. Besides yellow shades, polyester fibers were dyed fast orange shades [16]. It was shown that dye prepared from *p*-toluidine and 3-cyano-6-hydroxy-4-methyl-2-pyridone is useful for dyeing and printing hydrophobic synthetic fibers, e.g., polyester, in mixture with Disperse Yellow 54 and/or Disperse Yellow 64 [17].

By coupling diazotized 2,4,3,5-(NC)<sub>2</sub>Me<sub>2</sub>C<sub>6</sub>H<sub>2</sub>NH<sub>2</sub> with 3-cyano-6-hydroxy-1,4-dimethyl-2-pyridone in aqueous NaOH, the yellow azo dye was prepared and used for dyeing polyester fibers light- and sublimation fast yellow shades [18]. Another azo dye was prepared by coupling diazotized 3-H<sub>2</sub>NC<sub>6</sub>H<sub>4</sub>O<sub>3</sub>SPh with 3-cyano-6-hydroxy-1,4-dimethyl-2-pyridone and used for dyeing polyester fibers a fast greenish yellow shade [19]. In addition, azo dyes prepared by coupling diazotized 2,4-O<sub>2</sub>N(RO)C<sub>6</sub>H<sub>3</sub>NH<sub>2</sub> (R = Me(CH<sub>2</sub>)<sub>3</sub>CH<sub>2</sub>Et, Me(OCH<sub>2</sub>CH<sub>2</sub>)<sub>2</sub>, Me(CH<sub>2</sub>)<sub>9</sub>) with the same pyridone, were used to dye polyester fibers fast orange shades from aqueous dispersions and from tetrachloroethylene [20]. An improvement in azo dye synthesis in mean of yield, purity, and production efficiency, was achieved by using NO<sub>2</sub> in pentane at -8°C for diazotization followed by coupling in water at 0-5°C [21].

Brilliant yellow color was obtained by coupling of diazotized aniline 2,4-R<sub>1</sub>O(N O<sub>2</sub>)C<sub>6</sub>H<sub>3</sub>NH<sub>2</sub> (R<sub>1</sub> = C<sub>1-4</sub>) with two 1-substituted alkyl (R<sub>2</sub> = C<sub>1-4</sub>, (CH<sub>2</sub>)<sub>n</sub>OR<sub>3</sub>, R<sub>3</sub> = C<sub>1-4</sub> alkyl; n = 1-3) cyano(methyl)hydroxypyridones when used to dye polyester fabric [22]. Also, disperse dyes were prepared from 1-alkyl substituted cyano 2-pyridones where alkyl groups had 1-4 carbon atoms [23].

A fast greenish yellow shade on polyester fibers was obtained by using an azo dye prepared by coupling diazotized 4-ClC<sub>6</sub>H<sub>4</sub>OCH<sub>2</sub>CH<sub>2</sub>O<sub>2</sub>CC<sub>6</sub>H<sub>4</sub>NH<sub>2</sub> with 3-cyano-1-ethyl-2-hydroxy-4-methyl-6-pyridone [24].

When 1-butyl-3-cyano-6-hydroxy-4-methyl-2-pyridone was used as a coupling component and 4-H<sub>2</sub>NC<sub>6</sub>H<sub>4</sub>SO<sub>2</sub>NHCH<sub>2</sub>CH<sub>2</sub>Et was diazotized, disperse azo dye was obtained and used for dyeing polyester fibers light-, wet-, and heat fast greenish yellow shades [25].

Other 1-substituted 3-cyano-6-hydroxy-4-methyl-2-pyridones were used as coupling components. When 1-substituents were: (un)substituted Ph, C<sub>3-4</sub> alkenyloxy, C<sub>3-4</sub> alkynyloxy, PhO and (un)substituted C<sub>1-8</sub> alkoxy, azo dyes were obtained with different substituents in arylazo part of dye. Thus, 4-H<sub>2</sub>NC<sub>6</sub>H<sub>4</sub>CO<sub>2</sub>CH<sub>2</sub>CO<sub>2</sub>CH<sub>2</sub>Ph was diazotized and coupled with 1-butyl-3-cyano-6-hydroxy-4-methyl-2-pyridone to give dye that gave brilliant greenish yellow on polyester fibers, both in polyester fabrics and in polyester-cotton blends [26]. By coupling diazotized 2-nitroaniline with 3-cyano-1-(2-ethylhexyl)-6-hydroxy-4-methyl-2-pyridone an azo dye insoluble in water was obtained which produce heat- and wet fast greenish yellow on polyester fibers [27]. When such dye was heated at 80-85 °C for 2 h, an azo dye in a specified crystal form was obtained and used for dyeing of textured polyester yarns, giving rub-fast dyeing [28].

The water-soluble disperse azo dyes including light yellow, yellow, orange, red, violet and blue colours were obtained from 3-cyano-6-hydroxy-4-methyl-2-pyridone or 1-substituted 3-cyano-6-hydroxy-4-methyl-2-pyridones (substituents Me, OMe, SO<sub>2</sub>CH<sub>2</sub>COOH) [29].

Dyes having formula **1** (Figure 2.1; R = H or optionally substituted alkyl; Q = CN, CONH<sub>2</sub>; X = halogen), were obtained from (disulfoanilino)dihalotriazines and the appropriate azo pyridine, were useful in dyeing or printing of hydroxy- or nitrogen-containing substrates [30].

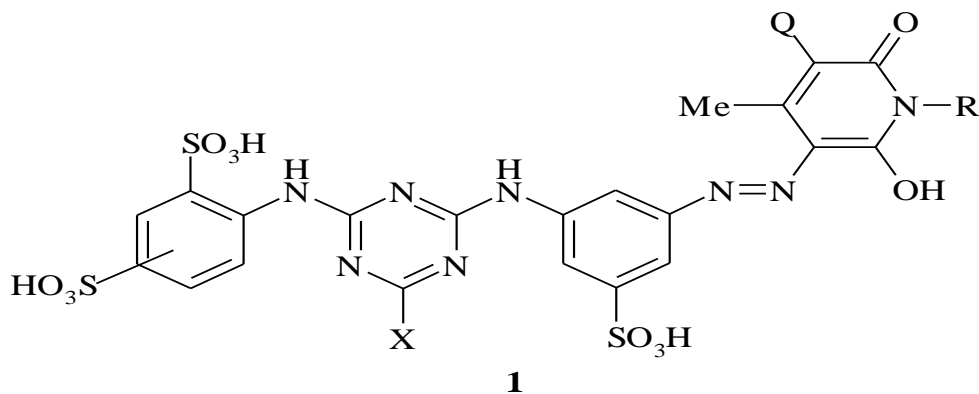


Figure 2.1. Disperse dyes obtained from (disulfoanilino)dihalotriazines.

Disperse azo dyes prepared from phthalimidyl and pyridone moieties showed improved washfastness in dyeing of hydrophobic fibers (Figure 2.2, R<sup>1</sup> = C<sub>1-12</sub> alkyl or C<sub>n</sub>H<sub>2n</sub>(OCH<sub>2</sub>CH<sub>2</sub>)<sub>m</sub>OR<sub>3</sub>, n = 2-8, m = 0-4, R<sub>3</sub> = C<sub>1-12</sub> alkyl, C<sub>6-24</sub> aryl, or C<sub>6-24</sub> aralkyl, R<sup>2</sup> = Me, Et, Pr, Bu, 2-methoxyethyl or 2-ethoxyethyl, X = halo, Y = H, Cl, or Br) [31].

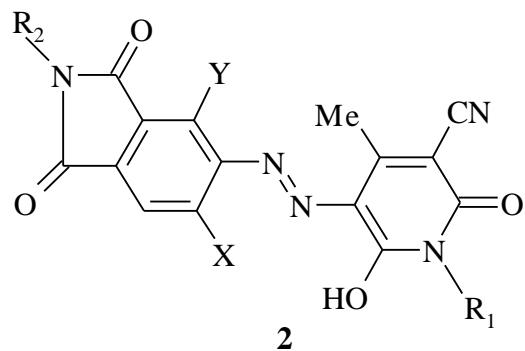
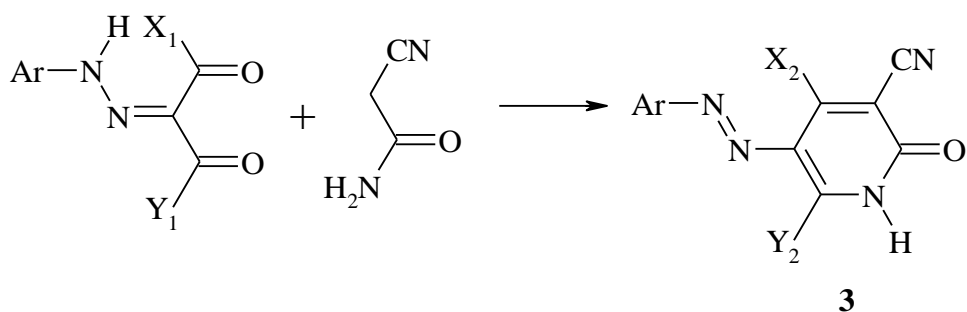


Figure 2.2. Disperse dyes prepared from phthalimidyl and pyridone moieties.

Azo dyes for dyeing of polyester fabrics were in addition prepared by coupling diazotized *p*-substituted anilines (H, Me, NO<sub>2</sub>) with 1-substituted 5-cyano-6-hydroxy-4-methyl-2-pyridones (N-substituents = H, Me, HOCH<sub>2</sub>CH<sub>2</sub>, Me<sub>2</sub>NCH<sub>2</sub>CH<sub>2</sub>, C<sub>12</sub>H<sub>25</sub>) [32].

Recently a synthesis of new azo dyes was reported. These dyes were prepared by diazotisation, coupling and cyclization reactions, starting from various aryldiazonium salts and different β-diketoesters followed by condensation with cyanoacetamide, as given in Scheme 2.2. The pyridone moiety was substituted by Me or Ph group in position 4 and with OH or C<sub>6</sub>H<sub>5</sub>NH in position 6 [33].



Scheme 2.3. Disperse dyes with pyridone moiety substituted by Me or Ph group in position 4 and with OH or C<sub>6</sub>H<sub>5</sub>NH in position 6.

Azo dyes given in Figure 2.3 were prepared from 3-cyano-4-hydroxy-2-phenyl-2-pyridone (**4**) as well as from 3-cyano-6-hydroxy-4-phenyl-2-pyridone (**5**) and coupling with aniline and *p*-substituted anilines (Me, OMe, Cl) [34].

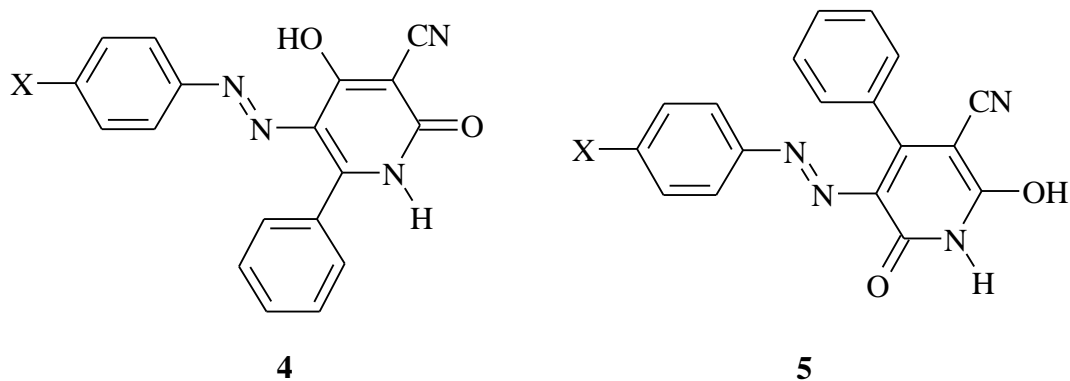


Figure 2.3. Azo dyes prepared from 3-cyano-4-hydroxy-2-phenyl-2-pyridone (**4**) and 3-cyano-6-hydroxy-4-phenyl-2-pyridone (**5**).

Thiopyridones (Figure 2.4) were prepared by the reaction of thiocyanacetamides with sodium ethoxide and then with  $\text{MeCOC}(\text{COMe})=\text{NNHPh}$  to give cyanodimethyl-(phenylhydrazono)-pyridinethione (**6**). Alternatively, **6** was chlorinated with  $\text{Cl}_2$  in  $\text{CHCl}_3$  to give chloropyridine derivative (**7**) [8].

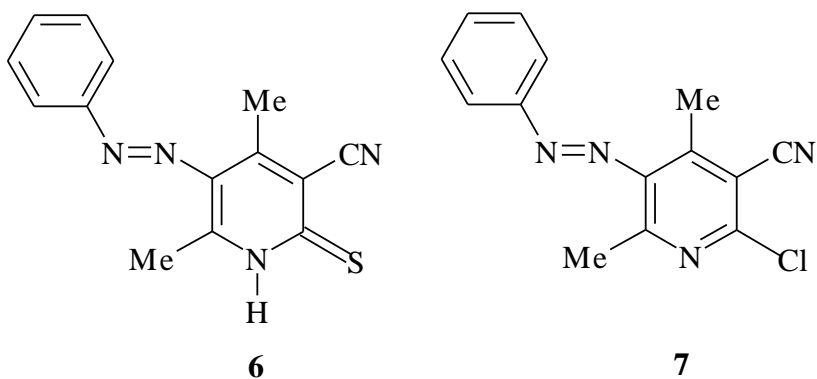


Figure 2.4. Cyanodimethyl(phenylhydrazono)pyridinethione (**6**) and its chloropyridine derivative (**7**).

It should be mentioned that disperse dyes were also prepared from 2-aminothiophene derivatives (2-amino-4,5,6,7-tetrahydro[b]thiophene-3-carbonitrile and ethyl 2-amino-4,5,6,7-tetrahydrobenzo[b]thiophene-3-carboxylate) and 5-cyano-6-hydroxy-4-methyl-2-pyridone and 5-cyano-1-ethyl-6-hydroxy-4-methyl-2-pyridone. The dyes had generally good coloration and fastness properties on polyester [35,36].

### Reactive dyes

Five reactive azo dyes for cotton were prepared from 1-(2-aminoethyl)-3-cyano-2-hydroxy-4-methyl-6-pyridone. Also, a cationic azo dye for polyacrylonitrile fiber, a disperse azo dye for hydrophobic fibers, and an acid azo dye for nylon were prepared [37].

More yellow reactive azo dyes (Figure 2.5; M = H, alkali metal; R<sup>1</sup>, R<sup>2</sup> = H, optionally substituted C<sub>1-4</sub>-alkyl; R<sup>3</sup> = H, optionally substituted C<sub>1-4</sub>-alkyl or -alkoxy, halogen, carboxy, Ph; R<sup>4</sup> = C<sub>1-4</sub>-alkyl, Ph; R<sup>5</sup> = carbonamido, cyano, sulfomethyl; R<sup>6</sup> = C<sub>1-4</sub>-alkyl; X = vinyl or vinyl-forming group; n = 0-2) were obtained from cyanuric fluoride, the requisite aromatic amines, and a pyridone derivate coupling component [38].

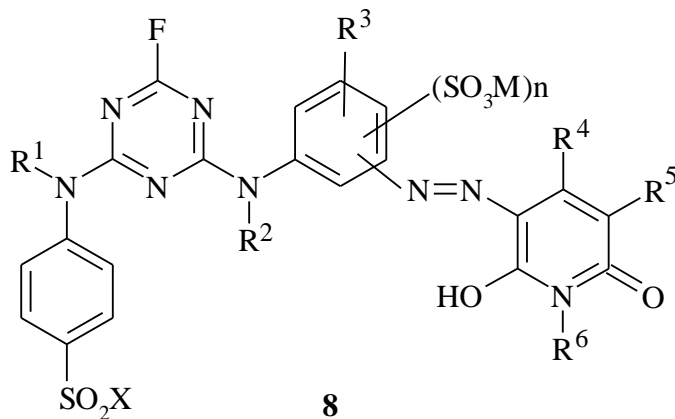


Figure 2.5. Yellow reactive azo dyes obtained from cyanuric fluoride.

### Basic dyes

Nine basic dyes, based on 2-pyridone moiety, were manufactured and used to dye polyacrylonitrile fast yellow shades. Thus, [ $\alpha$ -(4-aminobenzenesulfonamido)ethyl]pyridinium chloride was diazotized and coupled with 1-ethyl-3-cyano-2-hydroxy-4-methyl-6-pyridone to give an azo dye. A number of variations were applied in arylazo part as well as in substituent in position 1 of pyridone part [39].

Basic dyes, given in Figure 2.6, were prepared in one step by coupling diazotized aromatic primary amines with 6-hydroxy-2-pyridones and used to dye acrylic fibers fast yellow shades. 3-Pyridinium (**9**) or 3-cyano-2-pyridone (**10**) dyes were 1-substituted with at least one alkyl group with more than 5 C-atoms [40].

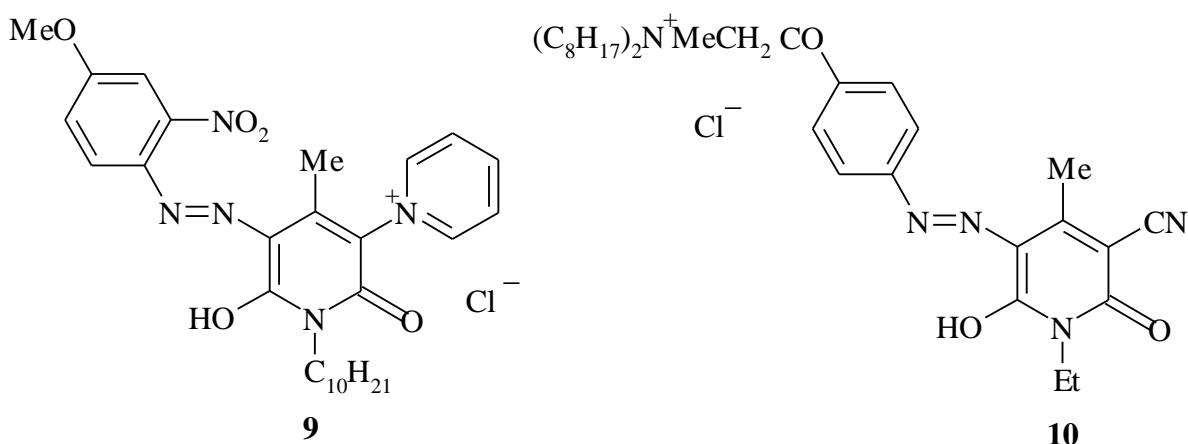


Figure 2.6. Basic azo pyridone dyes used to dye acrylic fibbers.

### ***Monoazo dyes for other uses***

Azo pyridone dyes were further used for paints and printing inks with yellow to blue shades. This printing inks were based on a monoazo dye e.g. 1-ethyl-3-cyano-4-methyl-5-[(3-nitrophenyl)azo]-6-hydroxy-2-pyridone. Besides a dye, a film-forming binder and a solvent were used [41].

Azo dyes obtained from 1-substituted pyridones ( $C_{1-8}$  alkyl, allyl) e.g. 1-butyl-3-cyano-2-hydroxy-4-methyl-6-pyridone, were used do dye coating components, organic solvents and mineral oil products in yellow shades. Different substituted anilines were used like 3,4-Me(H<sub>2</sub>N)C<sub>6</sub>H<sub>3</sub>SO<sub>2</sub>NBu<sub>2</sub> [42].

A yellow dye derived from substituted 3-cyano-6-hydroxy-2-pyridones with different groups in positions 1 and 4 were used for the preparation of a powder toner composition comprised a thermoplastic polymer blended with 0.5-10 % of a yellow dye. The dyes can be used where images are fixed by thermal fusion [43].

Cyano hydroxy pyridones were also used as colorants to prepare color filters for liquid-crystal displays. The dyes have the structure presented in Figure 2.7 [M = H, cation; R<sup>1</sup>, R<sup>3</sup> = H, (un)substituted C<sub>1-8</sub> organic group, A; R<sup>2</sup> = (un)substituted C<sub>1-8</sub> organic group; R<sup>4</sup>, R<sup>5</sup>, X, Y, Z = H, CN, substituent; c = 2-6; m, n = 0-2], containing ≥ 1 SO<sub>3</sub>M or PO<sub>3</sub>M<sub>2</sub> group, with certain specified exclusions [44].

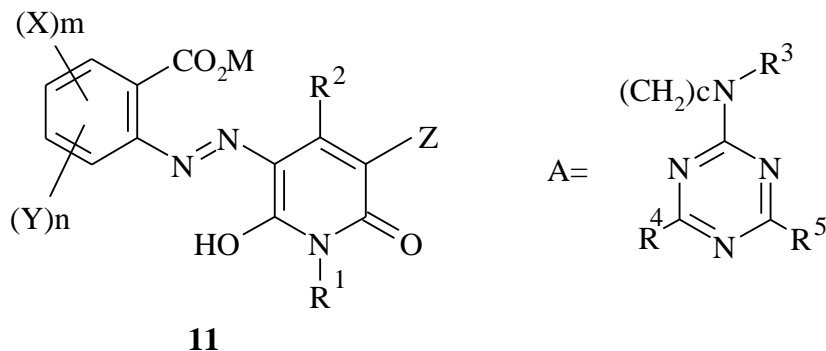


Figure 2.7. Cyano hydroxy pyridone dyes for liquid-crystal displays.

The pyridone azo dyes given in Figure 2.8 (A = diazo component residue;  $R^1 = H$ , optionally hydroxyl- or phenyl-substituted  $C_{1-6}$ -alkyl, azo pyridone derivative, ester, amide, keto;  $R^2 =$  azo pyridone derivative, ester, amide, keto;  $R^1R^2N$  may form a heterocycle; Y = cyano,  $CONH_2$ ,  $CH_2SO_3H$ ;  $n = 2-6$ ) were used in the production of colored plastics or polymeric color particles [45].

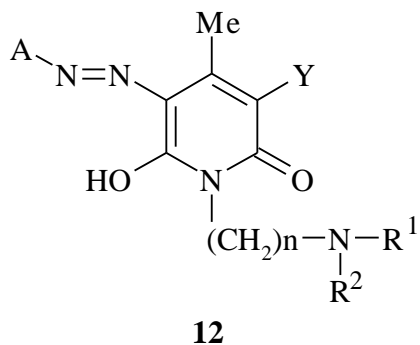


Figure 2.8. Pyridone azo dyes used in the production of colored plastics.

Azo dyes presented in Figure 2.9 ( $X = H, Cl, Br, CN, SO_2Me, OH, OMe, NO_2$ ; Y = H, Cl, Br, Cl; Z = coupling component group like 1-butyl-3-cyano-6-hydroxy-4-methyl-2-pyridone) were prepared, and used in dyeing and in jet and hot-melt printing. These dyes are suited for application to hydrophobic and synthetic textiles with good fastness in yellow shade [46].

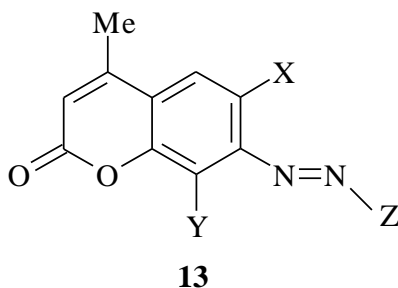


Figure 2.9. Azo dyes used in jet and hot-melt printing.

The yellow dyes [Figure 2.10,  $R^1 = C_{3-8}$  branched or cyclic (substituted) alkyl;  $R^2 = C_{5-10}$  branched or cyclic (substituted) alkoxyalkyl] were derived from 1-substituted 4-methyl-3-cyano-6-hydroxy-2-pyridones, and used to produce ink which contained a binder resin, and an organic solvent and/or  $H_2O$ . The ink was used for thermal-transfer recording. The dyes gave images with good storage stability [47].

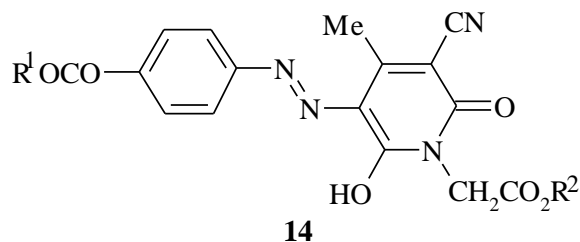


Figure 2.10. Yellow dyes derived from 1-substituted 3-cyano-6-hydroxy-4-methyl-2-pyridones which are used in inks for thermal-transfer recording.

Similarly, dyes were prepared having formula  $AN=NR$  [ $A =$  halogenated phenyl;  $R = 1-C_{2-6}$  alkyl(or alkoxy)-5-cyano-2-hydroxy-3-methyl-6-pyridon-3-yl group] and used to get inks for a transfer sheet which was used with a thermal receiving sheet [48].

In another patent pyridone-based yellow monoazo dyes were used to obtain ink by dissolving 2-8% dye and 2-8% binder in 84-96% organic solvent for thermal transfer printing [49].

Azo pyridone dyes, which structure is given in Figure 2.11 [ $A =$  (substituted) aromatic ring;  $B =$  single bond or divalent linking group;  $X = N$  or  $CY^1$ ;  $Y^{1-4} = H$ , halo, straight-chain or branched alkyl which may be substituted, aryl, heteroaryl, alkoxy, cycloalkyl, alkenyl, allyl, aralkyl, dialkylamino, alkylamino, the plural groups of  $Y^{1-4}$  may be condensed to form a 5- to 7-membered ring;  $R^1 =$  straight-chain or branched alkyl which may be substituted;  $R^2 =$  straight-chain or branched alkyl which may be substituted, cycloalkyl, alkenyl, aryl, aralkyl, allyl] were prepared and used in a thermal-

transfer printing material comprises the dye-donating material and a dye image-receiving material possessing an image-receiving layer containing a dye-fixing material [50].

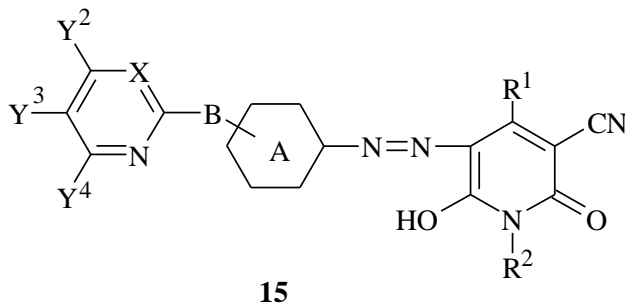


Figure 2.11. Azo pyridone dyes used in a thermal-transfer printing material.

Monoazo dyes derived from 1-substituted 3-cyano-6-hydroxy-4-methyl-2-pyridones were used in thermal-transfer printing. Different substituted anilines were used with substituents like (un)substituted succinimido or maleimido or glutarimido; halo, C<sub>1-4</sub> alkyl, alkoxy groups [51].

It is interesting to mention that dyes derived from different anilines and 3-cyano-6-hydroxy-2-pyridones were used in a media useful for recording and/or reading information by using blue laser [52].

Azo pyridones are also useful as colorants in phase change inks. Different derivatives of 3-cyano-6-hydroxy-2-pyridones were used [53,54].

Other inks were produced from azo pyridone dyes, as given in Japan patent [55], where was claimed that ink shows good storage stability while image formed from the ink showed optical density 1.1 and good water and light resistance.

The dyes obtained from 1-substituted 4-alkyl (C<sub>1-10</sub> alkyl, methoxymethyl, trifluoromethyl)-3-cyano-6-hydroxy-2-pyridones were used for ink-jet inks, liquid crystal displays, plasma display panels, and solid-state image sensors (e.g., CCD, CMOS) [56].

Tanaka *et al.* [57] claimed yellow toners prepared from azo pyridone dyes obtained from substituted 6-hydroxy-2-pyridones. As an example the following preparation can be given: *o*-nitrobenzoic acid and SOCl<sub>2</sub> were heated at 60 °C for 1 h, and then Et<sub>3</sub>N and di(2-ethylhexyl)amine were added therein and reacted at 80 °C for 2 h; the resulting 2-nitrobenzoyl 2-diethylhexylamide was reduced, diazotized, and coupled with 1,2-dihydro-6-hydroxy-4-methyl-2-oxo-3-pyridinecarbonitrile to give a pyridone derivative.

### ***Metal complexed dyes***

Azo pyridone dyes were used in order to provide an optical recording medium. This medium had a recording layer improved in light stability capable of recording and regeneration of high-density optical information by short-wavelength laser beams. The recording layer contained a metal complex of pyridone azo compounds as given in Figure 2.12 ( $R^{1-10} = H$ , monovalent functional group). The metal complex was obtained from a 6-hydroxy-2-pyridone structure as a coupler component and an isoxazole, 1,2,4-triazole or pyrazole structure as a diazo component and an ion of bivalent metal, such as Ni, Co, Fe, Zn, Cu or Mn [58].

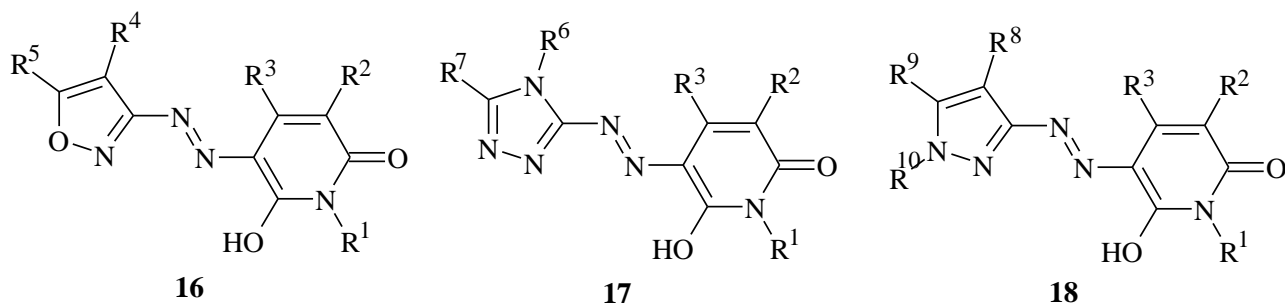


Figure 2.12. Azo pyridone dyes from 6-hydroxy-2-pyridone and isoxazole (**16**), 1,2,4-triazole (**17**) or pyrazole (**18**).

Also, Cr-complex azo dyes were obtained from *o,o'*-dihydroxyphenylazopyridone intermediates and ammonium chromium sulfate [59].

### ***Pigments***

Except dyes and their metal complexes, azo pyridone colorants can be prepared as pigments. So, by treatment of azo pyridone dye, obtained from 2-pyridones (e.g. 3-cyano-6-hydroxy-4-methyl-2-pyridone) with BaCl<sub>2</sub> yellow azo pigments were obtained and used in printing inks [60].

Thermally stable yellow pigments obtained by coupling diazotized 2,5-R<sup>1</sup>CO(R<sup>2</sup>CO)C<sub>6</sub>H<sub>3</sub>NH<sub>2</sub> (R<sup>1</sup>, R<sup>2</sup> = MeO, NH<sub>2</sub>) with 5-cyano-2-hydroxy-4-methyl-6-pyridone as an aqueous solution of Na or K salt or aqueous dispersion at pH 3-10 and 0-30 °C were dried at 105 °C and grounded. The pigments were stable up to 350 °C and resistant to organic solvents and suitable for plastics and baking varnishes [61].

### 2.1.1.2. Disazo dyes

#### *Disperse dyes*

5-(4-Arylazophenyl)azo-3-cyano-6-hydroxy-4-methyl-2-pyridones (Figure 2.13, X = H, Me, Cl, O<sub>2</sub>N; Y = H, Me, MeO, O<sub>2</sub>N; Z = H, MeO) were prepared (57-87% yield) by coupling the appropriate amino azo compound with 3-cyano-6-hydroxy-4-methyl-2-pyridone. When used on polyester yellow, orange, brown, and red shades with pick-up poor to excellent were obtained and light fastness was fair to excellent, and sublimation fastness was fair to very good [62].

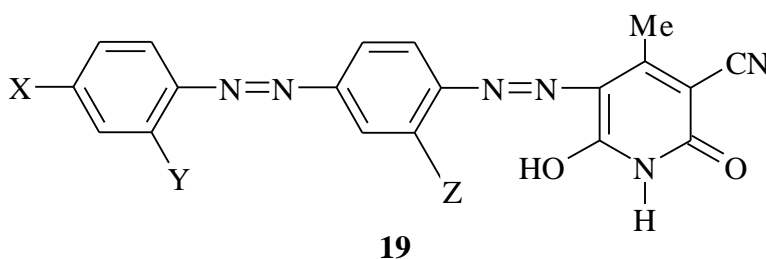


Figure 2.13. 5-(4-Arylazophenyl)azo-3-cyano-6-hydroxy-4-methyl-2-pyridones.

#### *Reactive dyes*

Disazo reactive dyes, which dyed cotton in yellow shades, containing hydroxyl pyridone and fluorotriazine groups were prepared. Thus, pyridone dye was obtained from 5-[(3-amino-6-sulfophenyl)azo]-1-ethyl-6-hydroxy-4-methyl-3-(sulfomethyl)-2-pyridone and *p*-phenylenediamine [63].

Reactive disazo pyridone dyes (Figure 2.14, R<sup>1</sup> = H, optionally substituted C<sub>1-4</sub>-alkyl; R<sup>2</sup> = H, optionally substituted C<sub>1-4</sub>-alkyl with substituents including fiber reactive groups; R<sup>3</sup>, R<sup>4</sup> = diazo component group optionally containing fiber-reactive group; X = SO<sub>3</sub>H, SO<sub>3</sub>Na, OH; Z = C<sub>2-4</sub>-alkylene, arylene, heterocyclic diradical) with improved solubility were obtained. In this preparations, e.g. a yellow disazo reactive dye was obtained by condensation of 2 mol 1-ethyl-6-hydroxy-2-pyridone with 1 mol glutaraldehyde-NaHSO<sub>3</sub> to provide a bis-pyridone coupling component which was then treated with 2 mol of diazotized 4-(2-sulfatoethylsulfonyl)aniline [64].

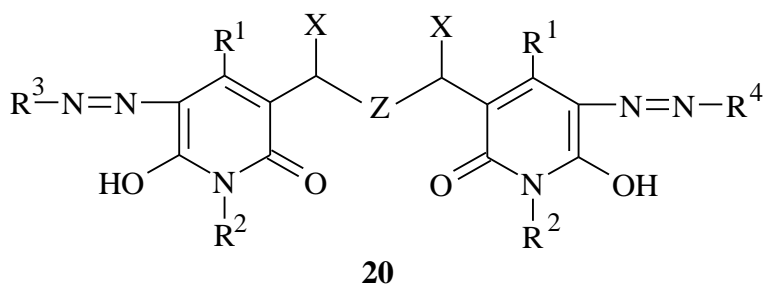


Figure 2.14. Reactive disazo pyridone dyes.

### *Disazo dyes for other uses*

Disazo dyes were prepared by tetrazotizing a dianiline and coupling it with a pyridone or by diazotizing aniline and coupling it with a dipyridone. Obtained colorants (Figure 2.15,  $R^1$  = alkylene, arylene, arylalkylene, alkylarylene, alkyleneoxy, aryleneoxy, arylalkyleneoxy, alkylaryleneoxy, polyalkyleneoxy, polyaryleneoxy, polyarylalkyleneoxy, polyalkyl-aryleneoxy, heterocyclic, silylene, siloxane, polysilylene, polysiloxane group;  $R^2, R^{2'}$  = alkyl, aryl, arylalkyl, alkylaryl, alkoxy, aryloxy, arylalkyloxy, alkylaryloxy, polyalkyleneoxy, polyaryleneoxy, polyarylalkyleneoxy, polyalkylaryleneoxy, heterocyclic, silyl, siloxane, polysilylene, polysiloxane group, etc.;  $R^3, R^{3'}$  = alkyl, aryl, arylalkyl, alkylaryl group;  $X, X'$  = direct bond, O, S, N-containing linking group, alkylidene group;  $Z, Z'$  = H, halogen, nitro, alkyl, aryl, arylalkyl, alkylaryl, etc.) can be used in phase change inks [65-67]. Diazopyridone colorants were also prepared by coupling substituted pyridone with a diazonium salt to form diazopyridone compounds [68].

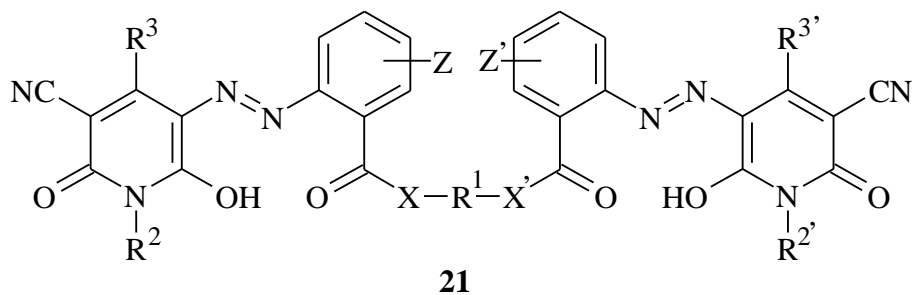


Figure 2.15. Disazo pyridone dyes used in phase change inks.

Another example of disazo dyes which are useful as colorants for phase change inks is given in Figure 2.16 ( $R^1, R^2 = \text{hydrocarbyl}$ ;  $R^3, R^6 = \text{H, halogen, nitro, org. group}$ ;  $R^4, R^5 = \text{organic group}$ ;  $X, X' = \text{direct bond, O, S, imino, optionally substituted methylene}$ ;  $Z = \text{unsaturated alkylene}$ ;  $m, n \text{ are integers}$ ). In this synthesis, bispyridone derivative was obtained first and then coupled with diazotized moiety [69,70].

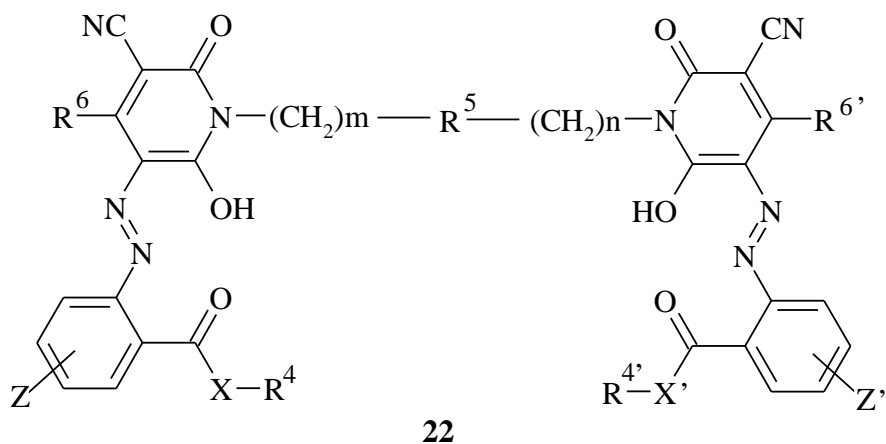


Figure 2.16. Disazo dyes obtained from bispyridone derivative.

Disazo yellow pyridone dyes given in Figure 2.17 ( $Y = \text{CN, CONH}_2, \text{CH}_2\text{SO}_3\text{H}$ ;  $R = \text{organic group}$ ) were described and used in the production of colored plastics or polymeric color particles. Dyes had good heat resistance, migration resistance, tinctorial strength, and fastness when used for bulk coloration [71].

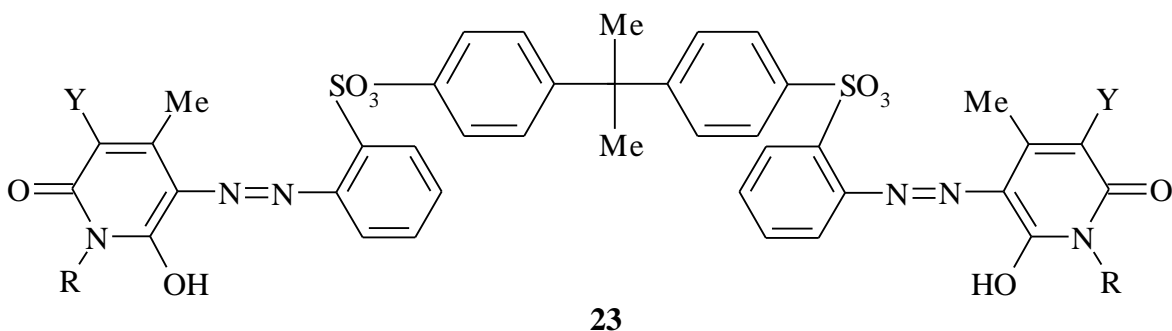


Figure 2.17. Disazo yellow pyridone dyes used in the production of colored plastics.

Dyes presented in Figure 2.18 ( $R = H$ , alkyl, alkenyl, cycloalkyl, aryl, or aromatic heterocyclyl;  $R^1 =$  alkyl, aryl, or aromatic heterocyclyl;  $R^2 = H$ , cyano, carbamoyl, carboxyl, ester, or acyl;  $Z =$  a divalent linking from an aromatic or heterocyclic moiety) were used as electrophotographic photoconductors having a high photosensitivity and excellent characteristics in repeated use [72].

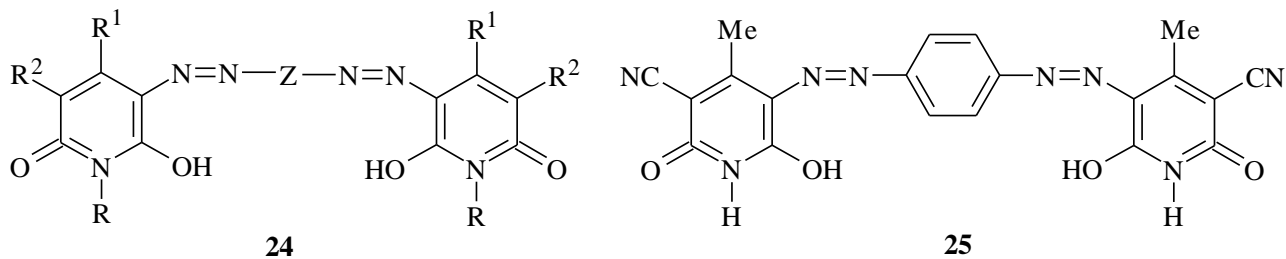


Figure 2.18. Disazo dyes from substituted 6-hydroxy-2-pyridones (**24**) and 4-methyl-3-cyano-6-hydroxy-2-pyridones (**25**) which are used as electrophotographic photoconductors.

Some new disazo dyes were synthesized by diazotization of 5-amino-3-methyl-4-hetarylazo-1H-pyrazoles and 5-amino-3-methyl-4-hetarylazo-1-phenylpyrazoles and coupling with 3-cyano-6-hydroxy-4-methyl-2-pyridone and 3-methyl-1H-pyrazole-5-one [73].

### 2.1.1.3. Trisazo dyes

Except mono and disazo pyridone dyes, trisazo pyridone dyes were prepared. So, pyridone dyes shown in Figure 2.19 (in a free acid form; R = H, C<sub>1-6</sub>-alkyl; X = H, aminocarbonyl, sulfomethyl, sulfo; Y = H, Me, Et, CF<sub>3</sub>, Cl, NO<sub>2</sub>; m = 0-2) were obtained and used to dye nylon 6 [74].

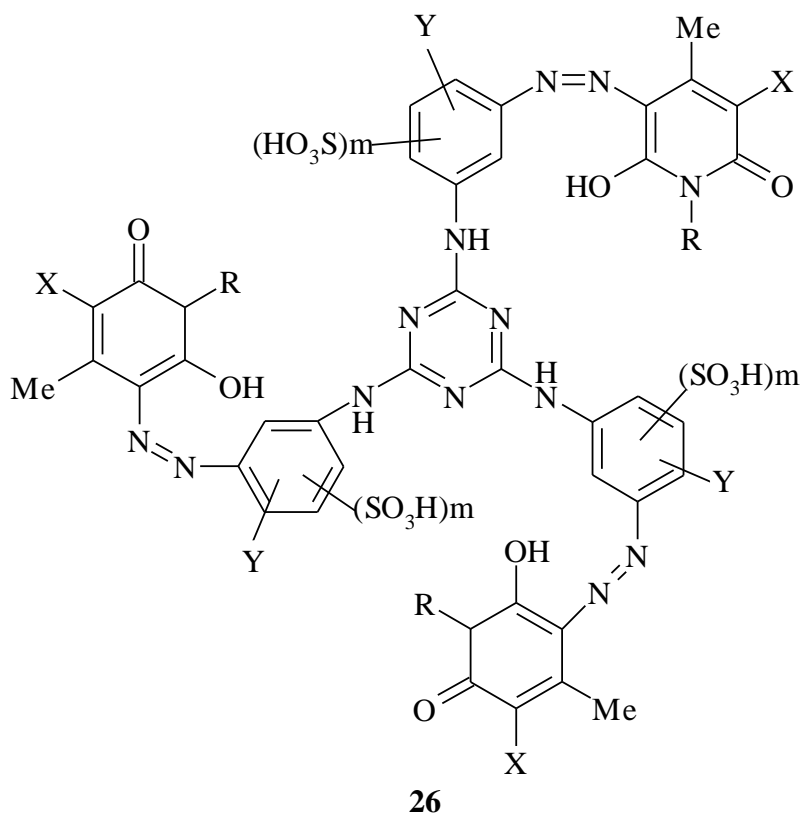


Figure 2.19. Trisazo pyridone dyes used to dye nylon 6.

In another example of trisazo colorants, compounds having 3 azopyridone moieties (Figure 2.20) bonded to a central atom, a monomeric group of atoms, an oligomer, or a polymer were produced for use as yellow dyes for hot-melt inks. Typically, a dye was manufactured by reaction of dodecylamine with ethyl cyanoacetate, cyclization of the intermediate with ethyl acetoacetate, and reaction of the resulting pyridone derivative with dipentaerythritol hexaanthranilate [75].

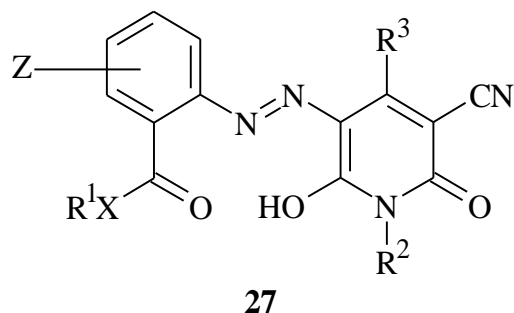


Figure 2.20. Azopyridone moieties used for the synthesis of trisazo colorants.

### 2.1.2. Properties of azo pyridone dyes

Pyridone azo dyes generally produce yellow shades on fabrics but other shades were also reported [12-20,25-27,29]. Dye structural effects on the intensity of color (yellow, green, and orange) and fastness properties on nylon 66 and polyester knits were also discussed [76].

Many authors have reported the fastness properties [31,35,36,46,62,71] of azo pyridone dyes and some have studied the photofading kinetics of 3-(*p*- and *o*-substituted arylazo)-5-cyano-2-hydroxy-4-methyl-6-pyridone dyes in amide solvents (DMF, HCONH<sub>2</sub>, and AcNMe<sub>2</sub>) and n-hexane. It was established that a fair linear correlation existed between the observed rate constant and the free energies of transfer, suggesting the possibility that the photofading rate increased with increasing solvation of dyes. The rate was increased by the presence of two electron-withdrawing substituents (NO<sub>2</sub> and Cl) on the benzene ring [77]. The same authors have also studied photostability of 3-(mono- and di-substituted arylazo)-5-cyano-2-hydroxy-4-methyl-6-pyridones in *N,N*-dimethylformamide. Photodegradation was observed when dyes were irradiated by 254 nm light. It was established that the primary photochemical reaction with pyridone azo dyes involved hydrogen abstraction from the amide solvent. Also, it was found out that the simultaneous presence of two electron-withdrawing substituents in diazo component of dyes caused a bathochromic effect and an increase of fading rate, while introduction of an alkylol group to coupling component resulted in hypsochromic shifts and in decrease of fading rate [78]. Besides direct photodegradation, photocatalytic degradation of 5-(4-sulpho phenylazo)-3-cyano-6-hydroxy-4-methyl-2-pyridone in the presence of commercial TiO<sub>2</sub>, in aqueous solutions by simulated sunlight was studied [79].

In another work, yellow disperse azo dye was synthesized from 2,6-dichloro-4-nitroaniline and 3-cyano-6-hydroxy-1,4-dimethyl-2-pyridone and its dyeing, fastness, and photodegradation behavior on polyester fabric was investigated. It was found that the build-up and lightfastness of dye derived from pyridone was not good [80]. Introduction of various substituents can have different impact on dye properties. So when in dyes presented in Figure 2.21 ( $R^1 = \text{H, Me, C}_3\text{H}_7, \text{C}_4\text{H}_9, \text{C}_6\text{H}_{13}, \text{C}_8\text{H}_{17}, \text{Ph}$ ;  $R^2 = \text{Me, CF}_3$ ;  $R^3 = \text{CF}_3, \text{C}_4\text{F}_9, \text{C}_6\text{F}_{13}, \text{C}_8\text{F}_{17}$ ) a long perfluoroalkyl group was introduced a lowered film-forming ability and sensitivity but good photostability was achieved [81]. When 5-(2-benzothiazolylazo)-3-cyano-1-ethyl-6-hydroxy-4-methyl-2-pyridone was compared to other unsymmetrical and symmetrical bis(hetaryl)azo dyes it was found that only pyridone derivative showed remarkable difference of decomposition temperature [82].

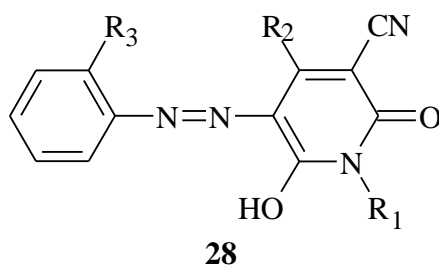


Figure 2.21. Azo pyridone dyes with good photostability.

### 2.1.3. Azo – hydrozone tautomerism of azo pyridone dyes

A number of studies can be found in literature in which series of pyridones were coupled with diazotized substituted anilines and than substituent and/or solvents effects were discussed. So dyes derived from 3-cyano-6-hydroxy-4-methyl-2-pyridone [83,84], 3-amino-5-cyano-1-ethyl-6-hydroxy-4-methyl-2-pyridone [85], 4-amino-6-hydroxy-2-pyridones, 4,6-diamino-2-pyridone-3-carbonitrile and 2,4-diamino-6-pyridone-3-carbonitrile [86], 5-(2-pyrido-5-yl)azo-thiophene derivatives [87], 4-(*p*-substituted) phenyl-2-(2-pyrido-5-yl)azo-thiazole derivatives [88], 5-(arylozo)-3-cyano-4-methyl-6-methyl/phenyl-2-pyridinones [76] and 1-butyl-3-cyano-6-hydroxy-4-methyl-2-pyridone [89] were studied among others. In these studies, often azo-hydrozone tautomerism was investigated. Thus, three series of dyes were prepared by coupling diazonium salts to 2-(ethylthio)- and 2-(butylthio)-4,6-diaminopyrimidine as well as to 3-cyano-6-hydroxy-

1,4-dimethyl-2-pyridone. IR spectra and visible absorption spectroscopy indicated that the arylazopyrimidines existed in the azo tautomeric form, while the pyridone dyes existed as hydrazones [90]. Also, absorption spectra of ten 5-(4-substituted arylazo)-3-cyano-6-hydroxy-4-methyl-2-pyridones have been recorded in fifteen solvents in the range 200-600 nm. Besides the effects of the substituents on the absorption spectra and the effects of solvent polarity and solvent/solute hydrogen bonding interactions, azo-hydrazone tautomerism (Figure 2.22, X = OH, OCH<sub>3</sub>, CH<sub>3</sub>, C<sub>2</sub>H<sub>5</sub>, H, Cl, Br, I, COOH, NO<sub>2</sub>) was studied and it was concluded that equilibrium depends on the substituents as well as the solvents [91]. In addition, twelve pyridone-based disperse dyes were synthesized from a variety of substituted pyridones and 3-amino-5-nitrobenzothiazole, 2-amino-6-nitrobenzothiazole and 2-chloro-4-nitroaniline. Here azo-quinohydrazone isomerism was discussed [92].

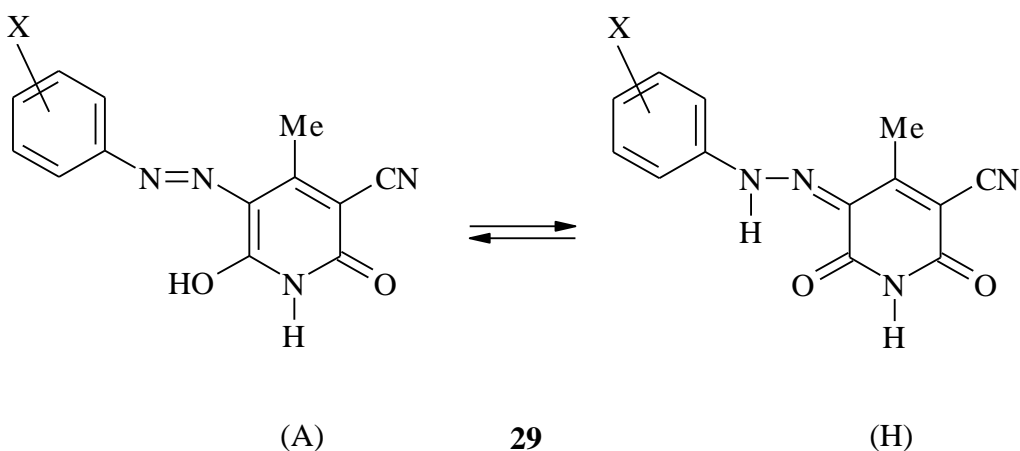


Figure 2.22. Azo (A) - hydrazone (H) tautomerism.

Azo-hydrazone tautomerism was also studied by crystallography. So 2-(2-methoxyethoxy)ethyl 4-[(5-cyano-1-ethyl-4-methyl-2,6-dioxo-1,2,3,6-tetrahydropyridin-3-ylidene)hydrazino]benzoate crystallizes in the hydrazone form [93]. The same conclusion was obtained for C.I. Disperse Yellow 114 (5-cyano-2-hydroxy-1,4-dimethyl-6-pyridone component) [94]. C.I. Disperse Yellow 119 and D.I. Disperse Yellow 211 (pyridine-1-ethyl-3-cyano-4-methyl-2,6-dione backbone) (Figure 2.23) also crystallize in the hydrazone form [95].

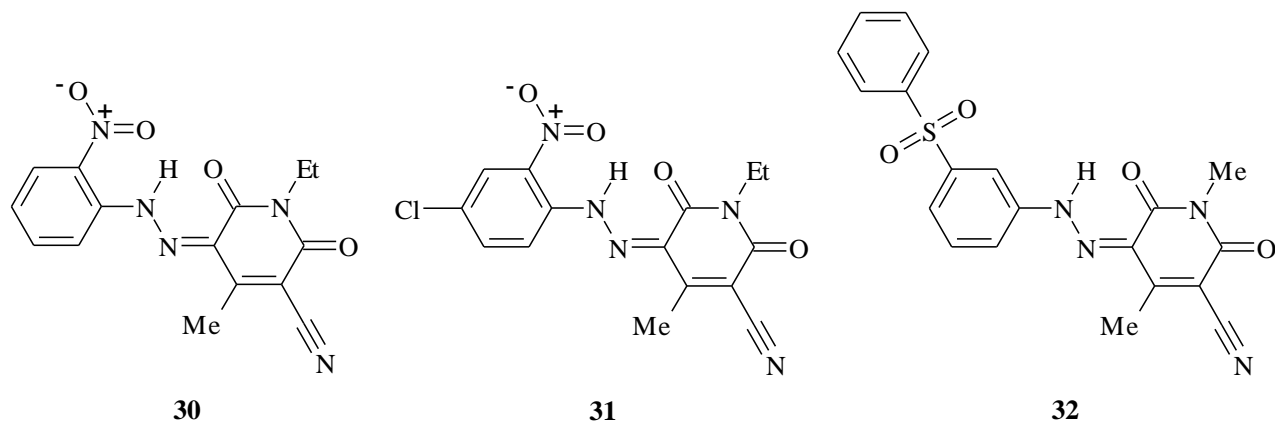


Figure 2.23. Structure of C.I. Disperse Yellow 119 (**30**), D.I. Disperse Yellow 211 (**31**) and C.I. Disperse Yellow 114 (**32**).

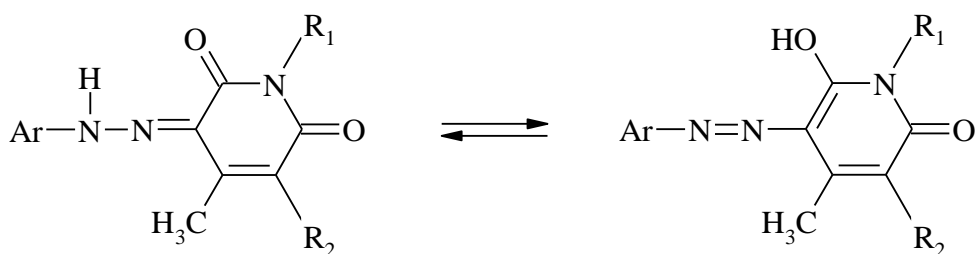
5-(3- and 4-Substituted arylazo)-3-cyano-4,6-dimethyl-2-pyridones and 3-cyano-4,6-diphenyl-5-(3- and 4-substituted phenylazo)-2-pyridones were prepared and their absorption spectra were recorded in different protic and aprotic solvents in the range 200–600 nm. The 2-pyridone/2-hydroxypyridine tautomeric equilibration was studied and it was found that it depends on the substituents as well as on the solvents [9,96,97]. 5-(3- and 4-substituted arylazo)-3-cyano-4,6-dimethyl-2-pyridones were also studied by RP C18 TLC in order to determine parameters such as lipophilicity which is important for dye application on fibers [98].

On the basis of above results, it may be concluded that the azo colourants containing hydroxyl and amino substituents *ortho* or *para* to the azo groups can in principle exist as mixture of azo and hydrazone tautomers. While azo – hydrazone tautomerism is quite interesting from a theoretical view point, it is also important from a practical stand point because the two tautomers have different technical properties and dyeing performances [99].

This phenomenon, called tautomerism involves the removal of a hydrogen from one part of the molecule, and the addition of a hydrogen to a different part of the molecule (Scheme 2.4). Tautomeric forms can be identified from their characteristic spectra. Ketohydrozones are normally bathochromic compared to their counter part hydroxyazo forms. Ketohydrozones also have higher molar extinction coefficient. However, not all azo dyes show tautomerism, and some tautomeric forms are more stable than others.

Since the work published by Zincke and Bindewald [100] the azo-hydrazone tautomerism has been investigated by numerous workers with a view to: (i) prove the existence of an equilibrium, if any (almost all) the available spectroscopic methods have been used; (ii) investigate the influence of factors such as: substituent, solvent, temperature; (iii) to gain an understanding of the (non) existence of such a thermodynamic equilibrium.

The intention of this part of theoretical study of azo-hydrazone tautomerism is to focus mainly in recent publications dealing with new aspect of tautomerism of pyridone arylazo derivatives, using  $^1\text{H}$  NMR,  $^{13}\text{C}$  NMR and UV-Vis spectroscopic methods and using quantum chemical *ab initio* methods.



Scheme 2.4. The equilibrium between hydrazone form and azo form

### 2.1.3.1. UV-Vis spectroscopic study of tautomerism

The use of UV-Vis spectroscopy for study of the tautomeric equilibrium between azo and hydrazone forms requires a knowledge of the molar extinction coefficient ( $\epsilon_{\text{max}}$ ) of the individual forms and the values of  $\lambda_{\text{max}}$ . Visible absorption spectral data of the azo dye **33** (Figure 2.24) is shown in the Table 2.1. and Figure 2.25 [85]. The visible spectra of the dye **33** were found to exhibit a strong solvent dependence.

Table 2.1. Absorption spectral data for the dye **33** ( $\lambda_{\text{max}}/\text{nm}$ ;  $\epsilon_{\text{max}}/10^4 \text{M}^{-1}\text{cm}^{-1}$ )

	Solvent				
	Ethanol	Acetone	Chloroform	DMF	DMSO
$\lambda_{\text{max}}$	488	486	482	535/492	535
$\epsilon_{\text{max}}$	2.55	3.75	2.29	1.49/1.53	0.83

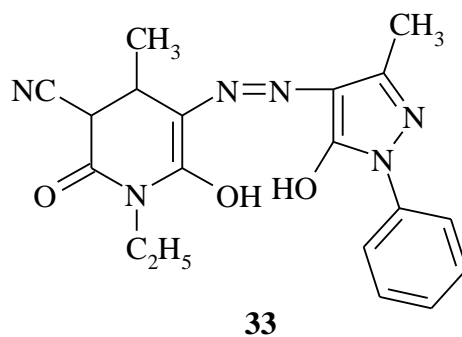


Figure 2.24. The chemical structure of the azo dye synthesized from 1-ethyl-3-cyano-6-hydroxy-4-methyl-5-amino-2-pyridone.

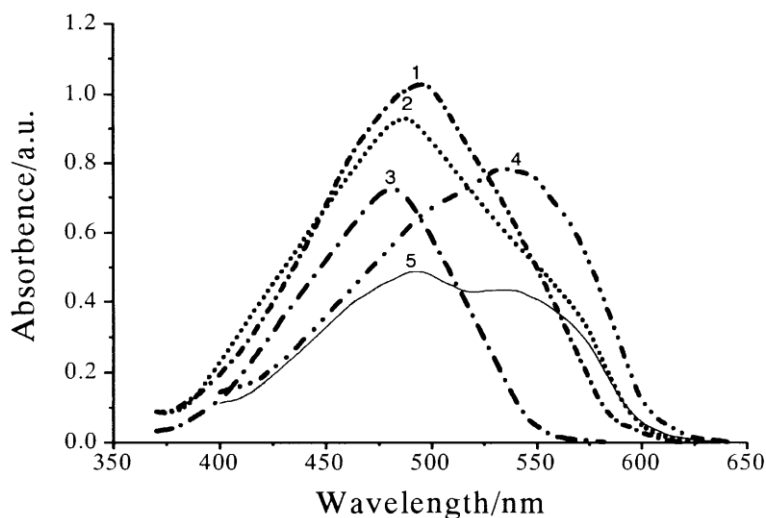


Figure 2.25. Absorption spectra of dye **33** in different solvents: (1. Acetone, 2. Ethanol, 3. Chloroform, 4. DMSO, 5. DMF).

It was observed that although in ethanol, acetone and chloroform the absorption spectra of the dye **33** does not change significantly,  $\lambda_{\max}$  of the dye shifted considerably in DMF and DMSO (Table 2.1.). The absorption spectra of dye **33** at different volume ratios of the mixture solvents of chloroform/DMSO are shown in Figure 2.26. From it one can see that there is an isobestic point in it, and with the increase of the volume content of DMSO, the absorption of the azo form increase, while that of the hydrazone form decreases.

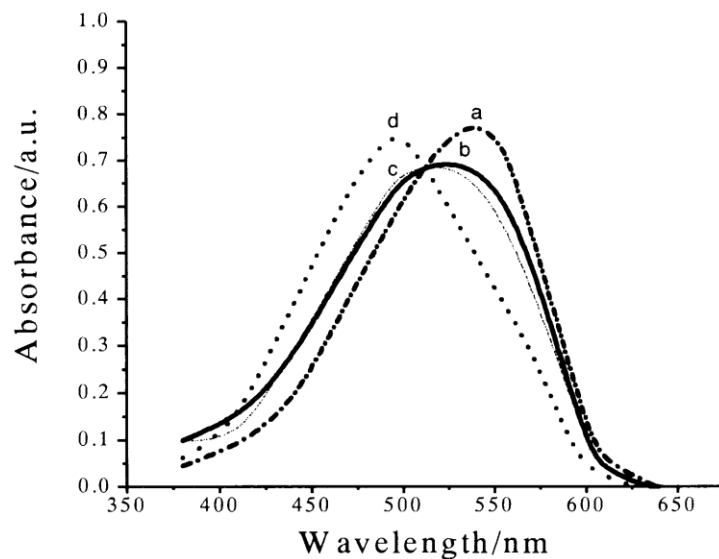


Figure 2.26. Absorption of dye **33** in different volume ratios (a.  $\frac{1}{4}$ ; b.  $\frac{3}{2}$ ; c.  $\frac{7}{3}$ ; d.  $\frac{4}{1}$ ) of chloroform/DMSO.

### 2.1.3.2. NMR Spectroscopic study of tautomerism

Q. Peng et al. [101] studied  $^1\text{H}$  NMR and  $^{13}\text{C}$  NMR spectra of 21 pyridone azo dyes in deuterated chloroform and deuterated dimethyl sulfoxide. It is shown that there is hydrazone – azo tautomerism in these dyes (Figure 2.27.).

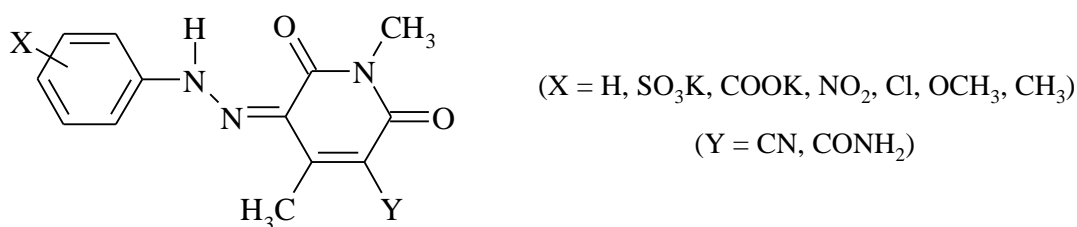


Figure 2.27. The chemical structures of the azo pyridone dyes investigated by Q. Peng et al. [101].

The chemical shifts of the imino group for investigated dyes (Figure 2.28.) are within the range 14.3 – 16.1 ppm. The colour change of the solutions was obvious when 20  $\mu\text{l}$  of an organic base (piperidine) was added to 0.5 ml of sample solutions (1:25,v/v). The peak for the imino group at lower field disappeared and moved to higher field ( $\delta$  3.6 – 8.0) and overlapped with the NH proton peak of piperidine in both  $\text{CDCl}_3$  and  $\text{DMSO-}d_6$ . A small amount of anhydrous sodium carbonate had the same effect on the

tautomerism as piperidine in DMSO- $d_6$ . This phenomenon suggests that perhaps the H atom of the imino group should transfer to a hydroxyl group.

The  $^{13}\text{C}$  NMR spectra were determined under the same conditions of concentration and temperatures as those used for the  $^1\text{H}$  NMR spectra. The chemical shifts of corresponding carbon atoms were nearly the same when the samples were measured in  $\text{CDCl}_3$  and DMSO- $d_6$ . Dye with substituent 4'-SO $_3\text{K}$  (Figure 2.27.) may be used as an example, as shown in Figure 2.28. When the sample is in DMSO- $d_6$  (0.4 M), the chemical shifts of the carbon atoms on the pyridone ring are similar to those reported by Cee et al. [102] and from the  $^1\text{H}$  NMR spectra, the dye exists in the hydrazone form (Figure 2.28.A). After adding piperidine, the spectrum transfers to B. If  $\text{Na}_2\text{CO}_3$  is added to the solution, the spectrum would transfer to C. According to the above discussion, the tautomer would be azo form in C.

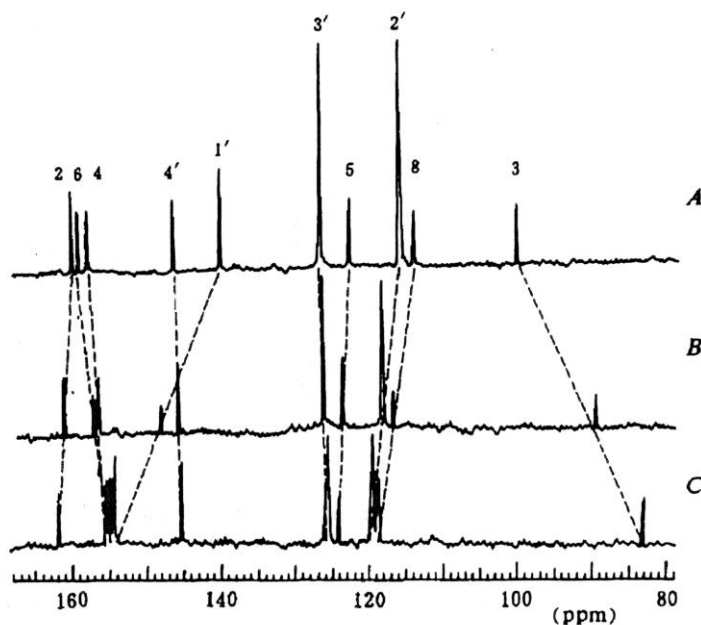
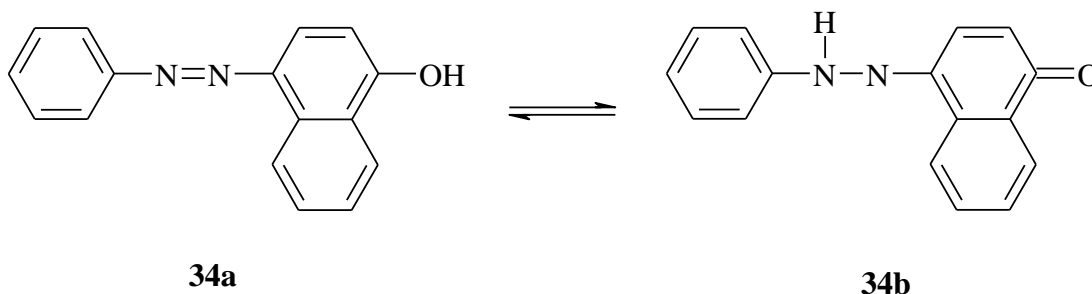


Figure 2.28. The  $^{13}\text{C}$  NMR spectra of azo pyridone dyes (Figure 2.27, substituent 4'-SO $_3\text{K}$ ) (at 90 °C). (A) in DMSO- $d_6$ ; (B) 20ml piperidine was added to (A); (C)  $\text{Na}_2\text{CO}_3$  was added to (A).

### 2.1.3.3. Analysis of solvent influence on the azo – hydrazone tautomerism using *ab initio* quantum chemical calculations

Since 92% of mono-azo dyes published in the Colour Index [103] are potentially tautomeric characters, and their spectral behaviour in solution (determined by the tautomeric ratio) is very relevant to industrial applications, the investigations over the solvent effect on the tautomeric equilibrium position are of present interest as in theoretical as well as in practical aspect. Modeling of the solvent effect on the azo – hydrazone tautomerism by using quantum – chemical method is valuable, because it could shed light on the root of the phenomenon.

L. Antonov et al. [104] reported results of the modeling of the solvent effect on the azo – hydrazone tautomeric equilibrium of 1-phenylazo-4-naftol (34a) (Scheme 2.5) by using *ab initio* quantum - chemical calculations.



Scheme 2.5. The equilibrium between azo (**34a**) and hydrazone (**34b**) tautomeric forms of 1-phenylazo-4-naftol

Quantum – chemical calculations have usually been carried out in the gas phase, but while gas phase predictions are suitable for many purposes, they are inadequate for describing the azo – hydrazone tautomeric equilibrium in solution, because the properties of the tautomers differ considerably between the gas phase and solution. Dye – solvent interactions were first modeled using the Gaussian '94 Onsager reaction field model [105] where the solvent is viewed as a continuous medium of uniform dielectric constant  $\epsilon$  and the solvent – solute interaction is the only dipole. The results from such modeling are presented in Table 2.2. As can be seen from Table 2.2 there is no correlation between the relative energies (hydrazone – azo gap) and the tautomeric constants in different

solvents, and these calculational results confirm the experimental fact that the interactions between tautomer and solvent are specific.

Table 2.2. Values of the energies of the H (hydrazo) and A (azo) forms (HF/6-31G level) in different solvents calculated according to the Onsager model [105]

Solvent	$\epsilon$	$E_{\text{RHF}}$	$E_{\text{RHF}}$	H-A	KT
		H (a.u.)	A (a.u.)	gap (kcal/mol)	
Gas phase		-796.630	-796.632	1.531	-
i-Octane	1.96	-796.630	-796.632	1.317	0.116
CH <sub>2</sub> Cl <sub>2</sub>	9.08	-796.631	-796.632	0.947	1.570
CH <sub>3</sub> OH	32.63	-796.631	-796.632	0.834	0.254
Water	80.37	-796.631	-796.632	0.803	1.934

The results of Antonov et al. [104] show that in methanol, methylene chloride and water there exists a strong hydrogen bonding between the particular tautomer and solvents, as well as dipole – dipole dye – solvent interactions. The results show that the hydrazo form is more stable in water and methylene chloride, while methanol and i-octan stabilize the azo form.

In this thesis DFT calculation was performed for different azo – hydrazone tautomers of 5-phenylazo-4-phenyl-6-hydroxy-3-cyano-2-pyridone dye (**A1**). The structure was preliminary optimized by semi – empirical PM3 method and the most stable geometries in vacuum were reoptimized at B3LYP/6-31G(d) level of theory [106,107]. The Gaussian 03 program package was used [108]. The results show that hydrazone tautomeric form (**B**) (Figure 2.29) of this azo pyridone dye is dominant.

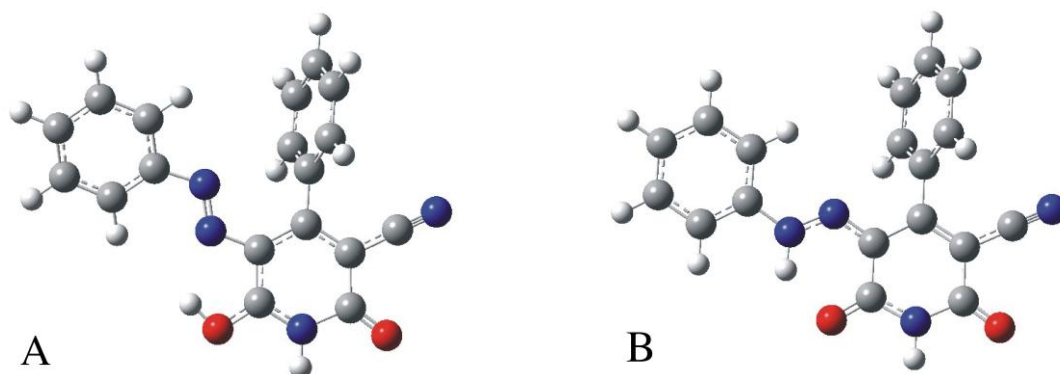


Figure 2.29. The most stable azo (**A**) and hydrazone (**B**) tautomer optimized structures of dye **A1**, at B3LYP/6-31G(d) level of theory.

## 2.2. Correlation analysis in organic chemistry

### 2.2.1. Substitution effects and linear free energy relationships

Two types of experiments for the study of reaction mechanisms are usually applied. First is an analysis of kinetics, which can tell us which molecules are involved in a mechanism prior to and/or during the rate-determining step. Kinetic results can be used to exclude mechanisms that are found experimentally not to conform to the predicted rate law. However, the kinetic results do not tell us the nature of any intermediates, nor do they indicate which bonds have been broken or formed during the reaction. To get this kind of information, we need to turn to second tools of physical organic chemistry, such as linear free energy relationships; this latter experiment gives us some limited structural information about the activated complex.

More indepth analysis of the structural of the transition state is obtained from studies of substituent effects. A substituent is any group on a molecule, such as a methyl, nitro, hydroxy, etc. A substituent effect is the manner in which the reactivity of the molecule changes when substituents are changed.

The studies of substituent effects represent a key pillar of physical organic chemistry. When they are carefully applied, substituent effects are used to determine how the free energies of reaction and activation vary as a function of chemical structure.

In the context of pharmaceutical studies, where activity, bioavailability, and other medically related data are collected as a function of the chemical structure of the drug, the substituent effect studies are referred to as structure-activity relationships (SAR). Most important for physical organic chemistry, the nature of the structure-reactivity relationship is often informative about the mechanism of the reaction.

The logic of conventional structure-function relationship should be familiar.

Experiment can be designed to test for changes in charges along a reaction coordinate by interchanging functional group, such as switching an electron donating group to an electron withdrawing group. If a positive charge is being created in a rate-determining step, then adjacent electron donating groups should stabilize the transition state and the reaction should speed up. Conversely, adjacent electron withdrawing groups should destabilize the transition state and therefore retard the reaction. Similar effects can be observed for equilibria. As we will see later, there are linear relationship (called linear free energy relationship or LFER) between the free energy of activation or reaction free energy change induced by a substituent and parameter that describes the electron donating or electron withdrawing characteristics of the substituent.

Changing substituent in the reactants or solvent should also influence the steric congestion, solvation, leaving group ability, nucleophilicity, acidity or basicity and a variety of other chemical attributes.

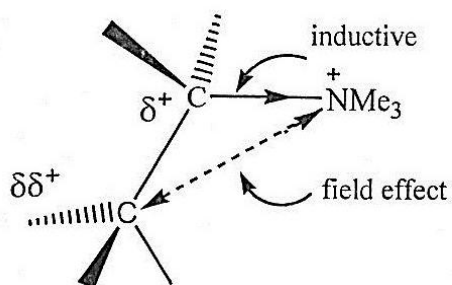
### **The origin of substituent effects [109]**

There are two different aspects of bonding valence bond theory (VBT) and molecular orbital theory (MOT). In MO theory orbitals that are spread out over all atoms in a molecule. When adding or changing substituents, new molecule orbitals are created that involve the atomic orbitals on the substituents. Although this theory can be used successfully to analyze substituent effects, the concept of delocalized molecule orbitals presents difficulties in visualizing localized changes in a molecule brought about by a substituent change.

## Inductive effects

An inductive effect (I), results from the ability of an atom or group of atom to withdraw or donate electrons through  $\sigma$  bonds [109]. + I means electron donating, - I electron withdrawing inductive effects [110,111].

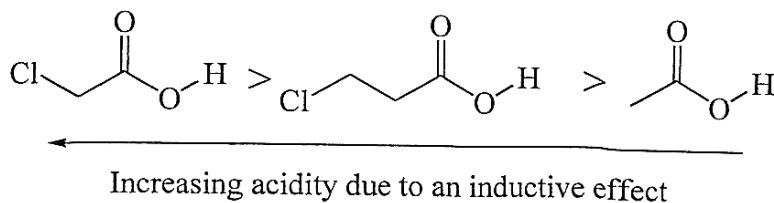
Perturbation evident from substituent constant results in the effect at *meta* position greater than that at *para*. This is clearly observable in substituent such as  $-N^+Me_3$  in Scheme 2.6.



Scheme 2.6. Inductive effect of  $-N^+Me_3$  substituent

The basis of this electronic displacement is probably complex but originates in part from difference in electronegativity which cause polarization of both  $\sigma$  – and  $\pi$  bonds and also from electrostatic effects experienced at the reaction center due to the changes and dipoles resident on the substituent. Two mechanisms for inductive polarization may be considered. The classical inductive effect is a polarization through bonds, both of  $\sigma$  and  $\pi$  types, becoming progressively attenuated. The other, known as a field effect, is propagated through space and depends more for its intensity on proximity than on the number of bonds separating source and receptor. In practice it is difficult to separate the two, which may both components of the I effect [110].

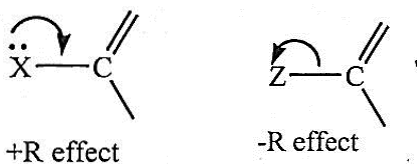
Strongly electronegative atoms or groups are best at drawing electrons to themselves. Conversely, a group can donate electrons *via* the  $\sigma$  bond framework [112]. The further away the group from the site of reaction, the lower its ability to effect the reaction *via* induction. For example, chloroacetic acid is substantially more acidic than acetic acid.



However, the increase in acidity induced by the electronegativity chlorine diminishes the further away from the carboxyl group.

### Resonance effect

A resonance effect reflects the ability of an atom or group of atoms to withdraw or donate electron through  $\pi$  bonds. This is also sometimes referred to as mesomeric effect in older literature [109]. Resonance effect is denoted R. Many substituents give rise to a perturbation that is greater when they are located *para* than when they are *meta*; this suggests the transmission mechanism is of a conjugative nature in which charge is relayed to alternate atoms. This effect is described as a '+R effect' if it results in donation of electrons from substituent to reaction center and as a '-R effect' if a withdrawal of electrons results [112].



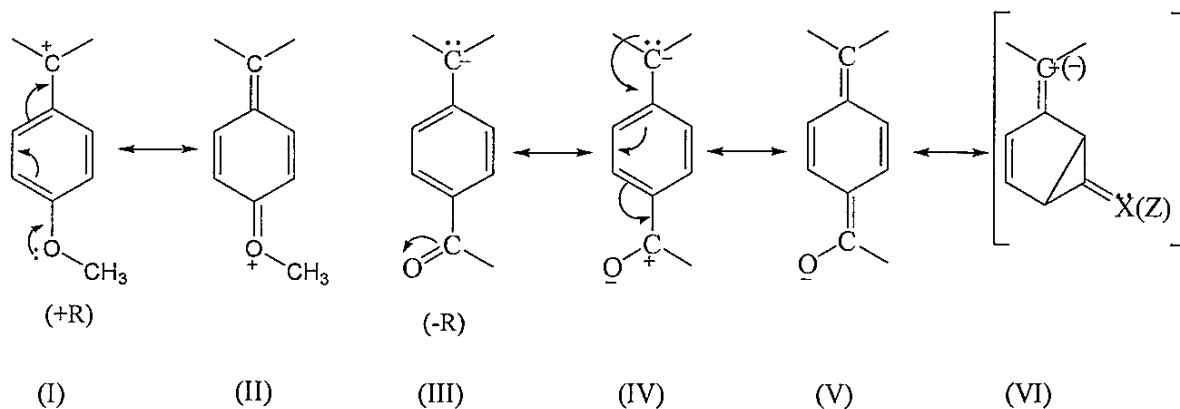
In order to exercise a resonance effect, a substituent must possess a p- or  $\pi$ -orbital which is available to conjugate with the  $\pi$ -MOs of the system. Two situations are important.

- a) X – is a donor group and typically possesses an unshared electron pair or  $\pi$ -electrons on an atom directly attached to the ring.

Examples are:



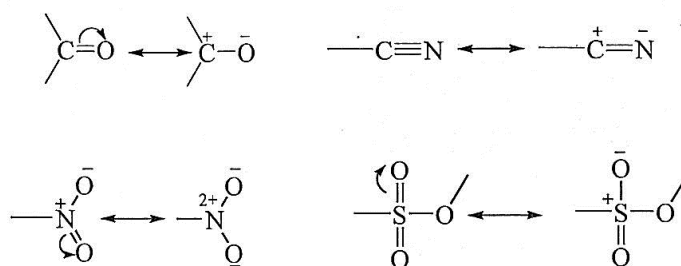
These groups are all capable of exerting a + R effect which stabilizes an acceptor centre. The extreme situation is depicted by the structures (I, II) in Scheme 2.7.



Scheme 2.7. Resonance effect

Little interaction between donor and acceptor centres will occur if they are located *meta* since quinoid resonance structure analogous to Scheme 2.7 (II, V) cannot be drawn and analogous structure (VI) in Scheme 2.7 is therefore of high energy and less important.

b) Substituent Z have a  $\pi$ -acceptor centre adjacent to the ring, since no commonly encountered substituents possess vacant bonding p-orbitals, this means in practice groups which can act as electron acceptors by simultaneously releasing  $\pi$  electrons to adjacent hetero atoms and whose contributing structures have a positively charged atom attached to the ring in Scheme 2.7 (III, V). Common examples are:



All such groups tend to accept electronic charge and stabilize donor centers (e.g. carbon bring some degree of carbanion character adjacent to the ring), illustrated by contributing structure (V) in Scheme 2.7. Again the stronger  $-R$  interaction occur when substituent and reaction center and located *ortho* or *para* (Scheme 2.7, V). It may be observed that there is no fundamental difference between these two situation; there is in each case a transfer of charge between two centers by conjugation and the differentiation

into +R and -R effects merely depends upon which part is designated as a substituent and which as the reaction centre .

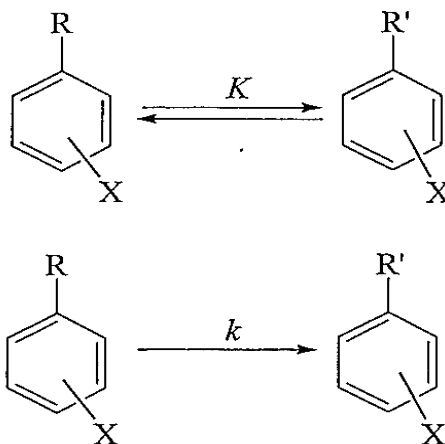
### Steric effect

Steric effects can also have a dramatic influence on the rate of a reaction, as well as conformation. Large atom or groups influence the manner in which molecules collide, often deflecting the reactants away from the angle or depth of collision necessary for the reaction to occur. For example, the  $S_N2$  reaction becomes slower due to steric effects as the carbon with the leaving group is more highly substituted with alkyl groups. The nucleophile cannot penetrate to the carbon with the leaving group when larger groups are attached [109].

### 2.2.2. The Hammett equation and its extension

The most important and the most widely applied structure reactivity relationship is due to L.P. Hammett which relates rates and the equilibria for many reactions of compounds containing substituted phenyl groups [113].

He dealt with systems of type:



R is a reaction site in the side chain attached to a benzene ring and X is a *meta* or *para* substituent. Hammett excluded *ortho* substituents on grounds that there would be specific steric interaction between reaction site and substituent which would not be amenable to a regular quantitative treatment. Aliphatic compounds are also not correlated with Hammett relationship [113,114].

In the early 1930s, Hammett [115,116] and Burkhard [117], discovered linear relationships involving  $\log k$  or  $\log K$  for a number of systems. This work led to the formulation of the Hammett equation, which describes the influence of polar *meta*- or *para* substituents on the side-chain reactions of benzene derivatives [118]. This relationship has become known as the Hammett equation, and is widely applied in the form:

$$\log (k/k_0) = \rho \sigma \quad (2.1)$$

$$\log (K/K_0) = \rho \sigma \quad (2.2)$$

Here  $k$  or  $K$  is the rate or equilibrium constant respectively, for a side-chain reaction of a *meta*- or *para*- substituted benzene derivative, and  $k_0$  or  $K_0$  are the rate or equilibrium constants respectively, for unsubstituted "parent" compound.  $\sigma$  is the substituent constant, which depends solely on the nature and position of the substituent X, and  $\rho$  is the reaction constant, which depends on the reaction conditions, such as the reaction medium and temperature, under which it takes place, and also on the nature of the side chain R.

The ionization of benzoic acids in water at 25 °C was chosen as the reference system with  $\rho$  equal to 1.00. This resulted in electron withdrawing substituent constants being positive and electron-releasing substituent constants being negative. The validity of equations 2.1 and 2.2 is restricted to substituents in the *meta*- and *para*- positions of the benzene ring [119,120].

The relationship may be exemplified by the rates of hydrolysis of substituted ethyl benzoates. The correlation is illustrated graphically in Figure 2.30, which shows  $\log k/k_0$ .

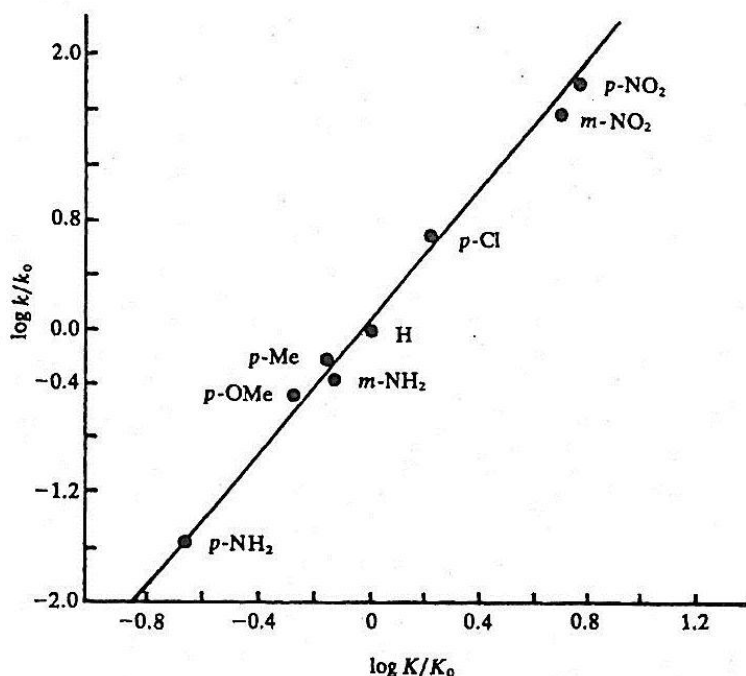


Figure 2.30. Hammett plot for the hydrolysis of ethyl benzoates.

where  $k_0$  is the rate constant for hydrolysis of ethyl benzoate and  $k$  is the rate constant for the substituted esters, plotted against  $\log K/K_0$  where  $K$  and  $K_0$  are the corresponding acid dissociation constants.

The Hammett equation is an example of linear free energy relationship. Equilibrium constants and rate constants are related to free energy relationship to free energy differences by the equation [113,121]:

$$\log K = -\Delta G^\ominus/2.3RT \quad (2.3)$$

Where  $\Delta G^\ominus$  is the standard free energy change of reaction. For chemical rate processes:

$$\log k = \log(k_B T/h) - \Delta G^\ddagger/2.3 RT \quad (2.4)$$

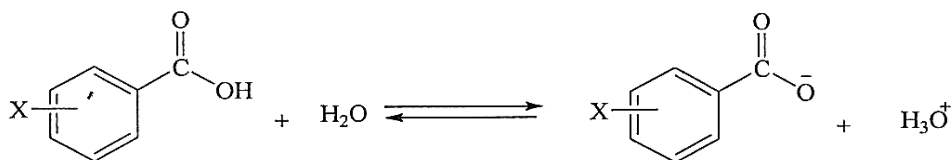
Where  $\Delta G^\ddagger$  is the standard free energy of activation ( $T$  is the Kelvin scale temperature;  $R$  is the gas constant,  $k_B$  is the Boltzmann constant, and  $h$  is the Plank constant).

$$\log (k/k_0) = \log k - \log k_0 = \Delta\Delta G/2.3RT = \rho \sigma \quad (2.5)$$

where the expression  $\Delta\Delta G$  is the second difference: the difference between  $\Delta G$  values for the substituted and unsubstituted reaction.

### Substituent constant ( $\sigma$ )

To show how reaction mechanisms vary as a function of the electronic changes induced by substituents, chemists use Hammett plots. Hammett defined a scale that measured the ability of substituents to influence the acidity of benzoic acid. The substituents are placed *meta* or *para* to the carboxylic group to eliminate any possible steric effects associated with an *ortho* substituent, and therefore only, field polarizability, inductive and resonance effects should be operative [109].



Equations 2.1 and 2.2 were used to define a substituent parameter  $\sigma_x$  for each substituent X. Hydrogen is the reference substituent. Thus, all acidity equilibrium constants for the substituted benzoic acids are compared to the equilibrium constant for benzoic acid itself ( $\sigma_{\text{H}} = 0$  by definition). Table 2.3 gives a number of  $\sigma$  value:

Table 2.3.  $\sigma$  Values for Several Commonly Encountered Substituents [122].

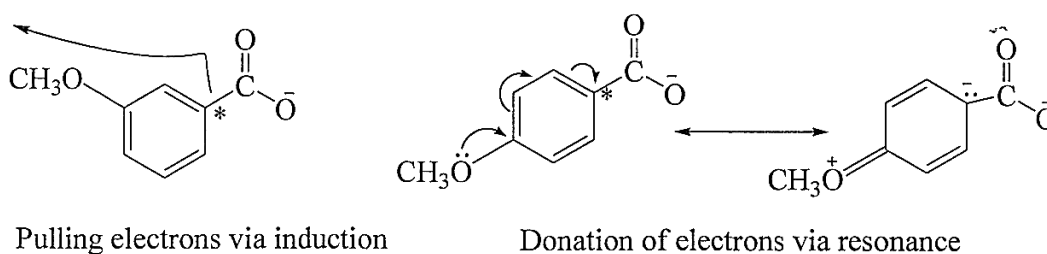
Substituents	$\sigma_m$	$\sigma_p$	$\sigma_p^+$	$\sigma_p^-$
-NH <sub>2</sub>	-0.09	-0.30	-1.3	-
-OH	0.13	-0.38	-0.92	-
-OCH <sub>3</sub>	0.10	-0.12	-0.78	-
-(CH <sub>3</sub> ) <sub>3</sub>	-0.09	-0.15	-0.26	-
-CH <sub>3</sub>	-0.06	-0.14	-0.31	-
-C <sub>6</sub> H <sub>6</sub>	0.05	0.05	-0.18	-0.08
-I	0.35	0.18	0.13	-
-Br	0.37	0.26	0.15	-
-Cl	0.37	0.24	0.11	-
-F	0.34	0.15	-0.07	-
-COCH <sub>3</sub>	0.36	0.47	-	0.82
-COOH	0.35	0.44	-	0.73
-OCOCH <sub>3</sub>	0.39	0.31	0.18	-
-NO <sub>2</sub>	0.71	0.81	-	1.23

Where,  $\sigma_m$ ,  $\sigma_p$  Hammett's substituent constant are defined by using the dissociation constants of *para*- and *meta*- substituted benzoic acids, which are composite substituent constants as both resonance and inductive / field effects are present.  $\sigma^+$  are composite substituent constants applied in cases when the reaction site is electron withdrawing, dissociation of dimethylphenyl-carbinyl chlorides.  $\sigma^-$  are composite substituent constants applied in cases when the reaction site is electron-donating, dissociation of phenols and anilines [123].

A different set of  $\sigma$  values is necessary for each different position on the benzoic acid, because the ability of substituent to influence the acidity of benzoic acid depends upon position relative to the carboxy group. When  $\sigma$  is negative, the substituted benzoic acid is less acidic than benzoic acid itself, and when  $\sigma$  is positive, the substituted benzoic acid is more acidic. Note that electron donating groups have negative  $\sigma$  values and electron withdrawing groups have positive  $\sigma$  values. This trend is exactly as predicted,

because electron withdrawing groups should stabilize the negative charge of carboxy ion and electron donating groups should destabilize this charge.

One interesting feature about the ionization of benzoic acid becomes apparent upon studying table 2.3. The  $\sigma_p$  value generally reflect a larger influence of the substituent at this position than do the  $\sigma_m$  values (the absolute value of  $\sigma_p > \sigma_m$ ) even though the *meta* position is closer to the ionizing group than is the *para* position. This difference in part reflects the ability of the *para* position to influence charge at the starred carbon (Scheme 2.8) *via* resonance, an influence that is not possible for the *meta* position. This difference is clearly evident with the hydroxy and methoxy groups.

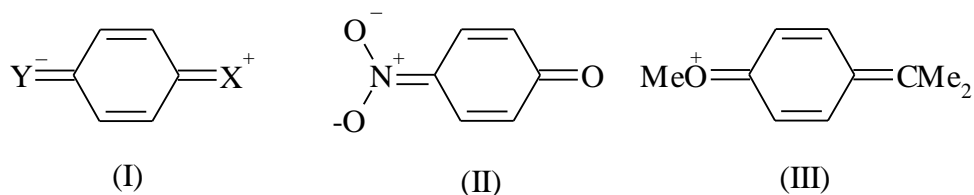


Scheme 2.8. Influence charge at the starred carbon

In the *meta* position these groups are found to be electron withdrawing to ware the starred carbon, an inductive effect. In the *para* position, these groups are electron donating, a resonance effect. Note that while this is a resonance effect, it is not resonance with the carboxylate anion. The negative charge of benzoate anion is not in conjugation with the aromatic ring and so can not be stabilized by resonance [109].

### Duality of substituent constant: $\sigma^+$ and $\sigma^-$

An early refinement was the suggestion of duality of substituents. Marked deviation from the Hammett equation were particularly noted for *para* substituents with important resonance effects, both electron-withdrawing + R and electron-releasing - R. These give rise to exalted resonance effect when such substituents are engaged in crose - conjugation with reaction sites of the opposite type, i.e. electron rich or electron deficient. This is exemplified by the structure (I) in Scheme 2.9.



Scheme 2.9. Duality of substituent constants

These *para* substituents given exalted electron withdrawal are assigned  $\sigma^-$  values [124]. These are based on the ionization of *meta*-substituted phenols in water at 25 °C, giving a defining  $\rho$  values for this reaction. This  $\rho$  value is then used to derive exalted or  $\sigma^-$  values for *para* substituents such as NO<sub>2</sub>, COMe, CN or CF<sub>3</sub>. The importance of structure such as (II) in (Scheme 2.9), for ionization of *p*-nitrophenol is thus estimated.

*Para* substituents giving exalted electron release are assigned  $\sigma^+$  value [125]. The reaction now used for determining such constants is S<sub>N</sub>1 solvolysis of substituted phenyl dimethylcarbinyl (*t*-cumyl) chlorides in 90% aqueous acetone at 25 °C, using *meta* substituents to define  $\rho$ . The exalted or  $\sigma^+$  values for *para* substituents such as OMe, Me, NH<sub>2</sub> and Cl can be calculated and demonstrate the importance of structures such as (III) in Scheme 2.9. It should be pointed out that, in defining  $\rho$  for use in estimating  $\sigma^-$ , strongly +R *meta* substituents are not used and for  $\sigma^+$  strongly –R *meta* substituents are not used. This precludes any relayed or secondary effects.

### Normal or unexalted substituent constant: $\sigma^n$ and $\sigma^0$

The duality of  $\sigma$  value was strongly criticized by Van Bekkum et al [126] who consider cross – conjugation or through - conjugation as a continuous process. A sliding extent of such interaction was considered to be present, depending on the reaction studied. Eight “primary”  $\sigma$  value of *meta* conjugation, including H, were considered to be of general applicability, together with *p*-COMe and *p*-NO<sub>2</sub> where cross – conjugation effect can be ruled out. All other *para* conjugation were excluded, as were –R *meta* substituents such as OMe<sup>+</sup> and NH<sub>2</sub> in case of relayed effects. These primary values were used to calculate  $\sigma$  values relevant that particular reaction for all other substituents.

This analysis did indicate a sliding scales for –R substituents and +R centers for +R substituents, average unexalted or ‘normal’ substituents were calculated and denoted  $\sigma^n$ . Large difference between  $\sigma$  and  $\sigma^n$  arise for substituents such as *p*-COMe, *p*-NH<sub>2</sub> and

p-OH, where cross-conjugation between the substituents and CO<sub>2</sub>H occur in the original reference reaction the ionization of benzoic acids. Ionization of *para*- substituted phenylacetic and 3-phenylpropionic acids and the alkaline hydrolysis of the corresponding ethyl phenylacetates and benzyl acetates. All these systems have substituents which are unaffected by cross-conjugation due to the insulating CH<sub>2</sub> group. These reaction series were then used to generate a series of  $\sigma^0$  values. Thus, *meta* and *para* substituents with + R effects have  $\sigma^0$  and  $\sigma$  values which are almost identical, whereas the substituents with – R effect deviate appreciably. The  $\sigma^n$  and  $\sigma^0$  scales are almost the same.

### Reaction constant ( $\rho$ )

Now that a scale for substituent effects has been established, it was possible to determine if other reactions respond to substituents the way benzoic acid does. The goal is to use benzoic acid ionization as a reference reaction that creates a negative charge and compare other reactions to it as a means to see if they also creates a negative charge, or conversely, a positive charge. Furthermore, it was necessary to determine if different reactions are more or less sensitive to the substituents than are the acidities of benzoic acid derivatives more used. To do this the Hammett relationships given in equations 2.7 and 2.8 for thermodynamic and kinetic analyses, respectively. To determine  $\rho$ , plot  $\log(K/K_0)$  or  $\log(k/k_0)$  versus  $\sigma$  for the new reaction under study. Rho ( $\rho$ ) is simply the slope of this plot.

$$\log (K/ K_0) = \rho \sigma \quad (2.7)$$

$$\log (k/ k_0) = \rho \sigma \quad (2.8)$$

$\rho$  describes the sensitivity of the new reaction to substituents effects relative to the influence of the substituent on the ionization of benzoic acids. It is called the reaction constant or sensitivity constant for each new reaction under study. The following values of  $\rho$  lead to the associated conclusions:

1. When  $\rho > 1$ , the reaction under study is more sensitive to substituents than benzoic acids and negative charge is building during the reaction.

2. When  $0 < \rho < 1$ , the reaction is less sensitive to substituents than benzoic acids, but negative charge is still building.

3. When  $\rho$  is equal to or close to 0, the reaction shows no substituent effects

This can mean no change in charge occurs in the equilibrium or rate - determining step.

4. When  $\rho$  is negative, the reaction is creating positive charge.

For example, Figure 2.31 shows a plot of the log data of ionization constant of substituted phenylacetic acids in water, and the ionization of substituted benzoic acids in ethanol.

The  $\rho$  for phenylacetic acid derivatives is 0.56, while that for benzoic acids derivatives in ethanol is 2.25. These indicate much lower and higher sensitivities of acidities to the substituent effects, respectively [109].

The smaller  $\rho$  for phenylacetic acid derives from the more remote position of the substituents to the carboxyl group relative to that in benzoic acid. The larger  $\rho$  value for the ionization of benzoic acid in ethanol reflects reduced stabilization of the negative charge in the carboxylate product in ethanol relative to that in water (remember  $\rho = 1$  in  $\text{H}_2\text{O}$ ). Hence, the substituents become more important in stabilizing or destabilizing the negative charge in the product. Interestingly, the lines are linear even though the  $\rho$  value is derived  $\sigma^-$  value of benzoic acid ionization in water.

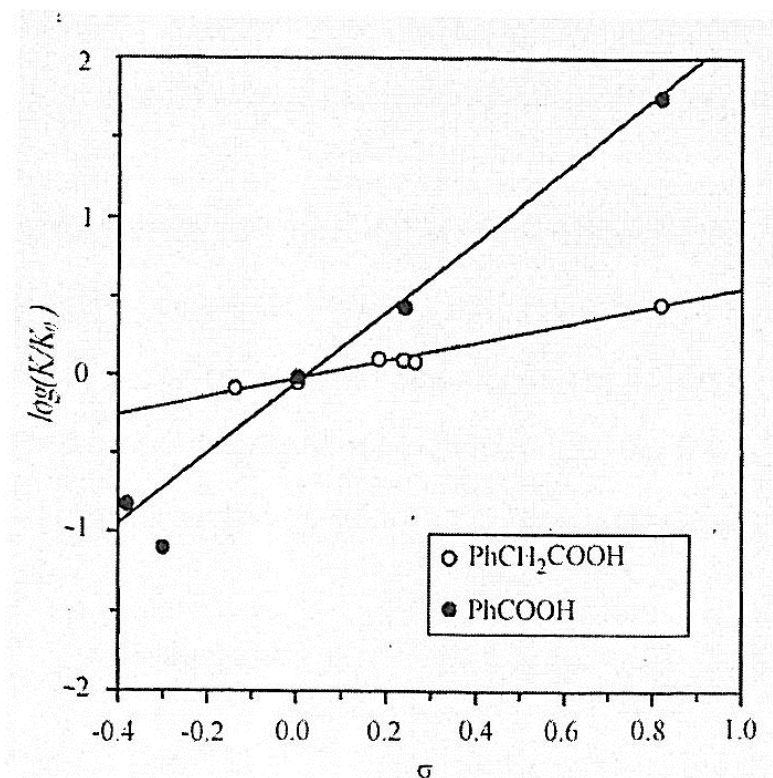


Figure 2.31. Hammett plots for phenylacetic acid and benzoic acid ionization in ethenol [127,128].

Very often the magnitude of  $\rho$  is used as a guide to the amount of charge that has been developed in transition state or in the product. Such an interpretation must be made with caution, because  $\rho$  really only relates the sensitivity of ionization to the substituents. In the examples just discussed, the amount of charge on the products is the same in all three reactions (phenylacetic acid, and benzoic acid in ethenol or water), but the  $\rho$  value are significantly different.

### 2.2.3. Separation of electronic effects

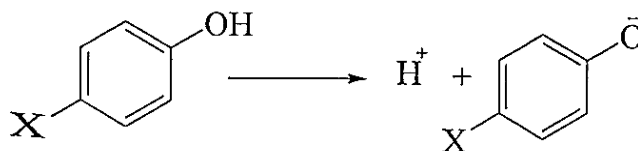
An important development was the concept that substituent electronic effects could be considered to be separable and additive. Substituent effects come in inductive resonance, and steric effects. Inductive and resonance are considered as electronic effects, whereas steric effects largely depend upon the size of the substituent. However, even steric effects are electronic in origin. They are repulsions brought about by atoms approaching within their respective Van der Waals contact distances where the electronic

clouds of the groups involved repel each other. Most chemists, however, separate the concepts of sterics and electronics [109].

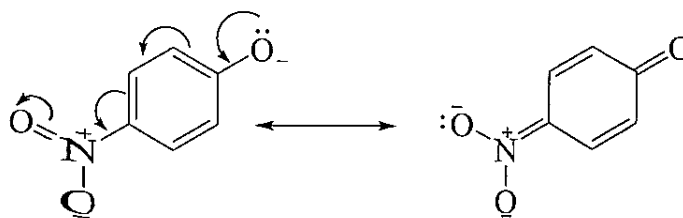
### Separation of inductive and resonance effects

Beside the  $\sigma_p$  and  $\sigma_m$  concept, tables of substituent constants usually list  $\sigma^-$  and  $\sigma^+$  values for the use of the classical Hammett equation.

As it was already mentioned, two new substituents effects scales were produced, one for groups that stabilize negative charges *via* resonance ( $\sigma^-$ ), and the other for groups that stabilize positive charges *via* resonance ( $\sigma^+$ ). The  $\sigma^-$  scale is based upon the ionization of *para*-substituted phenols (Scheme 2.10), for which groups like the nitro group can stabilize the negative charges *via* resonance (Scheme 2.11).

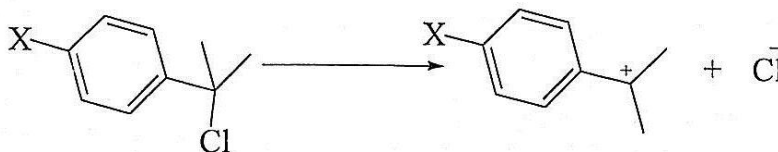


Scheme 2.10. Ionization of *p*-substituted phenols

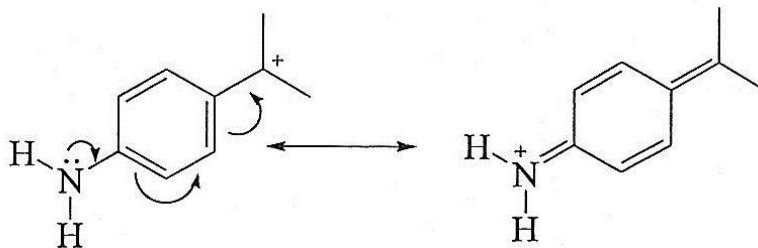


Scheme 2.11. Resonance in *p*-nitrophenolate

The  $\sigma^+$  scale is based upon the heterolysis reaction of *para*-substituted phenyldimethyl chloromethanes (Scheme 2.12), in which groups like amino can stabilize the positive charge *via* resonance (Scheme 2.13).



Scheme 2.12. Heterolysis reaction of *p*-substituted phenyldimethyl chloromethanes



Scheme 2.13. Resonance in *p*-aminobenzylic cation

Several  $\sigma^+$  and  $\sigma^-$  values are given in Table 2.3. Note that the  $\sigma^+$  values are defined so that negative  $\rho$  values correspond to the creation of positive charge, just as with normal Hammett plots. The electron withdrawing groups have positive  $\sigma^+$  values, and the electron donating groups have negative  $\sigma$  values, just as with  $\sigma$  values.

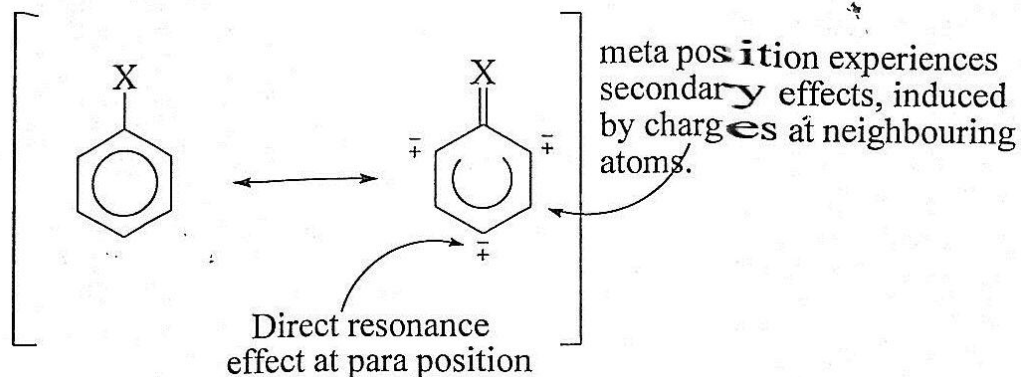
Hammett  $\sigma$  values measure the resultant of inductive and resonance effect. Taft and Lewis [129,130] suggested that the resultant effects should be quantitatively separable in the inductive and resonance contributions through equations 2.10 and 2.11.

$$\sigma_p = \sigma_I + \sigma_R \quad \text{or} \quad \sigma_p - \sigma_I = \sigma_R \quad \text{or} \quad \sigma_p - \sigma_R = \sigma_I \quad (2.10)$$

$$\sigma_m = \sigma_I + \alpha\sigma_R \quad (2.11)$$

The inductive effect, given by  $\sigma_I$ , is assumed to operate equally from the *meta*- and the *para*- position. The resonance effect, given by  $\sigma_R$ , contributes to  $\sigma_m$  indirectly,  $\alpha$  being the relay coefficient. Values  $\sigma_m$ ,  $\sigma_p$  and  $\sigma_I$  are sufficient to obtain value of  $\sigma_R$  and  $\alpha$ .

This assumes that the polar effect has the same force at the *meta*- and *para*-positions. The resonance (mesomeric) effect, on the other hand, is fully at the *para* position, but it is attenuated ( $\alpha < 1$ ) in transmission to the *meta*- position (Scheme 2.14) [113].



Scheme 2.14. Resonance effect at *meta*-position

Taft and Lewis set up a scale based on alicyclic and aliphatic reactivities. For ordinary Hammett  $\sigma$  values, based on the ionization of benzoic acid, a value for  $\rho$  of 0.33 was suggested. Selected value of  $\sigma_I$  and  $\sigma_R$  are in Table 2.4.

Table 2.4. Inductive and resonance values [124].

Substituent	$\sigma_I$	$\sigma_R^0$	$\sigma_R^{(BA)}$	$\sigma_R^-$	$\sigma_R^+$
-H	0	0	0	0	0
-N(CH <sub>3</sub> ) <sub>2</sub>	0.06	-0.52	-0.83	-0.34	-1.75
-NH <sub>2</sub>	0.12	-0.48	-0.82	-0.48	-0.161
-OCH <sub>3</sub>	0.27	-0.45	-0.61	-0.45	-1.02
-OC <sub>2</sub> H <sub>5</sub>	0.38	-0.34	-0.58	-	-0.87
-CH <sub>3</sub>	-0.04	-0.11	-0.11	-0.11	-0.25
-C <sub>6</sub> H <sub>5</sub>	0.10	-0.11	-0.11	0.04	-0.30
-F	0.50	-0.34	-0.45	-0.45	-0.57
-Cl	0.46	-0.23	-0.23	-0.23	-0.36
-Br	0.44	-0.19	-0.19	-0.19	-0.30
-I	0.39	-0.16	-0.16	-0.11	-0.25
-CN	0.56	0.13	0.13	0.33	0.13
-NO <sub>2</sub>	0.65	0.15	0.15	0.46	0.15
-COCH <sub>3</sub>	0.28	0.16	0.16	0.47	0.16

Taft [131] has obtained  $\sigma_R^0$  value by an extension of his F NMR method [113]. The analysis into resonance effect may also be performed for  $\sigma^0$  constant, giving  $\sigma_R^0$  value ( $\alpha = 0.5$ ) or with  $\sigma^+$  and  $\sigma^-$  constants (giving  $\sigma_R^+$  and  $\sigma_R^-$ , respectively) [132].

The importance of the separation of sigma parameters into  $\sigma_I$  and  $\sigma_R$  contribution is that it suggests the possibility of a ‘dual substituent – parameter’ DSP treatment for reaction series through equation 2.12.

$$\log (k/k_0) = \rho_I \sigma_I + \rho_R \sigma_R \quad (2.12)$$

Provided that the various  $\sigma_R$  type scales distinguished above are linearly related to each other, it should be satisfactory to characterize each substituent by  $\sigma_I$  and say  $\sigma_R^0$ , and apply equation 2.12 to *meta* and *para* reaction series separately. With the Hammett equation we have for each substituent, position – dependent sigma value,  $\sigma_m$  and  $\sigma_p$  (arbitrarily becoming  $\sigma^-$  or  $\sigma^+$  on occasion) but a single  $\rho$  value for each reaction series. In Taft's treatment, each substituent is characterized by position–independent  $\sigma_I$  and  $\sigma_R$  value, but the susceptibility to inductive and to resonance effect (variability of cross–conjugation) is to be expressed separately through position–dependent  $\rho_R$  and  $\rho_I$  values.

Taft and his colleagues use  $f = SD/RMS$  as measure of the success of correlation. SD is the root mean square of deviations and RMS is the root mean square of the  $\rho_i$ . If the  $f < 0.1$  the correlation is considered of good precision.

The ratio of  $\rho_R$  and  $\rho_I$  in the  $\lambda = \rho_R/\rho_I$  can be related to the importance of through – conjugation and can be used to detect the inhibition of the transmission of the resonance effects. Furthermore,  $\sigma_R$  and  $\sigma_I$  can be of opposite sign so the  $\lambda$  will be negative detecting that the opposing stabilization which can be afforded by inductive and resonance effect.

### 2.3. Solvent effects

One of the most important features for the success of the planned reaction is the selection of a suitable solvent. Since solvent effects on chemical reactivity have been known for more than a century, most chemists are familiar with the fact that solvents may have a strong influence on reaction rates and equilibria. The number of solvent systems and their associated solvent effects examined is so enormous that a complete description of aspects would fill several volumes.

The influence of solvents on the rates of chemical reactions [133] was first noted by Berthelot and Pean de Saint-Gilles in 1862 in connection with their studies on esterification of acetic acid and ethanol [134]. After thorough studies on the reaction of trialklamines with haloalkanes, Menshutkin in 1890 concluded that a reaction cannot be separated from the medium in which it is performed [135]. Menshutkin also discovered that, in reactions between liquids, one of the reaction partners may constitute an unfavourable solvent. Thus, in the preparation of acetanilide, it is not without importance whether aniline is added to an excess of acetic, or vice versa, since aniline in this case is an unfavourable reaction medium, Menshutkin related the influence of solvents primarily to their chemical, not their physical properties.

The influence of solvents on chemical equilibria was discovered in 1896, simultaneously with the discovery of keto-enol tautomerism in 1,3-dicarbonyl compounds and the nitro-isonitro tautomerism of primary and secondary nitro compounds [136]. The study of the keto-enol equilibrium of ethyl formylphenylacetate in eight solvents, led Wislicenus to the conclusion that the keto-form predominates in alcoholic solutions, the enol-form in chloroform or benzenes. He stated that the final ratio in which the two tautomeric forms coexist, must depend on the nature of the solvent and on its dissociating power, whereby he suggested that the dielectric constant were a possible measure of this 'power'.

Stobbe was the first to review these results [137]. He divided the solvents into two groups according to their ability to isomerize tautomeric compounds. His classification reflects, to some extent, the modern division into protic and aprotic solvents on constitutional and tautomeric isomerisation equilibria was later studied in detail by Dimroth [138] and Meyer [139]. The similarities in the relationships between solvent effects on reaction rate, equilibrium position, and absorption spectra has been related to the general solvating ability of the solvent in a fundamental paper by Scheibe et al [140]. Chemists have classified solvents according to [141]:

- Structure, comprising: protic solvents: solvents that contain relatively mobile protons, such as those bonded to oxygen, nitrogen, or sulphur (attached to an electronegative atom ); and aprotic solvents, in which all hydrogen's are bonded to carbon.

- Dielectric constant, comprising; polar solvents, those that have high dielectric constant (high polarizability); and non-polar solvents, are compound that have low dielectric constant (low polarizability), these solvents are not miscible with water:

Some of the more common solvents can be roughly classified as in table 2.5 on the basis of their structure and dielectric constant.

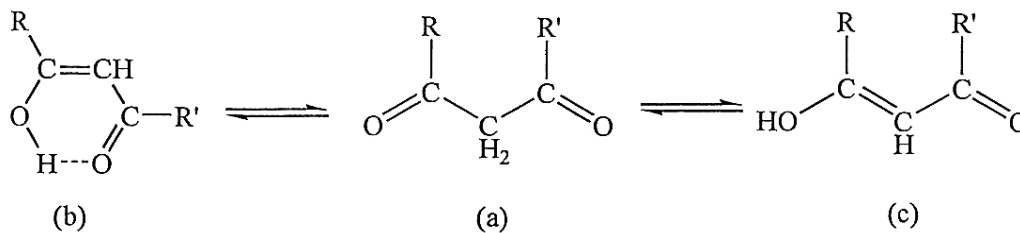
Table 2.5. Dielectric Constant of some common solvents<sup>a</sup>

Aprotic solvents			Protic solvents		
Nonpolar		Polar			
Hexane	1.9	Pyridine	12	Acetic acid	6.1
Dioxane	2.2	Acetone	21	Tert-Butanol	12.5
Benzene	2.3	Nitromethane	36	Ammonia	22
Diethyl ether	4.3	Dimethylformamide	37	Ethanol	24.5
Chloroform	8.4	Acetonitrile	38	Methanol	32.7
Tetrahydrofuran	7.6	Dimethyl sulfoxide	47	Water	78
Carbon tetrachloride	2.2	Hexamethyl phosphoramidate	30	Trifluoroacetic acid	8.6

<sup>a</sup> Dielectric Constant data are abstracted from the compilation of solvent properties in J.A Riddick and W. B .Bunger (eds.), Organic solvent , Vol . II of Techniques of Organic chemistry, Third Edition, Wiley-Interscience New York, 1970.

### 2.3.1. Solvent effects on the keto / enol equilibria [142]

In general, 1,3-dicarbonyl compounds, which include  $\beta$ -dialdehydes,  $\beta$ -ketoaldehydes,  $\beta$ -diketones and  $\beta$ -ketocarboxylic esters, may exist in solution or as pure compound in three tautomeric forms: the diketo form (Scheme 2.15 a), the cis-enolic (Scheme 2.15 b) , and the trans-enolic form (scheme 2.15 c).



Scheme 2.15. Keto / enol tautomeric form

Open-chain 1,3-dicarbonyl compounds are observed in the trans-enolic form only in rare cases [143]. When the trans-enolic form is excluded, the keto/enol equilibrium constant  $K_T$  (equilibrium constant of a tautomeric equilibrium) is given by equation 2.13.

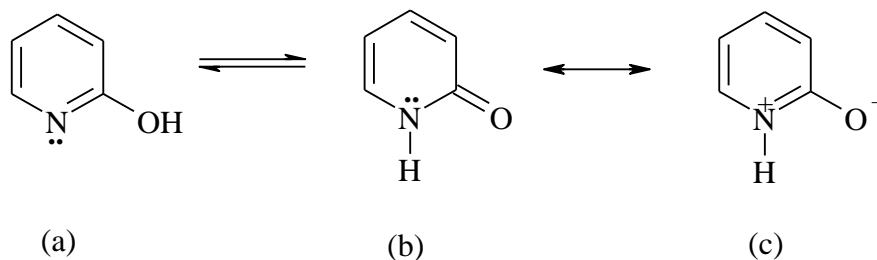
$$K_T = \frac{[\text{enol}]}{[\text{diketo}]} \quad (2.13)$$

In solution, open-chain 1,3-dicarbonyl compounds enolize practically exclusively to the cis-enolic form (scheme 2.15), which is stabilized by intermolecular hydrogen bonding. In contrast, cyclic 1,3-dicarbonyl compounds (e.g. cycloalkane-1,3-diones), can give either trans-enols (for small rings) or cis-enolic (for large rings). As the diketo form usually is more dipolar than the chelated cis-enolic form, the keto/enol ratio often depends on solvent polarity.

### 2.3.2. Solvent effects on the other tautomeric equilibria [143]

Solvent effects similar to those described for the keto/enol equilibrium can also be found for other tautomerisms, e.g. lactam/lactim, azo/hydrazone, ring/chain equilibria, etc [144,145]

One of the classic studies of lactam/lactim tautomerisms is the determination of the 2-hydroxypyridine (scheme 2.16 a)  $\rightleftharpoons$  2-pyridone (scheme 2.16 b) equilibrium [144,145]



Scheme 2.16. Lactam – lactim tautomeric forms

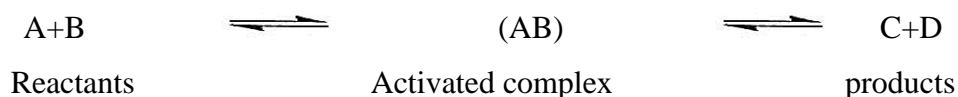
By considering the lactam–lactim equilibrium (Scheme 2.16 a)  $\rightleftharpoons$  (Scheme 2.16 b) in solvents of varying polarity it has been found that increasing solvent polarity shifts the equilibrium towards the pyridone-form. This form is more dipolar than the hydroxyl-form due to the contribution of the charge-separated mesomeric form (Scheme 16 c). Furthermore, the hydrogen-bonding ability of the solvent plays an important role since hydrogen-bond acceptors stabilize the enol-form.

### 2.3.3. Solvent effects on the rates of homogenous chemical reactions [142]

A change of solvent can considerably change both the rate and order of homogeneous chemical reactions. Already in 1890, Menschutkin demonstrated in his classical study on the quaternization of triethylamine with iodoethane in 23 solvents, that the rate of reaction varied remarkably depending on the choice of solvent. In diethyl ether, the rate was four times faster than in n-hexane, 36 times faster in benzene, 280 times faster in methanol, and 742 times faster in benzyl alcohol [146]. Thus, by means of a proper choice of solvent, decisive acceleration or deceleration of a chemical reaction can be achieved.

In solution, ions are produced by the heterolysis of covalent bonds in ionogens. This ionization reaction is favoured by solvents due to their cooperative EPD (electron pair donor) and EPA (electron pair acceptor) properties, and hence the behaviour of ions and molecules is dictated mainly by the solvent and only to a lesser extent by their intrinsic properties.

Consider a reaction between the starting compounds A and B, and suppose that during the course of the reaction these two first form an activated complex, which then decomposes to the end products, C and D. The reaction can then be described as follows



If the reaction takes place in solution, then the initial reactants, as well as the activated complex, will be solvated to a different extent, according to the solvating power of the solvent used. This differential solvation can retard or accelerate a reaction in the manner described below in Figure 2.32.

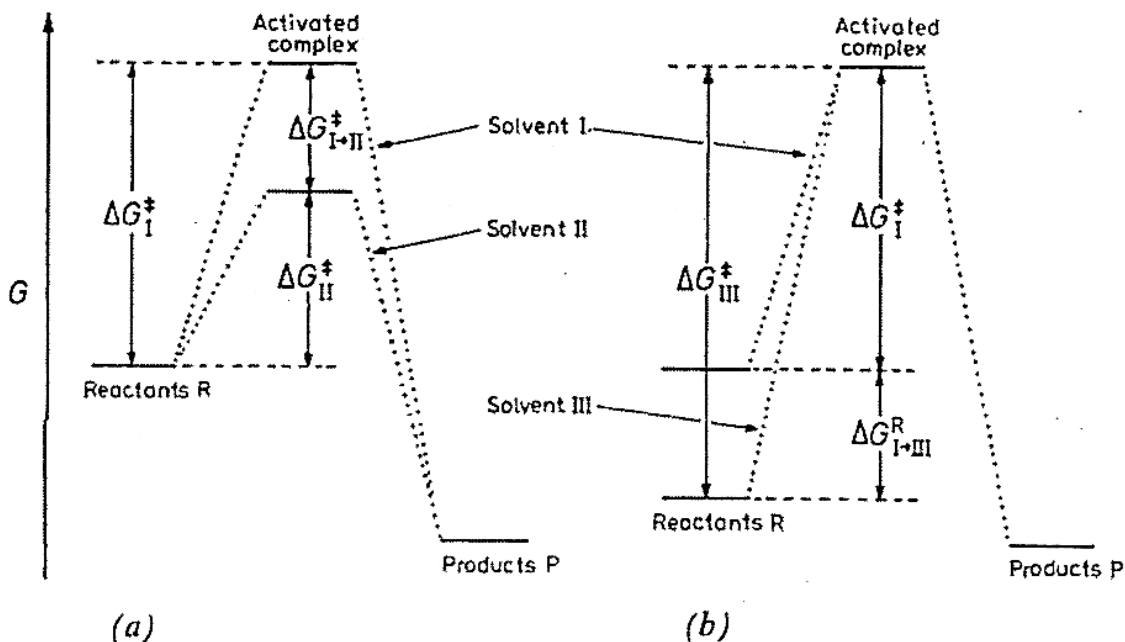


Figure 2.32. One dimensional Gibbs energy diagram for a chemical reaction in three different solvents I, II and III.

$\Delta G_I^\ddagger$  represents the Gibbs energy of activation for a given chemical reaction in an ideal solvent I. In such a case neither the reactants nor the activated complex are solvated. If in another solvent II only the activated complex is solvated, then  $\Delta G_{II}^\ddagger$  results. The Gibbs energy of activation is reduced by the Gibbs energy of transfer,  $\Delta G_I^\ddagger$  to  $\Delta G_{II}^\ddagger$  with consequent rate acceleration. If on the other hand, only the initial reactants are solvated as happens in solvent III, then  $\Delta G_{III}^\ddagger$  results. Gibbs energy of activation is increased by the Gibbs energy of transfer  $\Delta G_I^\ddagger$  to  $\Delta G_{III}^\ddagger$  with a consequent rate deceleration. The solvation of the products does not have any influence on the reaction rate. Because in reality the initial reactants as well as the activated complex are solvated, but usually to a different extent, the difference of both Gibbs transfer energies determines the reaction rate in solution.

### 2.3.3.1. The Grunwald – Winstein equation

The majority of these are based either on linear free energy relationships for chemical processes or on solvatochromic shifts in electronic spectra, for example in the former category.

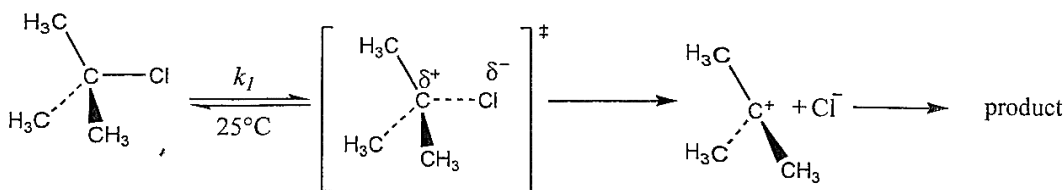
Grunwald and Winstein [147] are suggested treating solvent effects on rates in terms of equation 2.14, similar in form to the Hammett equation.

$$\log (\kappa / \kappa_0) = mY \quad (2.14)$$

$$\text{or } \log \kappa = \log \kappa_0 + mY \quad (2.15)$$

Log  $k$  refers to a given reaction in a given solvent,  $\log k^0$  to the same reaction in 80% v/v aqueous ethanol as a standard solvent,  $Y$  is a parameter characteristic of the given solvent and  $m$  is a parameter characteristic of the given reaction, which measures its susceptibility to changes in solvent; the analogy of  $Y$  and  $m$  to  $\sigma$  and  $\rho$  respectively is obvious. Scales of  $Y$  and  $m$  were established by taking  $Y = 0$  for 80 % ethanol, and selecting the solvolysis of t-butyl chloride at 25 °C as a standard reaction, for which  $m$  is defined as 1.0.  $Y$  values are known for various one-component solvents (mainly alcohols) and for various mixtures of organic solvents with water or second organic solvents.

Grunwald and Winstein [148] found that the  $S_N1$  solvolysis of 2-chloro-2-methylpropane (tert-butylchloride) is strongly accelerated by polar solvents, and is 335000 times faster in water than in the less polar solvent ethanol [147].



The authors defined a solvent ‘‘ ionizing power’’ parameter  $Y$  using equation 2.16,

$$Y = \log k_{t\text{-BuCl}} - \log k^0_{t\text{-BuCl}} \quad (2.16)$$

Where  $\log k^0_{t\text{-BuCl}}$  is the first order rate constant for the solvolysis of tert-butyl chloride at 25 °C in (80 % ethanol and 20% water,  $Y=0$ ) as reference solvent. Grunwald – Winstein equation 2.14 is fairly successful in a large number of cases.

Good linear relationships between  $\log k$  and  $Y$  are shown by the solvolysis of various tertiary halides and secondary alkyl sulphonates, i.e. reactions which proceed by an  $S_N1$  mechanism, like the standard reaction. The situation for  $S_N2$  reactions (e.g. solvolysis of primary haloalkanes) or for reaction borderline mechanism (e.g. solvolysis of secondary haloalkanes) is less satisfactory.

#### 2.3.4. Koppel – Palm solvatochromic treatment [149]

Solvent – solute interactions are classified as non-specific. The former are divided into polarization and polarizability effects, to be characterized by the parameters Y and P respectively. Specific interactions concern donor –acceptor interaction of solvent with solute. A solvent may function as a Lewis base (electron donor) capable of nucleophilic solvation, or as a Lewis acid (electron acceptor) capable of electrophilic solvation. These phenomena are characterized by the different parameters and may then be used in the correlation analysis of solvent effects by means of equation 2.17.

$$A = A_0 + yY + pP + bB + eE \quad (2.17)$$

A is the value of the solvent – dependent property (log K,  $\nu$ , etc.) in a given solvent,  $A_0$  is the statistical quantity (intercept term) corresponding to the value of the property in the gas-phase as reference ‘solvent’; y, p, b and e are the regression coefficients.

The setting–up of scales for Y and P depends on the assumption that capability of solvents for polarization and polarizability interactions is validly measured by dielectric constant and refractive index respectively.

Thus Y is defined either as  $(\epsilon - 1) / (2\epsilon + 1)$ , the Kirkwood function, or as  $(\epsilon - 1) / (2\epsilon + 1)$ , a function based on the expression for molar polarization.

#### 2.3.5. Kamlet – Taft solvatochromic treatment [150]

An interesting approach, called the solvatochromic comparison method, used to evaluate a  $\beta$ -scale of solvent hydrogen-bond acceptor (HBA) basicities (corresponding to the Koppel-Palm B scale), and an  $\alpha$ -scale of solvent hydrogen-bond donor (HBD) acidities (corresponding to the Koppel-Palm E scale), and  $\pi^*$ -scale of solvent dipolarity/polarizability using UV-Vis spectral data of solvatochromic compounds. A selection values of  $\beta$ ,  $\alpha$  and  $\pi^*$  are recorded in Table 2.6.

Table 2.6. Selected values of Kamlet-Taft parameters [151]

Solvent	$\beta$	$\alpha$	$\pi^*$	solvent	$\beta$	$\alpha$	$\pi^*$
n-Pentane	0.0	0.0	-0.08	n-Hexanol	0.84	0.80	0.40
n-Hexane	0.0	0.0	-0.04	c-Hexanol	0.84	0.66	0.45
n-Heptane	0.0	0.0	-0.08	Benzyl alcohol	0.52	0.60	0.98
c-Hexane	0.0	0.0	0.0	THF	0.55	0.0	0.58
Benzene	0.1	0.0	0.59	Acetonitrile	0.40	0.19	0.75
Methanol	0.66	0.98	0.60	Acetone	0.43	0.08	0.71
Ethanol	0.75	0.86	0.54	Formamide	0.48	0.71	0.97
n-Propanol	0.90	0.84	0.82	<i>N</i> -Methylformamide	0.80	0.62	0.90
i-Propanol	0.84	0.76	0.48	<i>N,N</i> -Dimethylformamide	0.69	0.0	0.88
n- Butanol	0.84	0.84	0.47	Dimethyl sulfoxide	0.76	0.0	1.0
i- Butanol	0.84	0.79	0.40	Dimethyl sulfide	0.34	0.0	0.57
s- Butanol	0.80	0.69	0.40	Formic acid	0.38	1.23	0.65
t- Butanol	0.93	0.42	0.41	Acetic acid	0.45	1.12	0.64
n-Pentanol	0.86	0.84	0.40	Propanoic acid	0.45	1.12	0.58
i- Pentanol	0.86	0.84	0.40	Acetic anhydride	0.29	0.0	0.76
t- Pentanol	0.93	0.28	0.40	Water	0.47	1.17	1.09

Kamlet and Taft have shown  $\beta$ ,  $\alpha$  and  $\pi^*$  may be applied in the correlation analysis by multiple regressions of reaction rates and equilibria, and of spectroscopic data; equation 2.18 applies:

$$XYZ = XYZ_0 + s \pi^* + a \alpha + b \beta \quad (2.18)$$

where  $XYZ_0$ ,  $a$ ,  $b$  and  $s$  are (solvent-independent) coefficients characteristic of the process and indicative of the sensitivity to the accompanying solvent properties.

Kamlet and Taft's solvatochromic parameters have been used in one-, two- and three-parameter correlation involving different combination of these parameters which are called linear solvation energy relationships (LSER's) [142].

### 2.3.6. Correlation analysis of solvent effects by means of substituent constants

It is sometimes possible to express aspects of solvent polarity in a series of structurally related solvents by means of appropriate substituent constants. Thus providing a link between solvent effects and Hammett or Taft equations. In a general way this may not be entirely straightforward, since substituent constants concern effects transmitted to a localized reaction centre, while solvent effects, in principle, involve the interaction of the reacting species with the solvent molecule in entirety.

In some series of solvents, however, a particular centre in the solvent molecule is likely to dominate solvent-solute interaction and in such cases the influence of substituents on that centre may play important role in solvent effects. Electronic or steric substituent constants may then be relevant as solvent parameters, usually in connection with multiple regression. Chapman et. al. [152] have established that the solvent effects is best interpreted in terms of the following properties: (a) the behaviour of the solvent as a dielectric in facilitating the separation of opposite charges in the formation of the activated complex; (b) the ability of the medium to solvate the carboxylic proton and thus stabilize the initial state relative to the transition state; and (c) the ability of protic solvents to form hydrogen bonds with the negative ends of the ion-pair, and thus stabilize the transition state relative to the initial state.

Multiple linear regression of  $\log k$  with  $f(\epsilon)$ ,  $\sigma^*$  and  $n_\gamma H$  gives equation 2.19.

$$\log k = \log k_0 + af(\epsilon) + b \sigma^* + cn_\gamma H \quad (2.19)$$

where  $f(\epsilon)$  is the Kirkwood function  $[(\epsilon-1)/(2\epsilon+1)]$  of dielectric constant,  $\sigma^*$  is the Taft constant for the alkyl group of the alcohol, and  $n_\gamma H$  is the number of  $\gamma$ -hydrogen atoms in the alcohol.

### 3. EXPERIMENTAL PART

#### General

All starting materials were obtained from Aldrich and Fluka, and were used without further purification.

The IR spectra were determined using a Bomem Fourier Transform-infrared (FT-IR) spectrophotometer, MB-Series in the form of the KBr pallets. The  $^{13}\text{C}$  and  $^1\text{H}$  NMR spectral measurements were performed on a Varian Gemini 2000 (200 MHz). The spectra were recorded at room temperature in deuterated dimethyl sulfoxide ( $\text{DMSO-}d_6$ ). The chemical shifts are expressed in ppm values referenced to TMS. The ultraviolet-visible (UV-vis) absorption spectra were recorded on a Shimadzu 1700 spectrophotometer in the region 200–600 nm. The spectra were run in spectroquality solvents (Fluka) using concentration of  $1 \times 10^{-5}$  M. All melting points were uncorrected and are in degree Celsius. Elemental analyses were performed using a VARIO EL III elemental analyzer.

#### 3.1. Preparation of 5-aryloxy-6-hydroxy-4-phenyl-3-cyano-2-pyridone dyes (A1-A12)

All the investigated aryloxy pyridone dyes were synthesized from the corresponding diazonium salts and 4-phenyl-6-hydroxy-3-cyano-2-pyridone using classical reaction for the synthesis of the azo compounds [32]. 4-Phenyl-6-hydroxy-3-cyano-2-pyridone was prepared from ethyl benzoylacetate and cyanoacetamide using a modified literature procedure [153].

#### General Procedure for the preparation of 4-phenyl-6-hydroxy-3-cyano-2-pyridone

4-Phenyl-6-hydroxy-3-cyano-2-pyridone was prepared from ethyl benzoylacetate and cyanoacetamide using a modified literature procedure. Equimolar amounts (10 mmol) of ethyl benzoylacetate and cyanoacetamide were heated under reflux in absolute ethanol (10 mL) in the presence of potassium hydroxide (10 mmol) as catalyst for 20 h. The product was isolated by filtration and purified by crystallization from ethanol. Characterization data are given below.

*4-Phenyl-6-hydroxy-3-cyano-2-pyridone*. White crystalline solid; m.p.: 279–280 °C (lit. m.p.: 280 °C [153]); yield: 62 %; IR (KBr,  $\nu/\text{cm}^{-1}$ ): 3419 (OH), 3321 (NH), 2227 (CN), 1654 (C=O);  $^1\text{H}$  NMR (200 MHz,  $\text{DMSO-}d_6$ ,  $\delta/\text{ppm}$ ): 6.26 (1H, s, PyrH); 7.60–7.40 (5H, m, PhH); 11.74 (1H, s, OH).

### **General Procedure for the preparation of 5-aryldazo-6-hydroxy-4-phenyl-3-cyano-2-pyridone dyes (A1–A12)**

All the investigated aryldazo pyridone dyes were synthesized from the corresponding diazonium salts and 4-phenyl-6-hydroxy-3-cyano-2-pyridone using classical reaction for the synthesis of the azo compounds. The obtained compounds were purified by crystallization from acetone and then analyzed. Characterization data are given below.

*5-Phenyldazo-6-hydroxy-4-phenyl-3-cyano-2-pyridone (A1)*. Orange crystalline solid; m.p.: 257–260 °C; yield: 75 %; anal. calcd. for  $\text{C}_{18}\text{H}_{12}\text{N}_4\text{O}_2$ : C, 68.35; H, 3.82; N, 17.71; found: C, 68.51; H, 3.75; N, 17.57; IR (KBr,  $\nu/\text{cm}^{-1}$ ): 3390 (NH of hydrazone form), 3153 (NH on heterocyclic), 2229 (CN), 1654, 1630 (C=O on heterocyclic);  $^1\text{H}$  NMR (200 MHz,  $\text{DMSO-}d_6$ ,  $\delta/\text{ppm}$ ): 7.42–7.10 (5H, m, ArH); 7.70–7.42 (5H, m, ArH); 12.22 (1H, s, NH on heterocyclic); 14.61 (1H, s, NH of hydrazone form);  $^{13}\text{C}$  NMR (50 MHz,  $\text{DMSO-}d_6$ ,  $\delta/\text{ppm}$ ): 163.24 (C2), 96.80 (C3), 162.02 (C4), 117.26 (C5), 161.29 (C6).

*5-(4-Hydroxyphenyldazo)-6-hydroxy-4-phenyl-3-cyano-2-pyridone (A2)*. Dark red crystalline solid; m.p.: 272–274 °C; yield: 58 %; anal. calcd. for  $\text{C}_{18}\text{H}_{12}\text{N}_4\text{O}_3$ : C, 65.06; H, 3.64; N, 16.86; found: C, 65.22; H, 3.72; N, 16.72; IR (KBr,  $\nu/\text{cm}^{-1}$ ): 3385 (NH of hydrazone form), 3153 (NH on heterocyclic), 2230 (CN), 1654, 1637 (C=O on heterocyclic);  $^1\text{H}$  NMR (200 MHz,  $\text{DMSO-}d_6$ ,  $\delta/\text{ppm}$ ): 7.27 (2H, d,  $J = 9$  Hz, ArH); 7.60–7.40 (5H, m, ArH); 8.77 (2H, d,  $J = 9.6$  Hz, ArH); 10.04 (1H, s, OH substituent); 12.12 (1H, s, NH on heterocyclic); 14.93 (1H, s, NH of hydrazone form);  $^{13}\text{C}$  NMR (50 MHz,  $\text{DMSO-}d_6$ ,  $\delta/\text{ppm}$ ): 163.40 (C2), 97.04 (C3), 162.26 (C4), 118.98 (C5), 161.53 (C6).

*5-(4-Methoxyphenyldazo)-6-hydroxy-4-phenyl-3-cyano-2-pyridone (A3)*. Brown crystalline solid; m.p.: 268–270 °C; yield: 60 %; anal. calcd. for  $\text{C}_{19}\text{H}_{14}\text{N}_4\text{O}_3$ : C, 65.89; H, 4.07; N, 16.18; found: C, 66.06; H, 3.96; N, 16.72; IR (KBr,  $\nu/\text{cm}^{-1}$ ): 3386 (NH of

hydrazone form), 3152 (NH on heterocyclic), 2231 (CN), 1664, 1642 (C=O on heterocyclic);  $^1\text{H}$  NMR (200 MHz, DMSO- $d_6$ ,  $\delta$ /ppm): 3.72 (3H, s, OCH<sub>3</sub> substituent); 7.60–7.45 (5H, m, ArH); 7.75–7.60 (4H, m, ArH); 12.15 (1H, s, NH on heterocyclic); 14.82 (1H, s, NH of hydrazone form);  $^{13}\text{C}$  NMR (50 MHz, DMSO- $d_6$ ,  $\delta$ /ppm): 163.31 (C2), 96.87 (C3), 162.11 (C4), 119.05 (C5), 161.44 (C6).

*5-(4-Methylphenylazo)-6-hydroxy-4-phenyl-3-cyano-2-pyridone (A4)*. Red crystalline solid; m.p.: 263–267 °C; yield: 54 %; anal. calcd. for C<sub>19</sub>H<sub>14</sub>N<sub>4</sub>O<sub>2</sub>: C, 69.08; H, 4.27; N, 16.96; found: C, 69.24; H, 4.13; N, 16.02; IR (KBr,  $\nu/\text{cm}^{-1}$ ): 3387 (NH of hydrazone form), 3135 (NH on heterocyclic), 2224 (CN), 1661, 1640 (C=O on heterocyclic);  $^1\text{H}$  NMR (200 MHz, DMSO- $d_6$ ,  $\delta$ /ppm): 2.30 (3H, s, CH<sub>3</sub> substituent); 7.60–7.42 (7H, m, ArH); 7.66 (2H, d,  $J = 9.6$  Hz, ArH); 12.19 (1H, s, NH on heterocyclic); 14.68 (1H, s, NH of hydrazone form);  $^{13}\text{C}$  NMR (50 MHz, DMSO- $d_6$ ,  $\delta$ /ppm): 163.28 (C2), 96.82 (C3), 162.04 (C4), 117.27 (C5), 161.31 (C6).

*5-(4-Chlorophenylazo)-6-hydroxy-4-phenyl-3-cyano-2-pyridone (A5)*. Light orange crystalline solid; m.p.: 272–274 °C; yield: 72 %; anal. calcd. for C<sub>18</sub>H<sub>11</sub>ClN<sub>4</sub>O<sub>2</sub>: C, 61.64; H, 3.16; N, 15.97; found: C, 61.48; H, 3.08; N, 15.76; IR (KBr,  $\nu/\text{cm}^{-1}$ ): 3406 (NH of hydrazone form), 3110 (NH on heterocyclic), 2217 (CN), 1660, 1631 (C=O on heterocyclic);  $^1\text{H}$  NMR (200 MHz, DMSO- $d_6$ ,  $\delta$ /ppm): 7.26 (2H, d,  $J = 9$ , ArH); 7.38 (2H, d,  $J = 8.4$  Hz, ArH); 7.70–7.44 (5H, m, ArH); 12.26 (1H, s, NH on heterocyclic); 14.52 (1H, s, NH of hydrazone form);  $^{13}\text{C}$  NMR (50 MHz, DMSO- $d_6$ ,  $\delta$ /ppm): 162.97 (C2), 96.80 (C3), 161.82 (C4), 118.77 (C5), 161.20 (C6).

*5-(4-Bromophenylazo)-6-hydroxy-4-phenyl-3-cyano-2-pyridone (A6)*. Yellow crystalline solid; m.p.: 269–271 °C; yield: 68 %; anal. calcd. for C<sub>18</sub>H<sub>11</sub>BrN<sub>4</sub>O<sub>2</sub>: C, 54.70; H, 2.81; N, 14.18; found: C, 54.82; H, 2.72; N, 14.06; IR (KBr,  $\nu/\text{cm}^{-1}$ ): 3385 (NH of hydrazone form), 3141 (NH on heterocyclic), 2223 (CN), 1672, 1654 (C=O on heterocyclic);  $^1\text{H}$  NMR (200 MHz, DMSO- $d_6$ ,  $\delta$ /ppm): 7.16 (2H, d,  $J = 8.4$ , ArH); 7.70–7.44 (7H, m, ArH); 12.26 (1H, s, NH on heterocyclic); 14.48 (1H, s, NH of hydrazone form);  $^{13}\text{C}$  NMR (50 MHz, DMSO- $d_6$ ,  $\delta$ /ppm): 163.06 (C2), 96.82 (C3), 161.88 (C4), 118.92 (C5), 161.23 (C6).

*5-(4-Iodophenylazo)-6-hydroxy-4-phenyl-3-cyano-2-pyridone (A7)*. Dark red crystalline solid; m.p.: 267–270 °C; yield: 52 %; anal. calcd. for C<sub>18</sub>H<sub>11</sub>IN<sub>4</sub>O<sub>2</sub>: C, 48.89; H, 2.51; N,

12.67; found: C, 48.66; H, 2.38; N, 12.48; IR (KBr,  $\nu/\text{cm}^{-1}$ ): 3398 (NH of hydrazone form), 3217 (NH on heterocyclic), 2225 (CN), 1684, 1651 (C=O on heterocyclic);  $^1\text{H}$  NMR (200 MHz, DMSO- $d_6$ ,  $\delta/\text{ppm}$ ): 7.04 (2H, d,  $J = 9$ , ArH); 7.70–7.44 (5H, m, ArH); 7.67 (2H, d,  $J = 8.4$  Hz, ArH); 12.24 (1H, s, NH on heterocyclic); 14.49 (1H, s, NH of hydrazone form);  $^{13}\text{C}$  NMR (50 MHz, DMSO- $d_6$ ,  $\delta/\text{ppm}$ ): 163.24 (C2), 96.80 (C3), 161.89 (C4), 119.23 (C5), 161.24 (C6).

*5-(4-Fluorophenylazo)-6-hydroxy-4-phenyl-3-cyano-2-pyridone* (**A8**). Brown crystalline solid; m.p.: 262–264 °C; yield: 50 %; anal. calcd. for  $\text{C}_{18}\text{H}_{11}\text{FN}_4\text{O}_2$ : C, 64.67; H, 3.32; N, 16.76; found: C, 64.42; H, 3.24; N, 16.58; IR (KBr,  $\nu/\text{cm}^{-1}$ ): 3385 (NH of hydrazone form), 3153 (NH on heterocyclic), 2224 (CN), 1654, 1628 (C=O on heterocyclic);  $^1\text{H}$  NMR (200 MHz, DMSO- $d_6$ ,  $\delta/\text{ppm}$ ): 7.20 (2H, d,  $J = 9$ , ArH); 7.62–7.40 (5H, m, ArH); 7.69 (2H, d,  $J = 8.4$  Hz, ArH); 12.22 (1H, s, NH on heterocyclic); 14.59 (1H, s, NH of hydrazone form);  $^{13}\text{C}$  NMR (50 MHz, DMSO- $d_6$ ,  $\delta/\text{ppm}$ ): 163.27 (C2), 96.85 (C3), 161.89 (C4), 119.28 (C5), 161.15 (C6).

*5-(4-Cyanophenylazo)-6-hydroxy-4-phenyl-3-cyano-2-pyridone* (**A9**). Dark red crystalline solid; m.p.: 270–272 °C; yield: 48 %; anal. calcd. for  $\text{C}_{19}\text{H}_{11}\text{N}_5\text{O}_2$ : C, 66.86; H, 3.25; N, 20.52; found: C, 66.71; H, 3.18; N, 20.38; IR (KBr,  $\nu/\text{cm}^{-1}$ ): 3386 (NH of hydrazone form), 3152 (NH on heterocyclic), 2231 (CN), 1668, 1652 (C=O on heterocyclic);  $^1\text{H}$  NMR (200 MHz, DMSO- $d_6$ ,  $\delta/\text{ppm}$ ): 8.03–7.40 (9H, m, ArH); 12.33 (1H, s, NH on heterocyclic); 14.29 (1H, s, NH of hydrazone form);  $^{13}\text{C}$  NMR (50 MHz, DMSO- $d_6$ ,  $\delta/\text{ppm}$ ): 163.28 (C2), 96.85 (C3), 161.70 (C4), 117.48 (C5), 161.13 (C6).

*5-(4-Carboxyphenylazo)-6-hydroxy-4-phenyl-3-cyano-2-pyridone* (**A10**). Dark red crystalline solid; m.p.: 260–262 °C; yield: 54 %; anal. calcd. for  $\text{C}_{19}\text{H}_{12}\text{N}_4\text{O}_4$ : C, 63.33; H, 3.36; N, 15.55; found: C, 63.52; H, 3.22; N, 15.38; IR (KBr,  $\nu/\text{cm}^{-1}$ ): 3382 (NH of hydrazone form), 3168 (NH on heterocyclic), 2231 (CN), 1683, 1654 (C=O on heterocyclic);  $^1\text{H}$  NMR (200 MHz, DMSO- $d_6$ ,  $\delta/\text{ppm}$ ): 7.60–7.40 (7H, m, ArH); 7.66 (2H, d,  $J = 9.6$  Hz, ArH); 12.30 (1H, s, NH on heterocyclic); 14.27 (1H, s, NH of hydrazone form);  $^{13}\text{C}$  NMR (50 MHz, DMSO- $d_6$ ,  $\delta/\text{ppm}$ ): 163.33 (C2), 96.83 (C3), 161.95 (C4), 116.96 (C5), 161.24 (C6).

*5-(4-Acetylphenylazo)-6-hydroxy-4-phenyl-3-cyano-2-pyridone* (**A11**). Dark red crystalline solid; m.p.: 264–266 °C; yield: 58 %; anal. calcd. for  $\text{C}_{20}\text{H}_{14}\text{N}_4\text{O}_3$ : C, 67.03;

H, 3.94; N, 15.63; found: C, 67.16; H, 3.68; N, 15.47; IR (KBr,  $\nu/\text{cm}^{-1}$ ): 3385 (NH of hydrazone form), 3145 (NH on heterocyclic), 2231 (CN), 1667, 1635 (C=O on heterocyclic);  $^1\text{H}$  NMR (200 MHz,  $\text{DMSO-}d_6$ ,  $\delta/\text{ppm}$ ): 2.50 (3H, s,  $\text{CH}_3\text{CO}$  substituent); 7.32 (2H, d,  $J = 8.4$  Hz, ArH); 7.65–7.43 (5H, m, ArH); 7.90 (2H, d,  $J = 8.6$  Hz, ArH); 12.34 (1H, s, NH on heterocyclic); 14.46 (1H, s, NH of hydrazone form);  $^{13}\text{C}$  NMR (50 MHz,  $\text{DMSO-}d_6$ ,  $\delta/\text{ppm}$ ): 163.27 (C2), 96.84 (C3), 161.80 (C4), 116.88 (C5), 161.22 (C6).

*5-(4-Nitrophenylazo)-6-hydroxy-4-phenyl-3-cyano-2-pyridone* (**A12**). Dark yellow crystalline solid; m.p.: 268–270 °C; yield: 60 %; anal. calcd. for  $\text{C}_{18}\text{H}_{11}\text{N}_5\text{O}_4$ : C, 59.84; H, 3.07; N, 19.38; found: C, 59.97; H, 2.98; N, 19.21; IR (KBr,  $\nu/\text{cm}^{-1}$ ): 3414 (NH of hydrazone form), 3112 (NH on heterocyclic), 2227 (CN), 1671, 1655 (C=O on heterocyclic);  $^1\text{H}$  NMR (200 MHz,  $\text{DMSO-}d_6$ ,  $\delta/\text{ppm}$ ): 7.40 (2H, d,  $J = 9$ , ArH); 7.65–7.45 (5H, m, ArH); 8.19 (2H, d,  $J = 9$  Hz, ArH); 12.37 (1H, s, NH on heterocyclic); 14.37 (1H, s, NH of hydrazone form);  $^{13}\text{C}$  NMR (50 MHz,  $\text{DMSO-}d_6$ ,  $\delta/\text{ppm}$ ): 161.58 (C2), 103.14 (C3), 161.09 (C4), 117.30 (C5), 161.78 (C6).

### 3.2. Preparation of 5-arylazo-6-hydroxy-4-(4-methoxyphenyl)-3-cyano-2-pyridone dyes (**A13 – A23**)

All the investigated arylazo pyridone dyes were synthesized from the corresponding diazonium salts and 6-hydroxy-4-(4-methoxyphenyl)-3-cyano-2-pyridone using classical reaction for the synthesis of the azo compounds [32]. 6-Hydroxy-4-(4-methoxyphenyl)-3-cyano-2-pyridone was prepared from ethyl 4-methoxyphenyl benzoylacetate and cyanoacetamide in absolute ethanol in the presence of potassium hydroxide using modified literature procedure [154]. All starting materials were obtained from Aldrich and Fluka and were used without further purification. The obtained compounds were purified by crystallization from acetone and then analyzed. Characterization data are given below.

#### *5-Phenylazo-6-hydroxy-4-(4-methoxyphenyl)-3-cyano-2-pyridone* (**A13**).

Orange crystalline solid; m.p.: 235–238 °C, yield 50%, anal. calcd. for  $\text{C}_{19}\text{H}_{14}\text{N}_4\text{O}_3$ : C, 65.89; H, 4.07; N, 16.18; found: C, 65.94; H, 3.89; N, 16.08; IR (KBr,  $\nu/\text{cm}^{-1}$ ): 3432

(NH of hydrazone form), 3137 (NH on heterocyclic), 2223 (CN), 1663, 1641 (C=O on heterocyclic);  $^1\text{H}$  NMR (200 MHz, DMSO- $d_6$ ,  $\delta$ /ppm): 3.88 (3H, s, OCH<sub>3</sub>); 7.12 (2H, d, J=8.4 Hz, ArOCH<sub>3</sub>); 7.28–7.42 (5H, m, ArH); 7.53 (2H, d, J=9 Hz, ArOCH<sub>3</sub>); 12.18 (1H, s, NH on heterocyclic); 14.69 (1H, s, NH of hydrazone form);  $^{13}\text{C}$  NMR (50 MHz, DMSO- $d_6$ ,  $\delta$ /ppm): 162.12 (C2), 99.82 (C3), 161.48 (C4), 117.25 (C5), 160.64 (C6).

*5-(4-Fluorophenylazo)-6-hydroxy-4-(4-methoxyphenyl)-3-cyano-2-pyridone (A14).*

Yellow crystalline solid; m.p.: 262–265 °C, yield 41%; anal.calcd. for C<sub>19</sub>H<sub>13</sub>F N<sub>4</sub>O<sub>3</sub>: C, 62.64; H, 3.60; N, 15.38; found: C, 62.48; H, 3.48; N, 15.34; IR (KBr,  $\nu/\text{cm}^{-1}$ ): 3425 (NH of hydrazone form), 3206 (HN on heterocyclic), 2221 (CN), 1697, 1659 (C=O on heterocyclic);  $^1\text{H}$ NMR (200 MHz, DMSO- $d_6$ ,  $\delta$ /ppm): 3.87 (3H, s, OCH<sub>3</sub>); 7.12 (2H, d, J=9Hz, ArF); 7.20–7.33 (4H, m, ArF + ArOCH<sub>3</sub>); 7.52 (2H, d, J=9Hz, ArOCH<sub>3</sub>); 12.17 (1H, s, NH on heterocyclic); 14.46 (1H, s, NH on hydrazone form);  $^{13}\text{C}$  NMR (50 MHz, DMSO- $d_6$ ,  $\delta$ /ppm): 161.98 (C2), 99.84 (C3), 161.40 (C4), 119.30 (C5), 160.65 (C6).

*5-(4-Chlorophenylazo)-6-hydroxy-4-(4-methoxyphenyl)-3-cyano-2-pyridone (A15).*

Light orange crystalline solid; m.p.: 265–268 °C, yield 44%; anal.calcd. for C<sub>19</sub>H<sub>13</sub>Cl N<sub>4</sub>O<sub>3</sub>: C, 59.93; H, 3.44; N, 14.71; found: C, 60.08; H, 3.34; N, 14.58; IR (KBr,  $\nu/\text{cm}^{-1}$ ): 3435 (NH of hydrazone form), 3213 (HN on heterocyclic), 2221 (CN), 1697, 1660 (C=O on heterocyclic);  $^1\text{H}$ NMR (200 MHz, DMSO- $d_6$ ,  $\delta$ /ppm): 3.88 (3H, s, OCH<sub>3</sub>); 7.12 (2H, d, J=8.8 Hz, ArOCH<sub>3</sub>); 7.35 (2H, d, J=8.8 Hz, ArCl); 7.45 (2H, d, J=7.6 Hz, ArCl); 7.52 (2H, d, J=7.4 Hz, ArOCH<sub>3</sub>); 12.19 (1H, s, NH on heterocyclic); 14.58 (1H, s, NH on heterocyclic);  $^{13}\text{C}$  NMR (50 MHz, DMSO- $d_6$ ,  $\delta$ /ppm): 161.93 (C2), 100.31 (C3), 161.32 (C4), 118.83 (C5), 160.49 (C6).

*5-(4-Bromophenylazo)-6-hydroxy-4-(4-methoxyphenyl)-3-cyano-2-pyridone (A16).*

Dark yellow crystalline solid; m.p.: 270–273 °C, yield 40%; anal.calcd. for C<sub>19</sub>H<sub>13</sub>Br N<sub>4</sub>O<sub>3</sub>: C, 53.67; H, 3.08; N, 13.18; found: C, 54.06; H, 3.02; N, 13.08; IR (KBr,  $\nu/\text{cm}^{-1}$ ): 3435 (NH of hydrazone form), 3206 (HN on heterocyclic), 2221 (CN), 1695, 1659 (C=O on heterocyclic);  $^1\text{H}$  NMR (200 MHz, DMSO- $d_6$ ,  $\delta$ /ppm): 3.88 (3H, s, OCH<sub>3</sub>); 7.12 (2H, d, J=8.4 Hz, ArBr); 7.28 (2H, d, J=8.4 Hz, ArOCH<sub>3</sub>); 7.51 (2H, d, J=8.4 Hz, ArBr); 7.58 (2H, d, J=9 Hz, ArOCH<sub>3</sub>); 12.20 (1H, s, NH on heterocyclic); 14.54 (1H, s, NH on hydrazone form);  $^{13}\text{C}$  NMR (50 MHz, DMSO- $d_6$ ,  $\delta$ /ppm): 161.91 (C2), 100.33 (C3), 161.31 (C4), 119.10 (C5), 160.45 (C6).

*5-(4-Iodophenylazo)-6-hydroxy-4-(4-methoxyphenyl)-3-cyano-2-pyridone (A17).*

Dark orange crystalline solid; m.p.: 257-260 °C, yield 25%; anal.calcd. for C<sub>19</sub>H<sub>13</sub>I N<sub>4</sub>O<sub>3</sub>: C, 48.32; H, 2.77; N, 11.86; found: C, 48.36; H, 2.58; N, 11.68; IR (KBr, v/cm<sup>-1</sup>): 3438 (NH of hydrazone form), 3202 (HN on heterocyclic), 2215 (CN), 1699, 1660 (C=O on heterocyclic); <sup>1</sup>H NMR (200 MHz, DMSO-*d*<sub>6</sub>, δ/ppm): 3.88 (3H, s, OCH<sub>3</sub>); 7.05–7.17 (4H, m, ArOCH<sub>3</sub> + ArI); 7.52 (2H, d, J=9 Hz, ArI); 7.74 (2H, d, J=8.4 Hz, ArOCH<sub>3</sub>); 12.19 (1H, s, NH on heterocyclic); 14.52 (1H, s, NH of hydrazone form); <sup>13</sup>C NMR (50 MHz, DMSO-*d*<sub>6</sub>, δ/ppm): 161.96 (C2), 100.28 (C3), 161.51 (C4), 119.27 (C5), 160.49 (C6).

*5-(4-Hydroxyphenylazo)-6-hydroxy-4-(4-methoxyphenyl)-3-cyano-2-pyridone (A18).*

Dark red crystalline solid; m.p.: 233-236 °C, yield 37%; anal.calcd. for C<sub>19</sub>H<sub>14</sub>N<sub>4</sub>O<sub>4</sub>: C, 62.98; H, 3.89; N, 15.46; found: C, 62.76; H, 3.66; N, 15.32; IR (KBr, v/cm<sup>-1</sup>): 3412 (NH of hydrazone form), 3218 (HN on heterocyclic), 2214 (CN), 1691, 1643 (C=O on heterocyclic); <sup>1</sup>H NMR (200 MHz, DMSO-*d*<sub>6</sub>, δ/ppm): 3.87 (3H, s, OCH<sub>3</sub>); 6.28 (2H, d, J=8.4 Hz, ArOH); 7.05 (2H, d, J=9 Hz, ArOH); 7.21 (2H, d, J=9 Hz, ArOCH<sub>3</sub>); 7.50 (2H, d, J=9 Hz, ArOCH<sub>3</sub>); 9.96 (1H, s, ArOH); 12.08 (1H, s, NH on heterocyclic); 14.69 (1H, s, NH of hydrazone form); <sup>13</sup>C NMR (50 MHz, DMSO-*d*<sub>6</sub>, δ/ppm): 162.27 (C2), 97.85 (C3), 161.85 (C4), 119.30 (C5), 160.89 (C6).

*5-(4-Methylphenylazo)-6-hydroxy-4-(4-methoxyphenyl)-3-cyano-2-pyridone (A19).*

Dark orange crystalline solid; m.p.: 233-236 °C, yield 42%; anal.calcd. for C<sub>20</sub>H<sub>16</sub>N<sub>4</sub>O<sub>3</sub>: C, 66.66; H, 4.48; N, 15.55; found: C, 66.52; H, 4.32; N, 15.35; IR (KBr, v/cm<sup>-1</sup>): 3425 (NH of hydrazone form), 3201 (NH on heterocyclic), 2214 (CN), 1654, 1643 (C=O on heterocyclic); <sup>1</sup>H NMR (200 MHz, DMSO-*d*<sub>6</sub>, δ/ppm): 2.30 (3H, s, CH<sub>3</sub>); 3.88 (3H, s, CH<sub>3</sub>); 3.88 (3H, s, OCH<sub>3</sub>); 7.54 (2H, d, J=9 Hz, ArCH<sub>3</sub>); 7.21 (4H, s, ArCH<sub>3</sub> + ArOCH<sub>3</sub>); 7.75 (2H, d, J=8.4 Hz, ArOCH<sub>3</sub>); 12.14 (1H, s, NH on heterocyclic); 14.52 (1H, s, NH of hydrazone form); <sup>13</sup>C NMR (50 MHz, DMSO-*d*<sub>6</sub>, δ/ppm): 162.13 (C2), 99.18 (C3), 161.40 (C4), 117.26 (C5), 160.98 (C6).

*5-(4-Methoxyphenylazo)-6-hydroxy-4-(4-methoxyphenyl)-3-cyano-2-pyridone (A20).*

Dark brown crystalline solid; m.p.: 232-235 °C, yield 27%; anal.calcd. for C<sub>20</sub>H<sub>16</sub>N<sub>4</sub>O<sub>4</sub>: C, 63.82; H, 4.28; N, 14.89; found: C, 63.78; H, 4.32; N, 14.54; IR (KBr, v/cm<sup>-1</sup>): 3347 (NH of hydrazone form), 3225 (NH on heterocyclic), 2212 (CN), 1662, 1648 (C=O on

heterocyclic);  $^1\text{H}$  NMR (200 MHz,  $\text{DMSO-}d_6$ ,  $\delta/\text{ppm}$ ): 3.76 (3H, s, N–ArOCH<sub>3</sub>); 3.88 (3H, s, OCH<sub>3</sub>); 6.59 (4H, m, N–ArOCH<sub>3</sub> + ArOCH<sub>3</sub>); 7.45 (2H, d,  $J=8.4$  Hz, N–ArOCH<sub>3</sub>); 7.50 (2H, d,  $J=8.4$  Hz, ArOCH<sub>3</sub>); 12.10 (1H, s, NH on heterocyclic); 14.63 (1H, s, NH of hydrazone form);  $^{13}\text{C}$  NMR (50 MHz,  $\text{DMSO-}d_6$ ,  $\delta/\text{ppm}$ ): 161.75 (C2), 99.02 (C3), 161.75 (C4), 119.01 (C5), 160.78 (C6).

*5-(4-Acetylphenylazo)-6-hydroxy-4-(4-methoxyphenyl)-3-cyano-2-pyridone (A21).*

Dark yellow crystalline solid; m.p.: 267–270 °C, yield 22%; anal.calcd. for  $\text{C}_{21}\text{H}_{16}\text{N}_4\text{O}_4$ : C, 64.94; H, 4.15; N, 14.43; found: C, 64.78; H, 3.98; N, 14.36; IR (KBr,  $\text{v}/\text{cm}^{-1}$ ): 3438 (NH of hydrazone form), 3206 (NH on heterocyclic), 2215 (CN), 1698, 1675 (C=O on heterocyclic);  $^1\text{H}$  NMR (200 MHz,  $\text{DMSO-}d_6$ ,  $\delta/\text{ppm}$ ): 3.76 (3H, s, N–ArOCH<sub>3</sub>); 3.88 (3H, s, OCH<sub>3</sub>); 6.59 (4H, m, N–ArOCH<sub>3</sub> + ArOCH<sub>3</sub>); 7.45 (2H, d,  $J=8.4$  Hz, N–ArOCH<sub>3</sub>); 7.50 (2H, d,  $J=8.4$  Hz, ArOCH<sub>3</sub>); 12.10 (1H, s, NH on heterocyclic); 14.63 (1H, s, NH of hydrazone form);  $^{13}\text{C}$  NMR (50 MHz,  $\text{DMSO-}d_6$ ,  $\delta/\text{ppm}$ ): 161.86 (C2), 101.22 (C3), 161.27 (C4), 116.81 (C5), 160.40 (C6).

*5-(4-Cyanophenylazo)-6-hydroxy-4-(4-methoxyphenyl)-3-cyano-2-pyridone (A22).*

Yellow crystalline solid; m.p.: 279–282 °C, yield 25%; anal.calcd. for  $\text{C}_{20}\text{H}_{13}\text{N}_5\text{O}_3$ : C, 64.69; H, 3.53; N, 18.86; found: C, 64.48; H, 3.32; N, 18.56; IR (KBr,  $\text{v}/\text{cm}^{-1}$ ): 3425 (NH of hydrazone form), 3221 (NH on heterocyclic), 2227 (CN), 1678, 1654 (C=O on heterocyclic);  $^1\text{H}$  NMR (200 MHz,  $\text{DMSO-}d_6$ ,  $\delta/\text{ppm}$ ): 3.88 (3H, s, OCH<sub>3</sub>); 7.05 (2H, d,  $J=9$  Hz, ArCN); 7.13 (2H, d,  $J=9$  Hz, ArOCH<sub>3</sub>); 7.21 (2H, d,  $J=9$  Hz, ArCN); 7.84 (2H, d,  $J=8.4$  Hz, ArOCH<sub>3</sub>); 12.28 (1H, s, NH on heterocyclic); 14.41 (1H, s, NH of hydrazone form);  $^{13}\text{C}$  NMR (50 MHz,  $\text{DMSO-}d_6$ ,  $\delta/\text{ppm}$ ): 161.75 (C2), 101.86 (C3), 161.24 (C4), 118.88 (C5), 160.75 (C6).

*5-(4-Nitrophenylazo)-6-hydroxy-4-(4-methoxyphenyl)-3-cyano-2-pyridone (A23).*

Dark yellow crystalline solid; m.p.: 275–278 °C, yield 23%; anal.calcd. for  $\text{C}_{19}\text{H}_{13}\text{N}_5\text{O}_5$ : C, 58.31; H, 3.35; N, 17.90; found: C, 58.22; H, 3.24; N, 17.72; IR (KBr,  $\text{v}/\text{cm}^{-1}$ ): 3431 (NH of hydrazone form), 3213 (NH on heterocyclic), 2214 (CN), 1689, 1675 (C=O on heterocyclic);  $^1\text{H}$  NMR (200 MHz,  $\text{DMSO-}d_6$ ,  $\delta/\text{ppm}$ ): 3.89 (3H, s, OCH<sub>3</sub>); 7.06 (2H, d,  $J=8.8$  Hz, ArOCH<sub>3</sub>); 7.15 (2H, d,  $J=9$  Hz, ArNO<sub>2</sub>); 7.52 (2H, d,  $J=8.4$  Hz, ArCH<sub>3</sub>); 8.24 (2H, d,  $J=9$  Hz, ArNO<sub>2</sub>); 12.31 (1H, s, NH on heterocyclic); 14.34 (1H, s, NH of

hydrazone form);  $^{13}\text{C}$  NMR (50 MHz,  $\text{DMSO-}d_6$ ,  $\delta/\text{ppm}$ ): 161.68 (C2), 102.28 (C3), 161.22 (C4), 119.85 (C5), 160.33 (C6).

### 3.3. Preparation of 5-aryloxy-6-hydroxy-4-(4-nitrophenyl)-3-cyano-2-pyridone dyes (A24–A33)

All then investigated arylazo pyridone dyes were synthesized from the corresponding diazonium salts and 6-hydroxy-4-(4-nitrophenyl)-3-cyano-2-pyridone using classical reaction for the synthesis of the azo compounds [32]. 6-Hydroxy-4-(4-nitrophenyl)-3-cyano-2-pyridone was prepared from ethyl-4-nitrophenyl benzoylacetate and cyanoacetamide in absolute ethanol in the presence of potassium hydroxide using modified literature procedure [154]. All starting materials were obtained from Aldrich and Fluka, and were used without further purification. The obtained compounds were purified by crystallization from acetone and then analyzed. Characterization data are given below.

#### *5-Phenylazo-6-hydroxy-4-(4-nitrophenyl)-3-cyano-2-pyridone (A24).*

Brown crystalline solid; m.p.: 260–263 °C; yield 50%; anal. calcd. for  $\text{C}_{18}\text{H}_{11}\text{N}_5\text{O}_4$ : C, 59.84; H, 3.07; N, 19.38; found: C, 59.62; H, 2.98; N, 19.18; IR (KBr,  $\text{v}/\text{cm}^{-1}$ ): 3439 (NH of hydrazone form), 3185 (NH on heterocyclic), 2223 (CN), 1692, 1668 (C=O on heterocyclic);  $^1\text{H}$ NMR (200 MHz  $\text{DMSO-}d_6$ ,  $\delta/\text{ppm}$ ): 6.71 (1H, m, Ar); 7.00–7.60 (4H, m, Ar); 7.85 (2H, d,  $J=9$  Hz,  $\text{ArNO}_2$ ); 8.45 (2H, d,  $J=9$  Hz,  $\text{ArNO}_2$ ); 12.34 (1H, s, NH on heterocyclic); 14.69 (1H, s, NH of hydrazone form);  $^{13}\text{C}$  NMR (50 MHz,  $\text{DMSO-}d_6$ ,  $\delta/\text{ppm}$ ): 161.64 (C2), 113.60 (C3), 161.02 (C4), 121.84 (C5), 159.16 (C6).

#### *5-(4-Methylphenylazo)-6-hydroxy-4-(4-nitrophenyl)-3-cyano-2-pyridone (A25).*

Light red crystalline solid; m.p.: 222–225 °C; yield 43%; anal. calcd. for  $\text{C}_{19}\text{H}_{13}\text{N}_5\text{O}_4$ : C, 60.80; H, 3.49; N, 18.66; found: C, 60.42; H, 3.27; N, 18.44; IR (KBr,  $\text{v}/\text{cm}^{-1}$ ): 3458 (NH of hydrazone form), 3157 (NH on heterocyclic), 2226 (CN), 1674, 1658 (C=O on heterocyclic);  $^1\text{H}$ NMR (200 MHz,  $\text{DMSO-}d_6$ ,  $\delta/\text{ppm}$ ): 2.26 (3H, s,  $\text{CH}_3$ ); 7.85 (2H, d,  $J=9$  Hz,  $\text{ArCH}_3$ ); 8.18 (2H, d,  $J=9$  Hz,  $\text{ArCH}_3$ ); 8.35 (2H, d,  $J=8.4$  Hz,  $\text{ArNO}_2$ ); 8.42 (2H, d,  $J=9$  Hz,  $\text{ArNO}_2$ ); 12.31 (1H, s, NH on heterocyclic); 14.69 (1H, s, NH on hydrozone form);  $^{13}\text{C}$  NMR (50 MHz,  $\text{DMSO-}d_6$ ,  $\delta/\text{ppm}$ ): 161.80 (C2), 115.15 (C3), 160.95 (C4), 123.35 (C5), 159.07 (C6).

*5-(4-Hydroxyphenylazo)-6-hydroxy-4-(4-nitrophenyl)-3-cyano-2-pyridone (A26).*

Dark red crystalline solid; m.p.: 285-287 °C, yield 37%; anal.calcd. for C<sub>18</sub>H<sub>11</sub>N<sub>5</sub>O<sub>5</sub>: C, 57.30; H, 2.94; N, 18.56; found: C, 55.25; H, 2.78; N, 18.33; IR (KBr, v/cm<sup>-1</sup>): 3426 (NH of hydrazone form), 3203 (HN on heterocyclic); <sup>1</sup>HNMR (200 MHz, DMSO-*d*<sub>6</sub>, δ/ppm): 6.78 (2H, d, J=9 Hz, ArOH); 7.17 (2H, d, J=9 Hz, ArOH); 8.18 (2H, d, J=9 Hz, ArNO<sub>2</sub>); 8.43 (2H, d, J=9 Hz, ArNO<sub>2</sub>); 9.96 (1H, s, ArOH); 12.23 (1H, s, NH on hydrazone form); <sup>13</sup>C NMR (50 MHz, DMSO-*d*<sub>6</sub>, δ/ppm): 161.97 (C2), 116.68 (C3), 161.04 (C4), 123.98 (C5), 158.92 (C6).

*5-(4-Chlorophenylazo)-6-hydroxy-4-(4-nitrophenyl)-3-cyano-2-pyridone (A27).*

Light brown crystalline solid; m.p.: 220-223 °C, yield 44%; anal. calcd. for C<sub>18</sub>H<sub>10</sub>ClN<sub>5</sub>O<sub>4</sub>: C, 54.63; H, 2.55; N, 17.70; found: C, 54.38; H, 2.32; N, 17.56; IR (KBr, v/cm<sup>-1</sup>): 3459 (NH of hydrazone form), 3170 (NH on heterocyclic), 2223 (CN), 1684, 1652 (C=O on heterocyclic); <sup>1</sup>HNMR (200 MHz, DMSO-*d*<sub>6</sub>, δ/ppm): 7.14–7.54 (4H, m, ArCl); 8.16 (2H, d, J=8.4 Hz, ArNO<sub>2</sub>); 8.43 (2H, d, J=9 Hz, ArNO<sub>2</sub>); 12.13 (1H, s, NH on heterocyclic); 14.58 (1H, s, NH of hydrazone form), <sup>13</sup>CNMR (50 MHz, DMSO-*d*<sub>6</sub>, δ/ppm): 162.98 (C2), 116.28 (C3), 161.04 (C4), 124.06 (C5), 159.09 (C6).

*5-(4-Bromophenylazo)-6-hydroxy-4-(4-nitrophenyl)-3-cyano-2-pyridone (A28).*

Red crystalline solid; m.p.: 242-245 °C; yield 42%, anal. calcd. for C<sub>18</sub>H<sub>10</sub>BrN<sub>5</sub>O<sub>4</sub>: C, 49.11; H, 2.29; N, 15.91; found: C, 48.88; H, 2.11; N, 15.78; IR (KBr, v/cm<sup>-1</sup>): 3433 (NH of hydrazone form), 3157 (NH on heterocyclic), 2206 (CN), 1683, 1662 (C=O on heterocyclic); <sup>1</sup>HNMR (200 MHz, DMSO-*d*<sub>6</sub>, δ/ppm): 7.20 (2H, d, J=8.8 Hz, ArBr); 7.54 (2H, d, J=8.4 Hz, ArBr); 8.16 (2H, d, J=9 Hz, ArNO<sub>2</sub>); 8.42 (2H, d, J=9 Hz, ArNO<sub>2</sub>); 12.35 (1H, s, NH on heterocyclic); 14.54 (1H, s, NH of hydrazone form); <sup>13</sup>C NMR (50 MHz, DMSO-*d*<sub>6</sub>, δ/ppm): 162.91 (C2), 114.99 (C3), 161.60 (C4), 123.45 (C5), 160.89 (C6).

*5-(4-Iodophenylazo)-6-hydroxy-4-(4-nitrophenyl)-3-cyano-2-pyridone (A29).*

Dark violet crystalline solid; m.p.: 218-221 °C, yield 35%, anal. calcd. for C<sub>18</sub>H<sub>10</sub>IN<sub>5</sub>O<sub>4</sub>: C, 44.37; H, 2.07; N, 14.37; found: C, 44.18; H, 1.98; N, 14.28; IR (KBr, v/cm<sup>-1</sup>): 3439 (NH of hydrazone form), 3145 (NH on heterocyclic), 2225 (CN), 1673, 1658 (C=O on heterocyclic); <sup>1</sup>H NMR (200 MHz, DMSO-*d*<sub>6</sub>, δ/ppm): 7.05 (2H, d, J=7.8 Hz, ArI); 7.69 (2H, d, J=7.8 Hz, ArI); 7.80 (2H, d, J=8.8 Hz, ArNO<sub>2</sub>); 8.42 (2H, d, J=8 Hz,

ArNO<sub>2</sub>); 12.34 (1H, s, NH on heterocyclic); 14.52 (1H, s, NH of hydrazone form); <sup>13</sup>C NMR (50 MHz, DMSO-*d*<sub>6</sub>, δ/ppm): 162.69 (C2), 114.98 (C3), 161.60 (C4), 123.44 (C5), 160.88 (C6).

*5-(4-Florophenylazo)-6-hydroxy-4-(4-nitrophenyl)-3-cyano-2-pyridone (A30).*

Dark brown crystalline solid; m.p.: 232-235 °C, yield 40%, anal. calcd. for C<sub>18</sub>H<sub>10</sub>FN<sub>5</sub>O<sub>4</sub>: C, 57.00; H, 2.66; N, 18.46; found; C, 48.36; H, 2.48; N, 18.23; IR (KBr, ν/cm<sup>-1</sup>): 3439 (NH of hydrazone form), 3196 (NH on heterocyclic), 2225 (CN), 1697, 1656 (C=O on heterocyclic); <sup>1</sup>H NMR (200 MHz, DMSO-*d*<sub>6</sub>, δ/ppm): 7.22 (2H, d, J=9 Hz, ArF); 7.77 (2H, d, J=9 Hz, ArF); 8.17 (2H, d, J=9 Hz, ArNO<sub>2</sub>); 8.40 (2H, d, J=9 Hz, ArNO<sub>2</sub>); 12.20 (1H, s, NH on heterocyclic); 14.46 (1H, s, NH of hydrazone form); <sup>13</sup>C NMR (50 MHz, DMSO-*d*<sub>6</sub>, δ/ppm): 162.67 (C2), 115.00 (C3), 161.67 (C4), 123.31 (C5), 160.58 (C6).

*5-(4-Acetylphenylazo)-6-hydroxy-4-(4-nitrophenyl)-3-cyano-2-pyridone (A31).*

Brown crystalline solid; m.p.: 235-238 °C, yield 25%, anal. calcd. for C<sub>20</sub>H<sub>13</sub>N<sub>5</sub>O<sub>5</sub>: C, 59.56; H, 3.25; N, 17.36; found; C, 59.14; H, 3.06; N, 17.34; IR (KBr, ν/cm<sup>-1</sup>): 3452 (NH of hydrazone form), 3209 (NH on heterocyclic), 2224 (CN), 1680, 1658 (C=O on heterocyclic); <sup>1</sup>H NMR (200 MHz, DMSO-*d*<sub>6</sub>, δ/ppm): 2.52 (3H, s, COCH<sub>3</sub>); 7.30 (2H, d, J=9 Hz, ArCOCH<sub>3</sub>); 7.83 (2H, d, J=9 Hz, ArNO<sub>2</sub>); 7.95 (2H, d, J=8.8 Hz, ArCOCH<sub>3</sub>); 8.45 (2H, d, J=8.8 Hz, ArNO<sub>2</sub>); 12.39 (1H, s, NH of heterocyclic); 14.41 (1H, s, NH of hydrazone form); <sup>13</sup>C NMR (50 MHz, DMSO-*d*<sub>6</sub>, δ/ppm): 161.47 (C2), 112.67 (C3), 160.85 (C4), 123.49 (C5), 159.05 (C6).

*5-(4-Cyanophenylazo)-6-hydroxy-4-(4-nitrophenyl)-3-cyano-2-pyridone (A32).*

Orange crystalline solid; m.p.: 255-258 °C, yield 30%, anal. calcd. for C<sub>19</sub>H<sub>10</sub>N<sub>6</sub>O<sub>4</sub>: C, 59.07; H, 2.61; N, 21.75; found; C, 58.88; H, 2.36; N, 21.64; IR (KBr, ν/cm<sup>-1</sup>): 3446 (NH of hydrazone form), 3229 (NH on heterocyclic), 2222 (CN), 1684, 1651 (C=O on heterocyclic); <sup>1</sup>H NMR (200 MHz, DMSO-*d*<sub>6</sub>, δ/ppm): 7.40 (2H, d, J=9 Hz, ArCN); 8.20 (2H, d, J=9 Hz, ArCN); 8.35 (2H, d, J=8.4 Hz, ArNO<sub>2</sub>); 8.45 (2H, d, J=9 Hz, ArNO<sub>2</sub>); 12.46 (1H, s, NH on heterocyclic); 14.38 (1H, s, NH of hydrazone form); <sup>13</sup>C NMR (50 MHz, DMSO-*d*<sub>6</sub>, δ/ppm): 162.91 (C2), 113.69 (C3), 161.40 (C4), 123.51 (C5), 160.75 (C6).

*5-(4-Nitrophenylazo)-6-hydroxy-4-(4-nitrophenyl)-3-cyano-2-pyridone (A33).*

Light brown crystalline solid; m.p.: 265-268 °C, yield 26%, anal. calcd. for C<sub>18</sub>H<sub>10</sub>N<sub>6</sub>O<sub>6</sub>: C, 53.21; H, 2.48; N, 20.68; found; C, 52.88; H, 2.32; N, 20.49; IR (KBr, v/cm<sup>-1</sup>): 3446 (NH of hydrazone form), 3268 (NH on heterocyclic), 2218 (CN), 1688, 1653 (C=O on heterocyclic); <sup>1</sup>H NMR (200 MHz, DMSO-*d*<sub>6</sub>, δ/ppm): 7.41 (2H, d, J=9.4 Hz, N-ArNO<sub>2</sub>); 7.80 (2H, d, J=8.8 Hz, ArNO<sub>2</sub>); 8.32 (2H, d, J= 8.4 Hz, N-ArNO<sub>2</sub>); 8.45 (2H, d, J=9 Hz, ArNO<sub>2</sub>); 12.46 (1H, s, NH on heterocyclic); 14.38 (1H, s, NH of hydrazone form); <sup>13</sup>C NMR (50 MHz, DMSO-*d*<sub>6</sub>, δ/ppm): 162.88 (C2), 112.62 (C3), 161.31 (C4), 123.60 (C5), 160.76 (C6).

## 4. RESULTS AND DISCUSSION

### 4.1. Solvent and structural effects on the UV-vis absorption spectra of 5-aryloxy-6-hydroxy-4-phenyl-3-cyano-2-pyridone dyes

The arylazo pyridone dyes prepared in this work may exist in two main tautomeric forms (Scheme 4.1). Generally, tautomers not only have different colors, but also have different tinctorial strength and different properties, *e.g.*, light fastness [78]. Due to the commercial importance of arylazo pyridone dyes, the azo-hydrazone tautomerism has been intensively studied [99–101]. It was concluded that the equilibrium between the two tautomers is influenced by the structure of the compound and the solvent used [99–101].

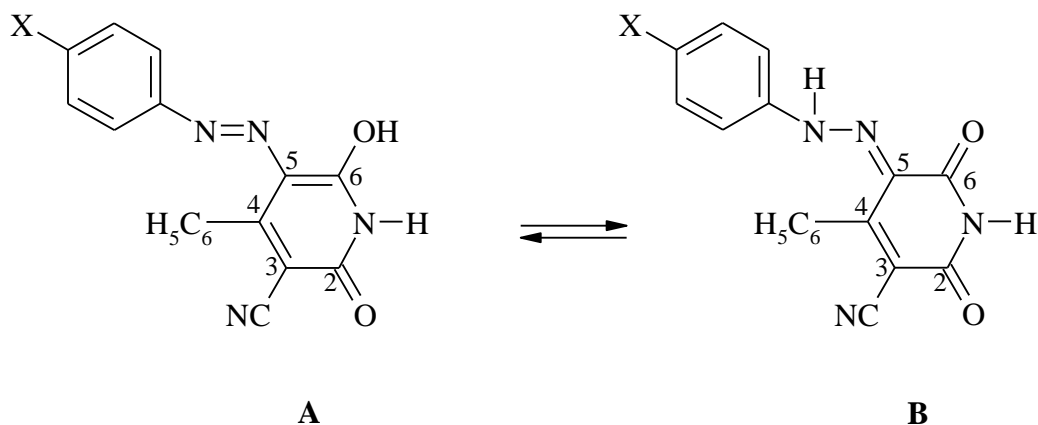
#### 4.1.1. Spectral characteristics and tautomerism

The infrared spectra of all the synthesized dyes showed two intense carbonyl bands at about 1630 and 1684  $\text{cm}^{-1}$ , which were assigned to the diketohydrazone form. The FT-IR spectra also showed a band at 3110–3217  $\text{cm}^{-1}$ , assigned to the imino group (N–H) of the heterocyclic (pyridine) ring and a band at 3382–3414  $\text{cm}^{-1}$  that was assigned to the N–H of hydrazone tautomeric form.

The  $^1\text{H}$  NMR spectra of the dyes exhibited a broad signal near 14.27–14.93 ppm. This signal corresponds to the imine N–H proton resonance of the hydrazone form (Scheme 4.1, Structure **B**).

N. Ertan *et al.* [83] reported the  $^1\text{H}$  NMR spectra of some azo pyridone dyes in  $\text{CF}_3\text{COOD} / \text{CDCl}_3$  and showed that these dyes existed in the hydrazone form with the N–H peak in the range 15.10–15.60 ppm. Q. Peng *et al.* [101] also reported the  $^1\text{H}$  NMR spectra of azo pyridone dyes in  $\text{CDCl}_3$  and concluded that the azo pyridone dyes exist in the hydrazone form and with the N–H peaks appearing within the range 14.30–16.09 ppm.

Lucka and Machacek [155] and Cee *et al.* [102] concluded from  $^{13}\text{C}$  NMR studies of some N-alkyl derivatives of azopyridones that pyridone azo dyes in  $\text{CDCl}_3$  and  $\text{DMSO}-d_6$  exist in the hydrazone form. Our results are in agreement with these results.



Scheme 4.1. The equilibrium between azo form (**A**) and hydrazone form (**B**) of 5-aryloxy-6-hydroxy-4-phenyl-3-cyano-2-pyridones (X = H (**A1**), OH (**A2**), OCH<sub>3</sub> (**A3**), CH<sub>3</sub> (**A4**), Cl (**A5**), Br (**A6**), I (**A7**), F (**A8**), CN (**A9**), COOH (**A10**), COCH<sub>3</sub> (**A11**), NO<sub>2</sub> (**A12**)).

#### 4.1.2. Solvent effects on the azo–hydrazone tautomerism

Since the tautomeric equilibria strongly depend on the nature of the media, the behavior of selected arylazo pyridone dyes in thirteen protic and aprotic solvents was studied. For this purpose, the absorption spectra of the pyridone dyes (**A1–A12**) at a concentration  $1 \times 10^{-5}$  mol dm<sup>-3</sup> were recorded over the  $\lambda$  range between 200 and 600 nm in the selected solvent set. The characteristic absorption spectra of the investigated azo dyes in methanol and dimethyl sulfoxide are shown in Figures 4.1 and 4.2.

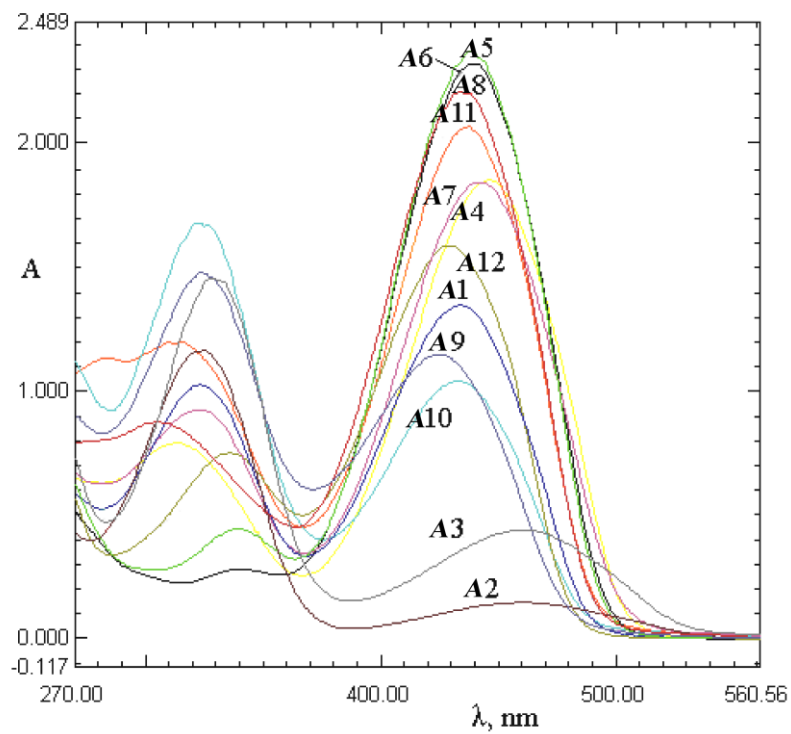


Figure 4.1. Absorption spectra of dyes **A1–A12** in methanol.

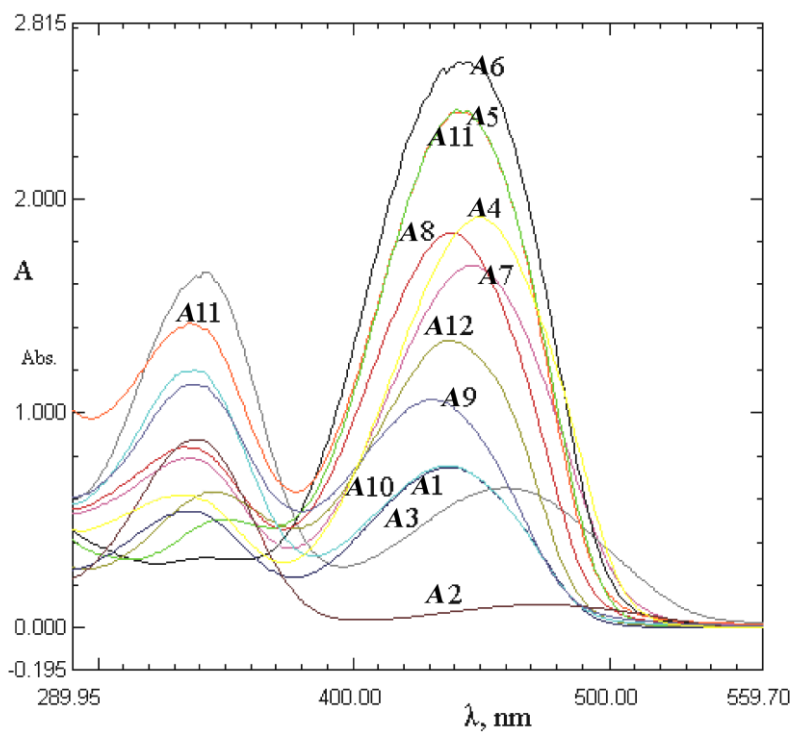


Figure 4.2. Absorption spectra of dyes **A1–A12** in dimethyl sulfoxide.

The UV-vis absorption spectra of all the dyes showed a weak band at about 260–370 nm, assigned to the azo tautomeric form and a strong band at 375–550 nm, which was assigned to hydrazone tautomeric form. The absorption maxima, which correspond to a transition in which electron density is transferred from the hydrazone –NH group to the pyridone carbonyl group (lower energy band), are presented in Tables 4.1 and 4.2. It was observed that, although slightly positive solvatochromism is evident, the absorption spectra of dyes **A1–A12** did not change significantly in all the employed solvents and the absorption maxima did not correlate with the polarity of the solvent.

Table 4.1. Absorption maxima of the hydrazone tautomer (B) of arylazo pyridone dyes (**A1–A12**) in protic solvents.

Dye No.	$\lambda_{\max}$ (nm)					
	Methanol	Ethanol	Propan-1-ol	Propan-2-ol	Butan-1-ol	2-Methyl-2-propanol
<b>A1</b>	433	434	434	433	433	431
<b>A2</b>	460	470	476	472	470	474
<b>A3</b>	460	458	458	455	448	454
<b>A4</b>	445	446	447	445	446	445
<b>A5</b>	437	435	438	439	439	439
<b>A6</b>	437	438	438	438	442	440
<b>A7</b>	440	442	443	442	442	442
<b>A8</b>	433	436	436	434	436	436
<b>A9</b>	424	426	425	425	425	424
<b>A10</b>	432	432	433	433	433	433
<b>A11</b>	437	436	436	435	435	435
<b>A12</b>	429	428	429	428	428	427

Table 4.2. Absorption maxima of hydrazone tautomer (**B**) of arylazo pyridone dyes (**A1**–**A12**) in aprotic solvents.

Dye No.	$\lambda_{\max}$ (nm)						
	Tetrahydrofuran	Dioxane	Methyl acetate	Ethyl acetate	<i>N,N</i> -Dimethylformamide	<i>N,N</i> -Dimethylacetamide	Dimethyl sulfoxide
<b>A1</b>	431	430	430	429	415	428	437
<b>A2</b>	466	461	460	460	470	470	473
<b>A3</b>	455	455	454	454	449	456	459
<b>A4</b>	442	442	441	440	423	441	449
<b>A5</b>	434	437	434	433	417	427	440
<b>A6</b>	436	437	434	433	421	425	441
<b>A7</b>	439	441	437	437	425	432	447
<b>A8</b>	432	432	431	429	410	422	437
<b>A9</b>	426	426	423	423	433	434	430
<b>A10</b>	431	432	429	429	431	433	437
<b>A11</b>	434	436	433	432	436	439	442
<b>A12</b>	429	430	427	427	451	452	437

Additional evidence for the solvent effect on the structure-property relationship of arylazo pyridone dyes was obtained from the correlation of the absorption frequencies ( $\nu = 1 / \lambda$  in  $\text{cm}^{-1}$ ) for the hydrazone tautomeric form (Tables 4.1 and 4.2) with the Kamlet-Taft Solvatochromic Equation 4.1 [150] of the following form:

$$\nu = \nu_0 + s\pi^* + b\beta + a\alpha \quad (4.1)$$

where  $\pi^*$  is an index of the solvent dipolarity / polarizability,  $\beta$  is a measure of the solvent hydrogen-bonding acceptor (HBA) basicity,  $\alpha$  is a measure of the solvent hydrogen-bonding donor (HBD) acidity and  $\nu_0$  is the regression value of the solute property in cyclohexane as the reference solvent. The regression coefficients  $s$ ,  $b$  and  $a$  in Eq. 4.1 are a measure the relative susceptibilities of the absorption frequencies to the indicated solvent parameters. The linear solvation energy relationship (LSER) concept

developed by Kamlet and Taft is one of the most ambitious and successful quantitative treatments of solvation effects. This treatment assumes attractive interactions between a solute and its environment and enables an estimation of the ability of the investigated compounds to form hydrogen bonds. The solvent parameters [151] are given in Table 4.3. The correlations of the absorption frequencies  $\nu_{\max}$  for hydrazone tautomer were realized by means of multiple linear regression analysis. It was found that  $\nu_{\max}$  in the selected solvent sets showed satisfactory correlation with the  $\pi^*$ ,  $\beta$  and  $\alpha$  parameters. The results of the multiple regressions are presented in Tables 4.4 and 4.5, and the coefficients  $\nu_0$ ,  $s$ ,  $b$  and  $a$  fitted at the 95 % confidence level are presented in Table 4.4. The negative sign of the  $a$  coefficient (Table 4.4) for all dyes (excluding the H, CN, COOH and NO<sub>2</sub> substituents) and the  $s$  and  $b$  coefficients for strong electron-donating substituents and strong electron-accepting substituents indicate a bathochromic shifts with increasing solvent dipolarity / polarizability and solvent hydrogen bond acidity and basicity. This suggests stabilization of the electron excited state relative to the ground state. The positive sign of the  $a$  coefficient for strong electron-accepting substituents and the  $s$  and  $b$  coefficients for moderate electron-donating and electron-accepting substituents indicate hypsochromic shifts with increasing solvent dipolarity / polarizability and both types of hydrogen bonding effects. These results showed that the solvent effect on the UV-vis absorption spectra of the investigated azo pyridone dyes is very complex and strongly dependent on the nature of the substituent on the arylazo component. They also indicated that the electronic behavior of the nitrogen atoms of hydrazone group are somewhat different between derivatives with electron-donating and electron-accepting substituents (Figure 4.3, Structures **C** and **D**). This phenomenon is caused by the difference in the conjugational or migrating ability of the electron lone pairs on the nitrogen atoms of the pyridone azo dyes. The strong electron-donating substituents in the phenyl group produce extensive delocalization in the arylazo group (Figure 4.3, Structure **D**), while the influence of the strong electron-accepting substituents are opposite, due to the positive charge on the nitrogen atom in the hydrazone tautomer (Figure 4.3, Structure **C**).

Table 4.3. Solvent parameters [151]

No.	Solvent	$\pi^*$	$\beta$	$\alpha$
1	Methanol	0.60	0.62	0.93
2	Ethanol	0.54	0.77	0.83
3	Propan-1-ol	0.52	0.83	0.8
4	Propan-2-ol	0.48	0.95	0.76
5	Butan-1-ol	0.47	0.88	0.79
6	2-Methyl-2-propanol	0.41	0.11	0.68
7	Tetrahydrofuran	0.58	0.55	0
8	Dioxane	0.55	0.37	0
9	Methyl acetate	0.60	0.42	0
10	Ethyl acetate	0.55	0.45	0
11	<i>N,N</i> -Dimethylformamide	0.88	0.69	0
12	<i>N,N</i> -Dimethylacetamide	0.88	0.76	0
13	Dimethyl sulfoxide	1.00	0.76	0

Table 4.4. Regression fits to the solvatochromic parameters (Eq. 4.1)

No.	Substituent	$\nu_0 \times 10^{-3}$ ( $\text{cm}^{-1}$ )	$s \times 10^{-3}$ ( $\text{cm}^{-1}$ )	$b \times 10^{-3}$ ( $\text{cm}^{-1}$ )	$a \times 10^{-3}$ ( $\text{cm}^{-1}$ )	$r^a$	$s^b$	$F^c$	Solvents used in the calculation <sup>d</sup>
<b>A1</b>	H	21.92 ( $\pm 0.180$ )	1.81 ( $\pm 0.240$ )	0.80 ( $\pm 0.170$ )	0.52 ( $\pm 0.100$ )	0.9789	0.078	46	1–11
<b>A2</b>	OH	21.34 ( $\pm 0.155$ )	-0.53 ( $\pm 0.269$ )	-0.86 ( $\pm 0.280$ )	-0.20 ( $\pm 0.191$ )	0.9417	0.099	21	2–13
<b>A3</b>	OCH <sub>3</sub>	23.02 ( $\pm 0.159$ )	-0.66 ( $\pm 0.089$ )	0.22 ( $\pm 0.078$ )	-0.31 ( $\pm 0.104$ )	0.9614	0.037	24	1–10,13
<b>A4</b>	CH <sub>3</sub>	23.02 ( $\pm 0.159$ )	-0.44 ( $\pm 0.222$ )	-0.19 ( $\pm 0.197$ )	-0.24 ( $\pm 0.118$ )	0.8128	0.099	5	1–10,12,13
<b>A5</b>	Cl	21.28 ( $\pm 0.183$ )	2.57 ( $\pm 0.246$ )	0.61 ( $\pm 0.176$ )	-0.31 ( $\pm 0.098$ )	0.9802	0.081	57	1–11
<b>A6</b>	Br	21.61 ( $\pm 0.194$ )	2.11 ( $\pm 0.260$ )	0.38 ( $\pm 0.186$ )	-0.27 ( $\pm 0.104$ )	0.9703	0.085	38	1–11
<b>A7</b>	I	21.39 ( $\pm 0.164$ )	2.01 ( $\pm 0.210$ )	0.50 ( $\pm 0.147$ )	-0.25 ( $\pm 0.083$ )	0.9812	0.067	52	1–9,11
<b>A8</b>	F	21.14 ( $\pm 0.256$ )	3.02 ( $\pm 0.344$ )	0.79 ( $\pm 0.246$ )	-0.43 ( $\pm 0.138$ )	0.9738	0.113	43	1–11
<b>A9</b>	CN	24.50 ( $\pm 0.102$ )	-1.21 ( $\pm 0.114$ )	-0.51 ( $\pm 0.097$ )	0.10 ( $\pm 0.051$ )	0.9862	0.042	71	1–7,10–12
<b>A10</b>	COOH	24.58 ( $\pm 0.097$ )	-1.25 ( $\pm 0.121$ )	-0.57 ( $\pm 0.098$ )	0.09 ( $\pm 0.055$ )	0.9823	0.046	64	1–7, 9–12
<b>A11</b>	COCH <sub>3</sub>	23.73 ( $\pm 0.050$ )	-0.92 ( $\pm 0.062$ )	-0.23 ( $\pm 0.057$ )	-0.16 ( $\pm 0.033$ )	0.9878	0.027	94	1–12
<b>A12</b>	NO <sub>2</sub>	27.02 ( $\pm 0.398$ )	-5.14 ( $\pm 0.533$ )	-1.71 ( $\pm 0.382$ )	0.47 ( $\pm 0.214$ )	0.9735	0.176	42	1–7,9,10, 12,13

<sup>a</sup> Correlation coefficient; <sup>b</sup> Standard error of the estimate; <sup>c</sup> Fisher's test; <sup>d</sup> Solvent number as given in Table 4.3.

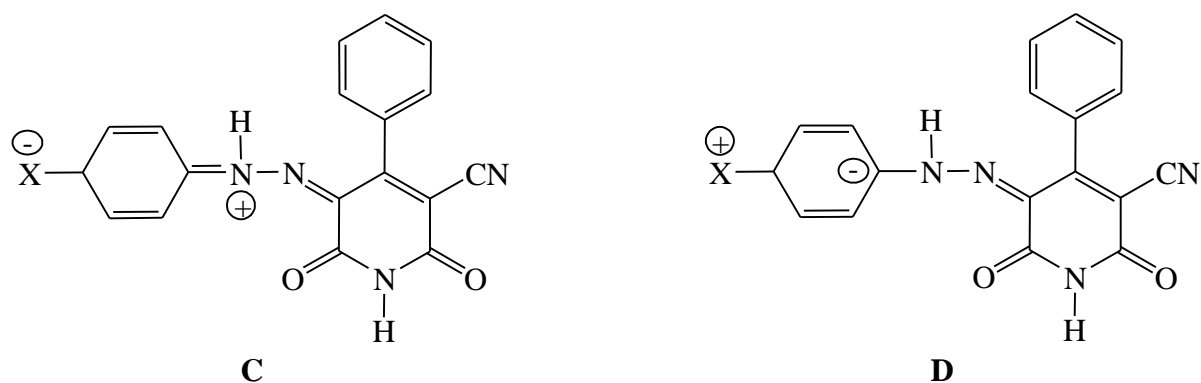


Figure 4.3. Resonance effect of electron-accepting (structure **C**) and electron-donating (structure **D**) substituents of the arylazo component on the hydrazone tautomer.

The percentage contributions of the solvatochromic parameters (Table 4.5) for the azo dyes with strong and moderate electron-accepting substituents on the arylazo group, showed that the most of the solvatochromism is due to the solvent dipolarity / polarizability rather than to the solvent acidity and basicity. These results could be explained by the effect of the positive charge on the nitrogen atom in the hydrazone tautomer (Figure 4.3, Structure **C**) and stabilization of this form mostly due to the solvent dipolarity / polarizability (non-specific solute-solvent interactions) than by hydrogen bond donating and hydrogen bond accepting properties (specific solute-solvent interactions).

Table 4.5. Percentage contribution of the solvatochromic parameters

Substituent	$P_{\pi^*}$ (%)	$P_{\beta}$ (%)	$P_{\alpha}$ (%)
H	58	25	17
OH	33	54	13
OCH <sub>3</sub>	55	19	26
CH <sub>3</sub>	50	22	28
Cl	74	17	9
Br	76	14	40
I	73	18	9
F	71	19	10
CN	66	28	6
COOH	65	30	5
COCH <sub>3</sub>	70	18	12
NO <sub>2</sub>	70	23	7

#### 4.1.3. Substituent effects on the azo–hydrazone tautomerism

As seen in Tables 4.1 and 4.2, the absorption spectra of the *p*-nitro derivative (dye **A12**) were shifted hypsochromically in all used solvents (excluding DMSO and DMF) when compared with dye **A1**. Moreover, the absorption spectra of the *p*-hydroxy and *p*-methoxy derivatives (dyes **A2** and **A3**) were shifted bathochromically in all used solvents when compared with dye **A1**. It is well known that the  $\lambda_{\max}$  values of the hydrazone tautomeric form of an azo dyes will show a general shift to shorter wavelengths when substituents of increasing electron withdrawing strength are introduced into the ring of the diazo component. In contrast, electron donor substituents produce strong bathochromic shifts [156]. The results presented in Tables 4.1 and 4.2 are in agreement with these conclusions. Thus, the observed relationship between the substituent constants and the  $\lambda_{\max}$  values strongly suggests that the lower energy absorption maxima of the investigated azo dyes originate from hydrazones (Scheme 4.1, Structure **B**).

In order to explain these results, the absorption frequencies were correlated by the Hammett Equation 4.2 using  $\sigma_p$  or  $\sigma_{p+}$  substituent constants [116]:

$$\nu = \nu_0 + \rho\sigma_p \quad (4.2)$$

where  $\rho$  is a proportionality constant reflecting the sensitivity of the absorption frequencies to the substituent effects. The substituent  $\sigma_p$  or  $\sigma_{p+}$  constants measure the electronic effect of the substituents. The plot  $\nu_{\max}$  vs. the  $\sigma_p$  substituent constants gave a correlation which showed deviations from the Hammett Equation in all dipolar aprotic solvents. However, a linear Hammett correlation was obtained in protic solvents. A better correlation of  $\nu_{\max}$  was obtained with the  $\sigma_{p+}$  substituent constants [125] than with the  $\sigma_p$  constants in all solvents, which indicates extensive delocalization in the arylazo group. The existence of the linear correlation with positive slope presented in Figure 4.4 and Equation 4.3 was interpreted as evidence of the diketohydrazone structure.

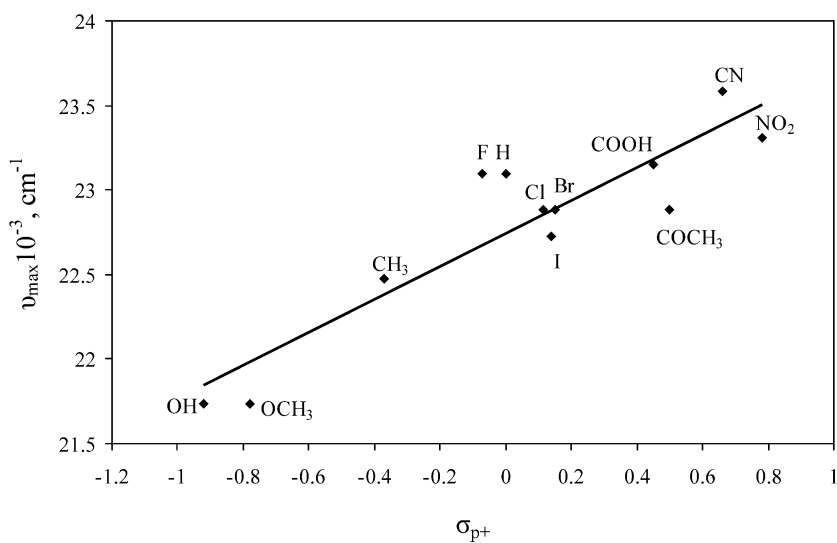


Figure 4.4. Relationship between  $\nu_{\max}$  and  $\sigma_{p+}$  for arylazo pyridone dyes **A1–A12** in methanol.

$$\nu_{\max} = 0.974 \sigma_{p+} + 22.744 \quad (4.3)$$

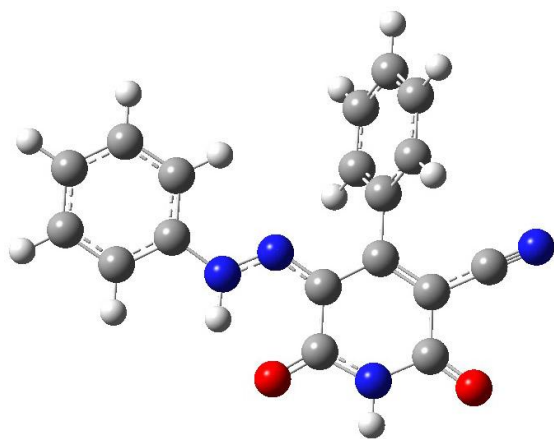
$(r = 0.9114, s = 0.25, F = 49, n = 12)$

#### 4.1.4. Quantum chemical calculations

DFT calculations were performed for different azo-hydrazone tautomers of dye **A1**. The structures were preliminary optimized by the semi-empirical PM3 method and the most stable geometries in vacuum were reoptimized at the B3LYP/6-31G(d) level of theory [106,107]. The Gaussian 03 program package was used [108]. The DFT calculations suggested that the diketohydrazone form (**a**) (Figure 4.5) is the most stable tautomer of dye **A1**. The relative energies and the statistical Boltzmann distribution weighted values of the most stable azo-hydrazone tautomers of dye **A1** are given in Table 4.6 and Figure 4.5.

Table 4.6. The relative energies and the statistical Boltzmann distribution weighted values of the most stable azo-hydrazone tautomers of dye **A1**

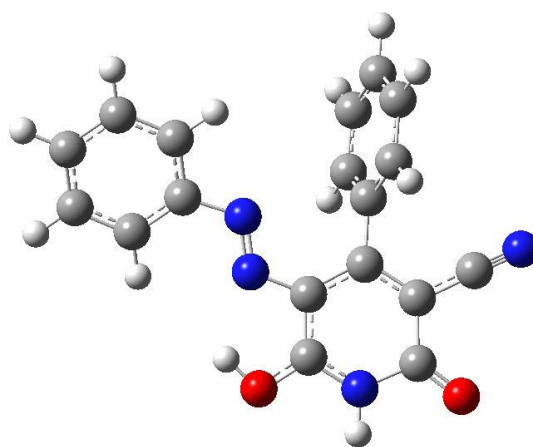
Tautomer of dye <b>A1</b>	Relative energies [kcal mol <sup>-1</sup> ]	Statistical Boltzmann distribution weighted values [%]
<b>(a)</b>	0.000	100.00
<b>(b)</b>	21.729	0.00



**(a)**

Relative energy = 0.000 kcal mol<sup>-1</sup>

Equilibrium population = 100.00%



**(b)**

Relative energy = 21.729 kcal mol<sup>-1</sup>

Equilibrium population = 0.00%

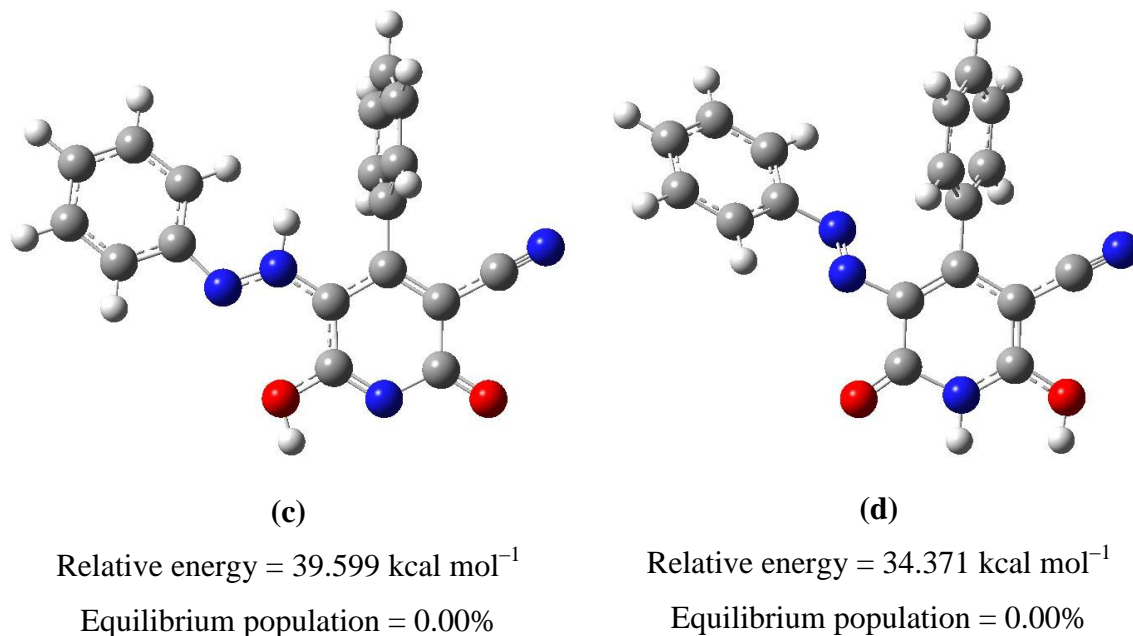
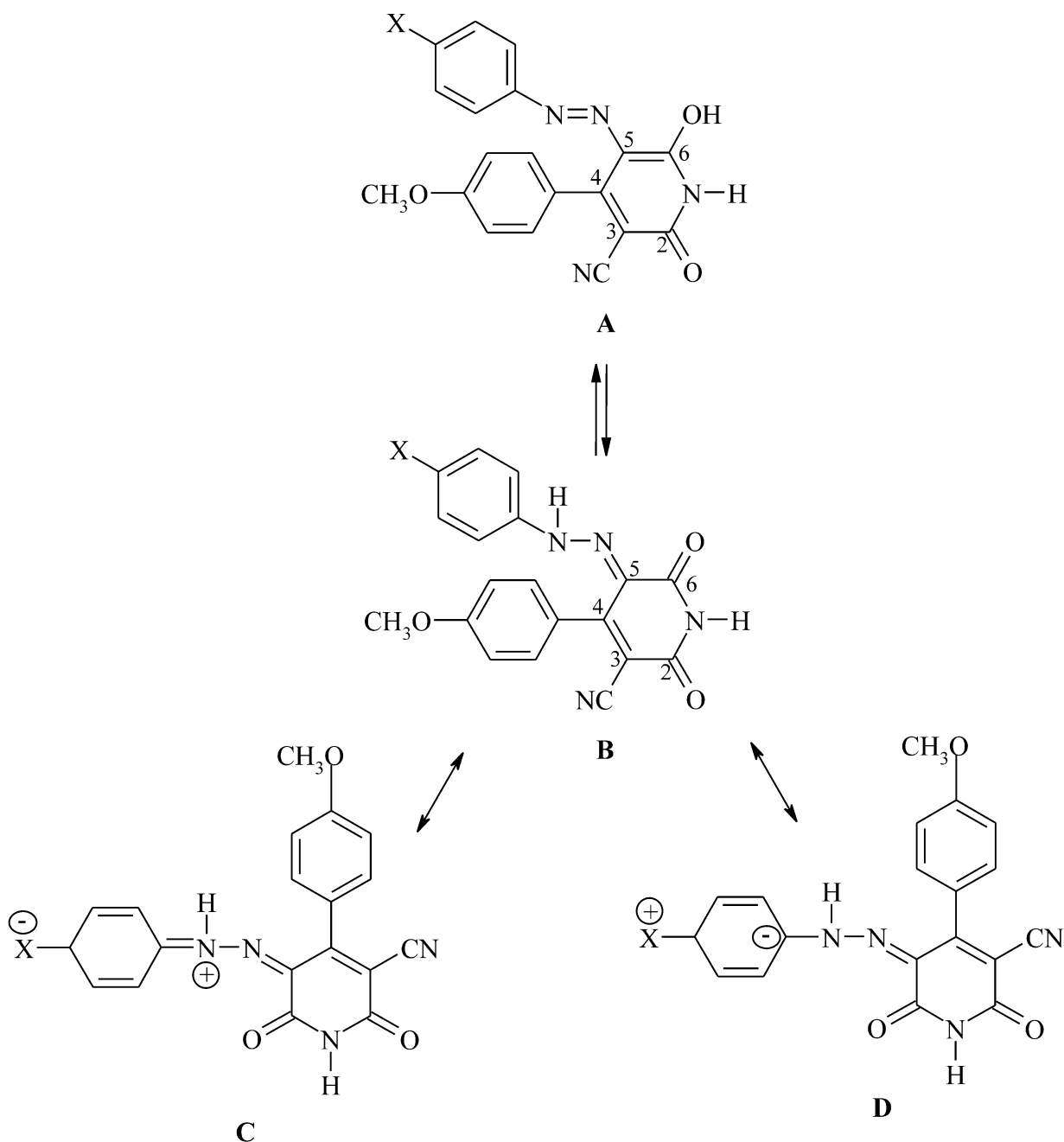


Figure 4.5. The most stable hydrazone tautomer (a) and some other azo-hydrazone tautomers of 5-phenylazo-6-hydroxy-4-phenyl-3-cyano-2-pyridone. (The geometries correspond to the energy minimum in vacuo).

#### 4.2. Solvent and structural effects on the UV-vis absorption spectra of 5-arylaazo-6-hydroxy-4-(4-methoxyphenyl)-3-cyano-2-pyridone dyes

In continuation of our investigations of novel arylazo pyridone dyes, eleven new 5-arylaazo-6-hydroxy-4-(4-methoxyphenyl)-3-cyano-2-pyridone dyes (Scheme. 4.2) were synthesized in order to characterize azo-hydrazone tautomerism, as well as to study the solvent and substituent effects on the electronic absorption spectra. The absorption spectra were recorded in the range from 300 to 600 nm in twenty solvents of different properties. Different solvent parameters, such as microscopic solvent polarity,  $E_T^N$ , relative permittivity,  $\epsilon_r$ , refractive index,  $n$ , the Kamlet-Taft and the Catalan parameters were used for describing the solute-solvent interactions and solvatochromic shifts of the UV-vis absorption band of the investigated arylazo pyridone dyes. For quantitative assessment of the substituent effects on the absorption frequencies, the simple Hammett equation was used.



**Scheme 4.2.** The equilibrium between azo form (**A**) and hydrazone form (**B**) of 5-aryldiazo-6-hydroxy-4-(4-methoxyphenyl)-3-cyano-2-pyridone dyes (X = H (**A13**), F (**A14**), Cl (**A15**), Br (**A16**), I (**A17**), OH (**A18**), CH<sub>3</sub> (**A19**), OCH<sub>3</sub> (**A20**), COCH<sub>3</sub> (**A21**), CN (**A22**), NO<sub>2</sub> (**A23**)). Resonance effect of electron-accepting (structure **C**) and electron-donating (structure **D**) substituents of the arylazo component on the hydrazone tautomer.

#### 4.2.1. Spectral characteristics of arylazo pyridone dyes

The 5-arylazo-6-hydroxy-4-(4-methoxyphenyl)-3-cyano-2-pyridone dyes can exist in two tautomeric forms (Scheme 4.2). The infrared spectra of all synthesized dyes showed two intense carbonyl bands at about 1642 and 1699  $\text{cm}^{-1}$ , which were assigned to the diketohydrazone form. The spectra exhibited broad bands in the region 3137–3225  $\text{cm}^{-1}$  and 3421–3438  $\text{cm}^{-1}$  which were assigned to the N–H group from pyridone ring and hydrazone form, respectively.

The  $^1\text{H}$ NMR spectra of the dyes exhibit a broad signal near 14.34–14.69 ppm. This signal corresponds to imine NH proton resonance of the hydrazone form (Scheme 4.2, Structure **B**). Ertan and Gurkan [83] have reported the  $^1\text{H}$  NMR spectra of some azo pyridone dyes in  $\text{CF}_3\text{COOD}/\text{CDCl}_3$  and showed that these dyes exist in the hydrazone form with NH peaks in the range of 15.1–15.6 ppm.  $^{13}\text{C}$  NMR studies of some N-alkyl derivatives of azopyridones in solutions in  $\text{CDCl}_3$  and  $\text{DMSO}-d_6$  by Lucka and Machacek [155] and Cee *et al.* [102] led to conclusion that pyridone azo dyes exist in the hydrazone form. Our experimental results are in agreement with these results.

Physical properties of the solvents including the Kamlet-Taft solvatochromic parameters  $\alpha$ ,  $\beta$  and  $\pi^*$  were taken from Ref. [150], whereas the Catalan SP, SdP, SA and SB solvent from Ref. [157], and the relative permittivity,  $\epsilon_r$ , refractive index,  $n$ , and the  $E_T^N$  solvent polarity from Ref. [142]. Substituent constants,  $\sigma_p$  and  $\sigma_{p+}$ , were taken from Ref. [125].

The correlation analysis was carried out using Microsoft Excel software, which considers the 95% confidence level. The goodness of the fit is discussed using the correlation coefficient ( $R$ ), the standard error of the estimate ( $s$ ) and Fischer's significance test ( $F$ ).

#### 4.2.2. Solvent effects on the UV-vis absorption spectra

The electronic absorption spectra of 5-arylazo-6-hydroxy-4-(4-methoxyphenyl)-3-cyano-2-pyridone dyes (**A13–A23**) were measured at room temperature in twenty solvents in the range 300–600 nm and the characteristic spectra in representative solvents are shown in Fig. 4.6. The UV-vis spectra of all dyes showed a weak band at about 330–

360 nm and a strong band at 420–480 nm which was assigned to azo and hydrazone tautomeric form, respectively. The absorption maxima, which correspond to a transition in which electron density is transferred from the hydrazone –NH group to the pyridone carbonyl group (lower energy band), is presented in Table 4.7 and were studied.

The physical parameters of the solvents used are listed in Table 4.8: relative permittivity,  $\epsilon_r$ , refractive index,  $n$ , the  $E_T^N$  and corresponding solvent parameters used for the Kamlet-Taft and Catalan parameters. The solvents are arranged with increasing their relative permittivity.

To explain the effects of solvents and substituents on electronic absorption spectra of azo pyridone dyes, the absorption maxima of the lower energy band of the unsubstituted dye (**A13**) in different solvents, was taken as the reference. The data from Table 4.7 confirm that the positions of the UV-vis absorption frequencies depend on the nature of the used solvent and substituent on the benzene ring of the coupling component. The introduction of electron-donating substituents in the benzene ring produced bathochromic shift of absorption maxima as compared to that of the unsubstituted azo dye in all solvents (Fig. 4.6). Electron-attracting substituents caused bathochromic or hypsochromic shifts when there is a change from polar to non-polar solvents, respectively.

Also, on going from aprotic to protic solvents, a bathochromic shift of the low-energy absorption band is observed. Azo pyridone dyes show positive solvatochromism i.e. the position of the absorption maxima of the lower energy band is shifted to a lower energy with increasing the solvent polarity / dipolarity. This behavior indicates that the azo pyridone dyes are more polar in the excited state than in their ground state.

Table 4.7. The absorption frequencies of the investigated compounds (**A13–A23**) in selected solvents.

Solvent / No.	$\nu_{\max} \times 10^{-3} \text{ (cm}^{-1}\text{)}$										
	<b>A13</b>	<b>A14</b>	<b>A15</b>	<b>A16</b>	<b>A17</b>	<b>A18</b>	<b>A19</b>	<b>A20</b>	<b>A21</b>	<b>A22</b>	<b>A23</b>
Dioxane	23.20	23.22	23.02	22.90	22.79	21.73	22.88	22.12	23.18	23.34	23.18
Disopropyl ether	23.32	23.26	23.10	23.06	22.90	21.70	22.80	22.00	23.24	23.59	23.54
Diethyl ether	23.28	23.27	23.13	23.12	22.92	21.70	22.94	22.22	23.19	23.54	23.51
Chloroform	22.78	22.78	22.52	22.57	22.32	21.57	22.40	21.48	22.73	23.09	22.96
Ethyl acetate	23.27	23.26	23.14	23.08	22.89	21.77	23.06	22.21	23.01	23.54	23.34
Methyl acetate	23.25	23.15	23.08	22.90	22.91	21.73	22.95	22.10	23.16	23.52	23.32
Tetrahydrofuran	23.18	23.15	23.07	23.00	22.84	21.56	22.95	22.14	23.02	23.40	23.22
Cyclohexanone	22.81	23.00	22.97	22.98	22.70	21.44	22.75	21.98	22.85	23.30	23.13
Butan-2-ol	22.96	22.92	22.92	22.83	22.60	21.03	22.73	22.37	23.08	23.24	22.88
Butan-1-ol	22.97	22.96	22.89	22.78	22.70	21.00	22.67	22.37	23.18	23.28	22.87
Propan-2-ol	23.06	23.10	22.90	22.87	22.90	21.12	22.98	22.94	22.86	23.32	23.42
Propan-1-ol	22.98	23.06	22.88	22.85	22.93	21.16	22.84	22.55	22.84	23.26	23.28
Acetone	23.21	23.12	23.10	23.14	22.84	21.65	22.86	22.16	23.23	23.47	23.35
Ethanol	23.07	23.12	22.92	22.90	22.97	21.74	23.05	22.63	22.93	23.42	23.39
Ethylene glycol	22.73	22.73	22.68	22.57	22.35	21.11	22.53	22.22	22.57	23.09	22.83
Methanol	23.09	23.00	22.89	22.84	22.85	21.28	22.79	22.50	22.95	23.38	23.25
Acetonitrile	23.18	23.13	23.00	23.00	22.73	21.68	22.77	22.18	22.95	23.37	23.18
<i>N,N</i> -Dimethylformamide	23.15	23.24	23.09	23.46	22.68	21.28	23.42	22.04	22.82	23.25	22.71
<i>N,N</i> -Dimethylacetamide	23.07	23.26	22.99	22.96	22.65	21.25	22.70	22.08	22.78	23.23	23.04
Dimethyl sulfoxide	22.95	23.04	22.77	22.84	22.43	21.14	22.65	21.83	22.65	23.04	22.78

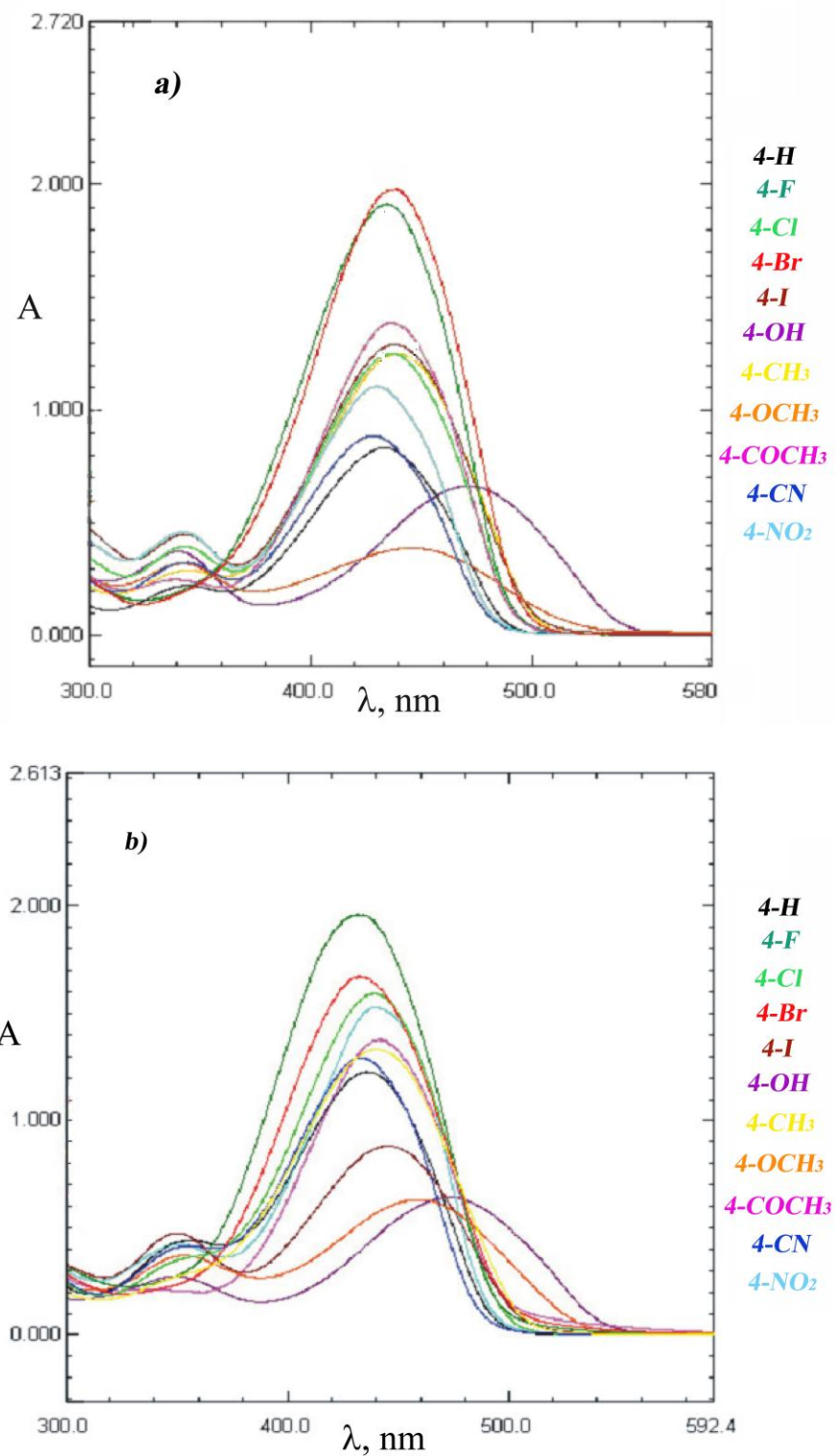


Figure 4.6. The UV-vis absorption spectra of 5-arylaazo-6-hydroxy-4-(4-methoxyphenyl)-3-cyano-2-pyridone dyes in ethanol (a) and dimethyl sulfoxide (b).

Table 4.8. The physical parameters of the solvents.

No.	Solvent	Kamlet-Taft						Catalan			
		$\epsilon_r$	n	$E_T^N$	$\pi^*$	$\beta$	$\alpha$	SP	SdP	SB	SA
1	Dioxane	2.21	1.4224	0.164	0.49	0.37	0.00	0.737	0.312	0.444	0.000
2	Disopropyl ether	3.80	1.3680	0.105	0.27	0.49	0.00	0.625	0.324	0.657	0.000
3	Diethyl ether	4.20	1.3524	0.117	0.24	0.47	0.00	0.617	0.385	0.562	0.000
4	Chloroform	4.81	1.4459	0.259	0.53	0.10	0.20	0.783	0.614	0.071	0.047
5	Ethyl acetate	6.02	1.3724	0.228	0.45	0.45	0.00	0.656	0.603	0.542	0.000
6	Methyl acetate	6.68	1.3614	0.253	0.60	0.42	0.00	0.645	0.637	0.527	0.000
7	Tetrahydrofuran	7.58	1.4072	0.207	0.55	0.55	0.00	0.714	0.634	0.591	0.000
8	Cyclohexanone	15.00	1.4648	0.281	0.68	0.53	0.00	0.760	0.745	0.482	0.000
9	Butan-2-ol	16.56	1.3971	0.506	0.40	0.80	0.69	0.656	0.706	0.888	0.221
10	Butan-1-ol	17.51	1.3993	0.586	0.47	0.84	0.84	0.674	0.655	0.809	0.341
11	Propan-2-ol	19.92	1.3772	0.546	0.48	0.84	0.76	0.633	0.808	0.830	0.283
12	Propan-1-ol	20.45	1.3856	0.617	0.52	0.90	0.84	0.658	0.748	0.782	0.367
13	Acetone	20.56	1.3587	0.355	0.62	0.48	0.08	0.651	0.907	0.475	0.000
14	Ethanol	24.55	1.3614	0.654	0.54	0.75	0.86	0.633	0.783	0.658	0.400
15	Ethylene glycol	31.69	1.4475	0.790	0.92	0.52	0.90	0.777	0.910	0.534	0.717
16	Methanol	32.66	1.3284	0.762	0.60	0.66	0.98	0.608	0.904	0.545	0.605
17	Acetonitrile	35.94	1.3441	0.460	0.66	0.40	0.19	0.645	0.974	0.286	0.044
18	<i>N,N</i> -Dimethylformamide	36.71	1.4305	0.386	0.88	0.69	0.00	0.759	0.977	0.613	0.031
19	<i>N,N</i> -Dimethylacetamide	37.78	1.4384	0.377	0.88	0.76	0.00	0.763	0.987	0.650	0.028
20	Dimethyl sulfoxide	46.45	1.4793	0.444	1.00	0.76	0.00	0.830	1.000	0.647	0.072

### 4.2.3. Absorption maxima of hydrazone form as a function of dispersive interaction

In order to explain the solvatochromic behavior of azo pyridone dyes, their spectral properties are correlated with different solvent polarity scales.

The dispersive interaction function,  $f(n)$  gives an indication of the atomic and electronic polarization part of the intermolecular interaction occurring between solutes dissolved in solutions. The dispersive function is given by the relation:

$$f(n) = \frac{n^2 - 1}{n^2 + 1} \quad (4.4)$$

where  $n$  is refractive index of solvent. The correlation between  $\nu_{max}$  of the studied compounds and the solvent dispersive function,  $f(n)$ , proves that dispersion forces can strongly influence the position of the azo pyridone dyes visible absorption band. Instead, in this case for all studied samples the plots  $\nu_{max}$  as a function of  $n$  or  $f(n)$  deviate from linearity for all used solvents. The linear relations are obtained for two isolated solvent classes (Table 4.9). The plot of  $\nu_{max}$  for all studied dyes versus relative permittivity gives correlation which shows deviation from linearity in all investigated solvents indicating that the relative permittivity is not the sole parameter governing the solvent shift (data not shown).

The nonlinear character of  $\nu_{max}$  as a function of  $f(n)$  show that specific solvent effects have an important influence on solvatochromism and is examined.

Table 4.9. The results of the correlation between  $v_{max}$  and the solvent disperzive function  $f(n)$ .

Dyes	$v_{max}$ vs. $f(n)$	Solvent excluded from the calculation <sup>a</sup>
<b>A13</b>	I. $v_{max} = -4.04 f(n) + 24.50$ (R = 0.935, n = 9)	
	II. $v_{max} = -5.09 f(n) + 24.61$ (R = 0.920, n = 11)	
<b>A14</b>	I. $v_{max} = -3.50 f(n) + 24.31$ (R = 0.976, n = 6)	(1, 16, 18, 19)
	II. $v_{max} = -6.50 f(n) + 25.06$ (R = 0.969, n = 10)	
<b>A15</b>	I. $v_{max} = -4.70 f(n) + 24.61$ (R = 0.906, n = 6)	(16, 17, 18)
	II. $v_{max} = -8.14 f(n) + 25.49$ (R = 0.923, n = 11)	
<b>A16</b>	I. $v_{max} = -3.41 f(n) + 24.11$ (R = 0.955, n = 7)	(8, 16, 18)
	II. $v_{max} = -5.83 f(n) + 24.62$ (R = 0.807, n = 10)	
<b>A17</b>	I. $v_{max} = -5.35 f(n) + 24.55$ (R = 0.919, n = 13)	
	II. $v_{max} = -6.60 f(n) + 24.71$ (R = 0.932, n = 7)	
<b>A18</b>	I. $v_{max} = -8.35 f(n) + 24.19$ (R = 0.943, n = 12)	(1, 4, 8)
	II. $v_{max} = -5.33 f(n) + 22.77$ (R = 0.923, n = 5)	
<b>A19</b>	I. $v_{max} = -5.56 f(n) + 24.73$ (R = 0.954, n = 8)	(16, 17, 18)
	II. $v_{max} = -7.78 f(n) + 25.22$ (R = 0.954, n = 9)	
<b>A20</b>	I. $v_{max} = -10.26 f(n) + 25.67$ (R = 0.921, n = 11)	(11)
	II. $v_{max} = -12.23 f(n) + 25.80$ (R = 0.955, n = 8)	
<b>A21</b>	I. $v_{max} = -5.09 f(n) + 24.73$ (R = 0.916, n = 8)	(1, 15, 18)
	II. $v_{max} = -3.35 f(n) + 23.92$ (R = 0.916, n = 9)	
<b>A22</b>	I. $v_{max} = -4.12 f(n) + 24.78$ (R = 0.940, n = 7)	(13, 14)
	II. $v_{max} = -3.52 f(n) + 24.38$ (R = 0.921, n = 11)	
<b>A23</b>	I. $v_{max} = -7.70 f(n) + 25.72$ (R = 0.905, n = 15)	
	II. $v_{max} = -8.19 f(n) + 25.52$ (R = 0.999, n = 5)	

<sup>a</sup>Solvent number as given in Table 4.8.

#### 4.2.4. Variation of absorption maxima with $E_T^N$

The empirical solvent polarity index,  $E_T^N$  is also used to study the solvent-solute interaction influence on electronic transitions for the all studied azo pyridone dyes. The plot of the absorption maxima of the dyes against the solvent empirical polarity scale gives nonlinear correlation for all used solvents. The linear relations are obtained for two separated solvent classes, each with good linearity but different slopes (Fig. 4.7). The deviation from linear correlation between  $\nu_{max}$  and  $E_T^N$  values can be explained by taking into account that  $E_T^N$  represent a dipolarity / polarizability and acidity contributions. These results indicated that basicity contributions of solvent play an important role on absorption spectra of the studied dyes and should be included in correlation.

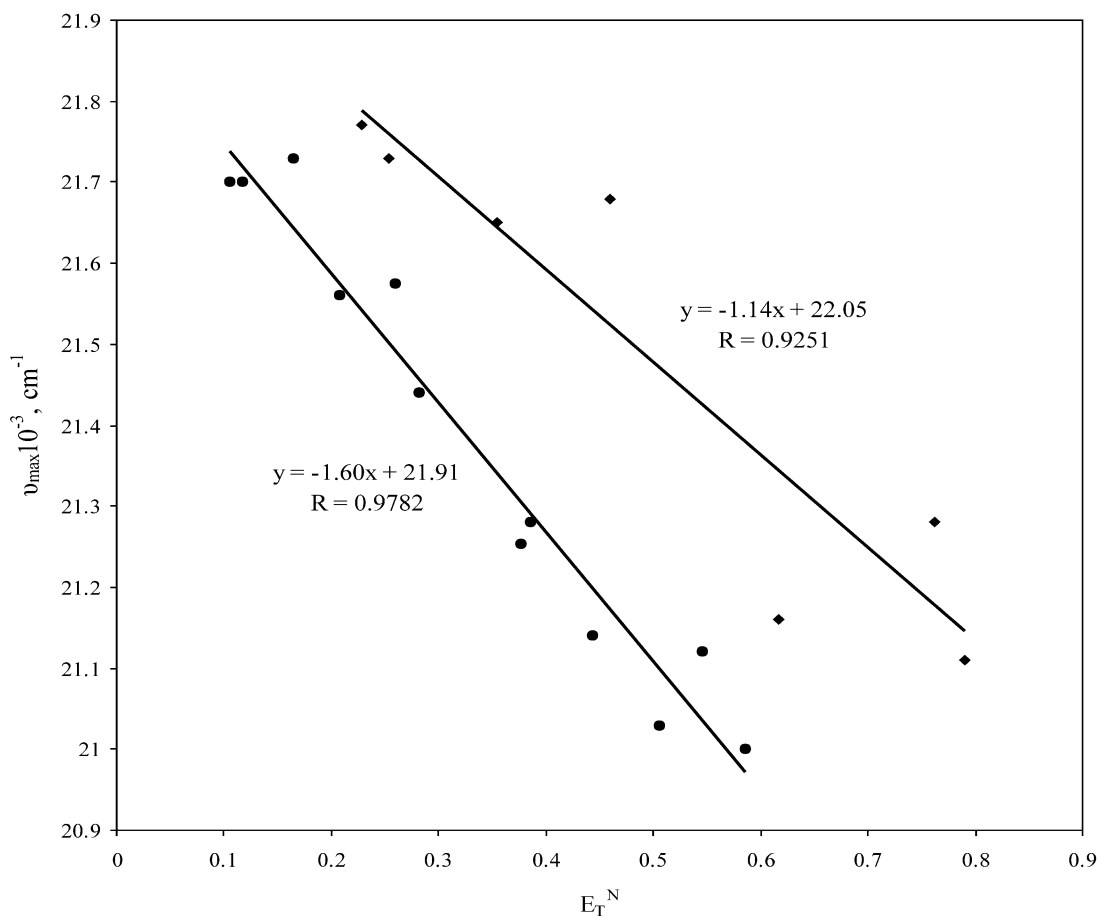


Figure 4.7. The correlation of  $\nu_{max}$  of the dye **A18** with  $E_T^N$  (excluded ethanol).

#### 4.2.5. Correlation with multiparameter solvent polarity scales

The effect of solvent dipolarity / polarizability and hydrogen bonding on the absorption spectra are interpreted by means of linear solvation energy relationship (LSER) using a Kamlet–Taft solvatochromic equation 4.1 (Kamlet et al., 1981) of the following form:

$$\nu = \nu_0 + s\pi^* + b\beta + a\alpha \quad (4.1)$$

The solvent parameters are given in Table 4.3. The correlations of the absorption frequencies  $\nu_{max}$  for hydrazone tautomer were carried out by means of multiple linear regression analysis. The results of the multiple regressions are presented in Tables 4.10 and 4.11, and coefficients  $\nu_0$ ,  $s$ ,  $b$  and  $a$  (Table 10) fit at the 95% confidence level.

Table 4.10. Regression fits to the solvatochromic parameters (Eq. 4.1).

No.	Substituent	$\nu_0 \cdot 10^{-3}$ ( $\text{cm}^{-1}$ )	$s \cdot 10^{-3}$ ( $\text{cm}^{-1}$ )	$b \cdot 10^{-3}$ ( $\text{cm}^{-1}$ )	$a \cdot 10^{-3}$ ( $\text{cm}^{-1}$ )	$R^a$	$s^b$	$F^c$	$n^d$
A13	H	23.30 ( $\pm 0.064$ )	-0.32 ( $\pm 0.063$ )	0.21 ( $\pm 0.100$ )	-0.40 ( $\pm 0.046$ )	0.9787	0.041	61	12
A14	F	23.30 ( $\pm 0.063$ )	-0.41 ( $\pm 0.065$ )	0.22 ( $\pm 0.105$ )	-0.31 ( $\pm 0.048$ )	0.9654	0.047	37	12
A15	Cl	23.41 ( $\pm 0.061$ )	-0.47 ( $\pm 0.060$ )	-0.20 ( $\pm 0.088$ )	-0.15 ( $\pm 0.036$ )	0.9593	0.042	38	14
A16	Br	23.05 ( $\pm 0.060$ )	-0.36 ( $\pm 0.062$ )	0.27 ( $\pm 0.101$ )	-0.34 ( $\pm 0.045$ )	0.9505	0.050	31	14
A17	I	22.87 ( $\pm 0.074$ )	-0.69 ( $\pm 0.077$ )	0.58 ( $\pm 0.124$ )	-0.16 ( $\pm 0.053$ )	0.9643	0.055	31	11
A18	OH	22.22 ( $\pm 0.127$ )	-0.39 ( $\pm 0.125$ )	-0.78 ( $\pm 0.198$ )	-0.35 ( $\pm 0.092$ )	0.9728	0.081	47	12
A19	CH <sub>3</sub>	23.34 ( $\pm 0.073$ )	-0.51 ( $\pm 0.077$ )	-0.24 ( $\pm 0.101$ )	-0.28 ( $\pm 0.046$ )	0.9714	0.048	33	10
A20	OCH <sub>3</sub>	22.39 ( $\pm 0.084$ )	-0.69 ( $\pm 0.111$ )	0.28 ( $\pm 0.131$ )	0.37 ( $\pm 0.050$ )	0.9670	0.065	48	14
A21	COCH <sub>3</sub>	23.39 ( $\pm 0.045$ )	-0.72 ( $\pm 0.158$ )	/ <sup>e</sup>	-0.16 ( $\pm 0.040$ )	0.9605	0.057	65	14
A22	CN	23.85 ( $\pm 0.064$ )	-0.55 ( $\pm 0.064$ )	-0.23 ( $\pm 0.104$ )	-0.12 ( $\pm 0.045$ )	0.9587	0.053	38	14
A23	NO <sub>2</sub>	23.93 ( $\pm 0.065$ )	-1.12 ( $\pm 0.084$ )	0.13 ( $\pm 0.046$ )	-0.17 ( $\pm 0.065$ )	0.9683	0.070	60	16

<sup>a</sup> Correlation coefficient.<sup>b</sup> Standard error of the estimate.<sup>c</sup> Fisher's test.<sup>d</sup> Number of solvents included in correlation.<sup>e</sup> Negligible value with high standard error.

Table 4.11. Percentage contribution of solvatochromic parameters (Eq. 4.1).

No.	Substituent	$P_{\pi^*}$ (%)	$P_{\beta}$ (%)	$P_{\alpha}$ (%)
<b>A13</b>	H	34.4	22.6	43.0
<b>A14</b>	F	43.6	23.4	33.0
<b>A15</b>	Cl	57.3	24.4	18.3
<b>A16</b>	Br	37.1	27.8	35.1
<b>A17</b>	I	48.2	40.6	11.2
<b>A18</b>	OH	25.7	51.3	23.0
<b>A19</b>	CH <sub>3</sub>	49.5	23.3	27.2
<b>A20</b>	OCH <sub>3</sub>	51.4	20.9	27.7
<b>A21</b>	COCH <sub>3</sub>	81.8	0.0	18.2
<b>A22</b>	CN	61.1	25.6	13.3
<b>A23</b>	NO <sub>2</sub>	78.9	9.2	11.9

The influence of solvent characteristics on the shift of  $\nu_{max}$  is additionally analyzed using the linear solvation energy relationship (LSER) model of Catalan [157], given by Eq. 4.5:

$$\nu = \nu_0 + aSA + bSB + cSP + dSdP \quad (4.5)$$

where  $SA$ ,  $SB$ ,  $SP$  and  $SdP$  characterize solvent acidity, basicity, polarizability and dipolarity of a solvent, respectively; and  $a-d$  are the regression coefficients describing the sensitivity of the absorption maxima to the different types of the solvent–solute interactions. The advantage of this concept in regard to Kamlet–Taft solvatochromic model is that it gives possibility to separate non-specific solvent effects into two terms: dipolarity and polarizability. The results of the multiple regressions are presented in Tables 4.12 and 4.13.

Table 4.12. Regression fits to solvatochromic parameters (Eq. 4.5).

No.	Substituent	$\nu_0 \cdot 10^{-3}$ ( $\text{cm}^{-1}$ )	$d \cdot 10^{-3}$ ( $\text{cm}^{-1}$ )	$c \cdot 10^{-3}$ ( $\text{cm}^{-1}$ )	$b \cdot 10^{-3}$ ( $\text{cm}^{-1}$ )	$a \cdot 10^{-3}$ ( $\text{cm}^{-1}$ )	$R^a$	$s^b$	$F^c$	$n^d$
A13	H	24.03 ( $\pm 0.132$ )	-0.11 ( $\pm 0.038$ )	-0.95 ( $\pm 0.169$ )	-0.16 ( $\pm 0.070$ )	-0.53 ( $\pm 0.041$ )	0.9936	0.024	136	12
A14	F	23.66 ( $\pm 0.175$ )	0.22 ( $\pm 0.094$ )	-1.31 ( $\pm 0.263$ )	0.51 ( $\pm 0.096$ )	-0.57 ( $\pm 0.074$ )	0.9542	0.059	25	15
A15	Cl	23.92 ( $\pm 0.105$ )	-0.29 ( $\pm 0.074$ )	-0.83 ( $\pm 0.158$ )	-0.20 ( $\pm 0.063$ )	-0.29 ( $\pm 0.047$ )	0.9776	0.033	48	14
A16	Br	23.70 ( $\pm 0.159$ )	0.15 ( $\pm 0.069$ )	-1.47 ( $\pm 0.215$ )	0.44 ( $\pm 0.094$ )	-0.56 ( $\pm 0.067$ )	0.9674	0.054	33	14
A17	I	24.35 ( $\pm 0.167$ )	-0.25 ( $\pm 0.081$ )	-2.25 ( $\pm 0.225$ )	0.40 ( $\pm 0.114$ )	-0.25 ( $\pm 0.067$ )	0.9664	0.055	35	15
A18	OH	23.69 ( $\pm 0.418$ )	-0.27 ( $\pm 0.111$ )	-1.61 ( $\pm 0.525$ )	-1.46 ( $\pm 0.216$ )	-0.46 ( $\pm 0.125$ )	0.9814	0.071	46	12
A19	CH <sub>3</sub>	23.97 ( $\pm 0.211$ )	-0.31 ( $\pm 0.103$ )	-1.72 ( $\pm 0.268$ )	0.64 ( $\pm 0.110$ )	-0.25 ( $\pm 0.083$ )	0.9580	0.067	25	14
A20	OCH <sub>3</sub>	23.51 ( $\pm 0.260$ )	0.29 ( $\pm 0.140$ )	-2.81 ( $\pm 0.382$ )	0.58 ( $\pm 0.122$ )	0.45 ( $\pm 0.111$ )	0.9638	0.084	36	16
A21	COCH <sub>3</sub>	24.09 ( $\pm 0.165$ )	-0.46 ( $\pm 0.080$ )	-1.11 ( $\pm 0.264$ )	<sup>e</sup>	-0.32 ( $\pm 0.079$ )	0.9633	0.059	47	15
A22	CN	24.61 ( $\pm 0.159$ )	-0.28 ( $\pm 0.082$ )	-1.30 ( $\pm 0.252$ )	-0.21 ( $\pm 0.104$ )	-0.25 ( $\pm 0.070$ )	0.9684	0.049	34	14
A23	NO <sub>2</sub>	25.02 ( $\pm 0.147$ )	-0.24 ( $\pm 0.065$ )	-2.50 ( $\pm 0.197$ )	0.23 ( $\pm 0.078$ )	-0.21 ( $\pm 0.062$ )	0.9792	0.051	70	17

<sup>a</sup> Correlation coefficient.<sup>b</sup> Standard error of the estimate.<sup>c</sup> Fisher's test.<sup>d</sup> Number of solvents included in correlation.<sup>e</sup> Negligible value with high standard error.

Table 4.13. Percentage contribution of solvatochromic parameters (Eq. 4.5).

No.	Substituent	P <sub>SdP</sub> (%)	P <sub>SP</sub> (%)	P <sub>B</sub> (%)	P <sub>A</sub> (%)
<b>A13</b>	H	6.3	54.3	9.1	30.3
<b>A14</b>	F	8.4	50.2	19.5	21.9
<b>A15</b>	Cl	18.0	51.6	12.4	18.0
<b>A16</b>	Br	5.7	56.1	16.9	21.3
<b>A17</b>	I	7.9	71.4	12.8	7.9
<b>A18</b>	OH	7.1	42.4	38.4	12.1
<b>A19</b>	CH <sub>3</sub>	10.6	58.9	21.9	8.6
<b>A20</b>	OCH <sub>3</sub>	7.0	68.0	14.0	11.0
<b>A21</b>	COCH <sub>3</sub>	24.3	58.7	0.0	17.0
<b>A22</b>	CN	13.7	63.7	10.3	12.3
<b>A23</b>	NO <sub>2</sub>	7.5	78.6	7.2	6.7

It was found that absorption frequencies of hydrazone form for azo dyes in selected solvents show satisfactory correlation with  $\pi^*$ ,  $\beta$  and  $\alpha$  as well as with *SdP*, *SP*, *SB* and *SA* parameters. However, the multiple regression analysis of the  $\nu_{max}$  data using Kamlet-Taft model in which non-specific solvent effects are included in single parameter  $\pi^*$ , leads to a smaller correlation quality (R) and / or smaller number of solvents (n) which are included in correlations. The advantage of Catalan solvatochromic model stems from separation of non-specific interaction on polarity and polarizability solvent effects. As it can see from Tables 4.11 and 4.13 the solvent polarizability is the main factor that influences on the spectral shifts of all investigated compounds.

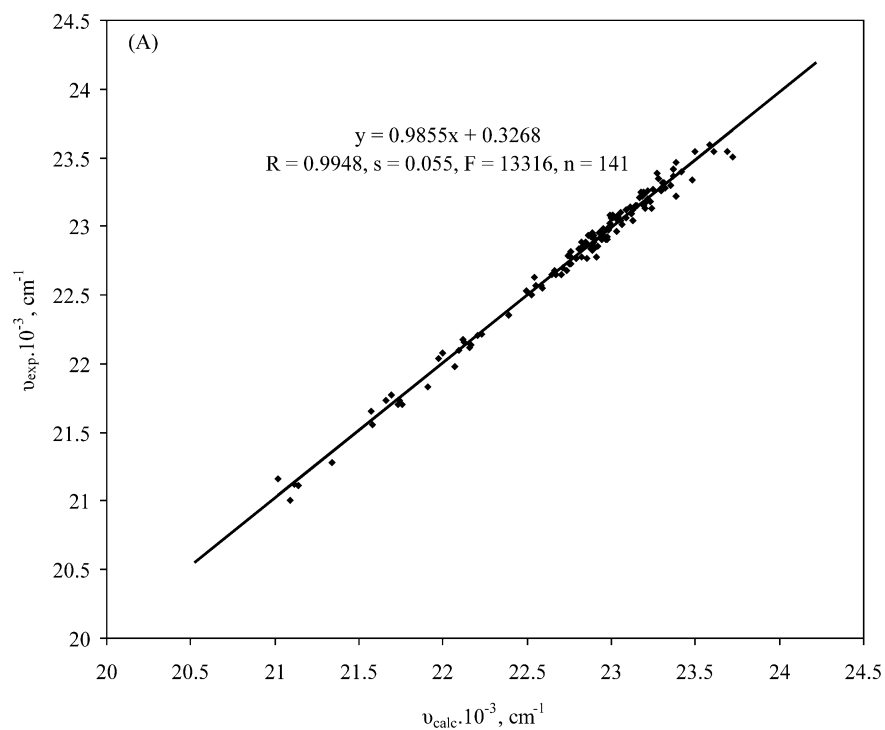
From the analysis of absorption frequencies according to Kamlet-Taft equation 4.1 it was found that the negative sign of *a* coefficient (excluding CH<sub>3</sub>O substituent) and *s* coefficient for all arylazo dyes (Table 4.10) indicate a bathochromic shifts with both increasing solvent hydrogen-bond acidity and solvent polarity. This suggests stabilization of the electron excited state relative to the ground state. The positive sign of *b* coefficient for all investigated dyes (excluding **A15**, **A18**, **A19** and **A22**) indicate a hypsochromic shifts with increasing of solvent hydrogen-bond acceptor basicity which suggests stabilization of the ground state relative to the electronic excited state.

The percentage contribution of solvatochromic parameters (Table 4.11) examined separately, for all azo dyes showed (excluding **A13** and **A18**) that the most of the solvatochromism is due to solvent dipolarity / polarizability rather than on the hydrogen-bond acidity or basicity. The percentage contribution of solvatochromic parameters for **A18** where hydrogen-bond basicity is the most important parameter can be explained by the effect of the positive charge on oxygen atom (from hydroxyl group in arylazo component) in the hydrazone tautomer (Scheme 4.2, Structure **D**) and stabilization of this form rather due to the solvent hydrogen bond acceptor basicity than through hydrogen bond donating acidity and solvent polarity.

Moreover, the multiparameter regression analysis according to Catalan equation 4.5 showed negative sign of *a* coefficient (excluding CH<sub>3</sub>O substituent) and *c* coefficient for all arylazo dyes (Table 4.12) indicate a bathochromic shifts with increasing of solvent hydrogen-bond acidity and solvent polarizability. The positive sign of *b* coefficient for all investigated dyes (excluding **A13**, **A15**, **A19** and **A22**) indicate a hypsochromic shifts with increasing solvent hydrogen-bond acceptor basicity. The negative sign of *d* coefficient (excluding **A14**, **A16** and **A20**) indicate a bathochromic shifts with increasing solvent dipolarity. The percentage contribution of solvatochromic parameters (Table 4.13) for all azo dyes showed that solvent polarizability is the most important parameter which influences the absorption frequencies shifts. Solvent hydrogen-bond acidity and basicity have a moderate influence on solvatochromism, whereby the effect of solvent acidity has a more significant impact compared with the solvent basicity. Solvent dipolarity (Table 4.13) has negligible impact on solvatochromism (excluding **A21**).

All the results obtained using Kamlet-Taft and Catalan model indicate that the solvent effects on azo-hydrazone equilibrium and UV-vis absorption spectra of the investigated azo pyridone dyes are very complex and strongly dependable on the nature of the substituent on the arylazo component. This also indicated that the electronic behavior of the nitrogen atoms of hydrazone group is somewhat different between derivatives with electron-donating and electron-accepting substituents (Scheme 4.2, Structures **C** and **D**). In all cases, the use of Catalan scale gives better regressions than the Kamlet-Taft model. The advantage of Catalan model derived from the division of non-specific solvent characteristics on solvent polarizability and dipolarity which allows

better insight into influence of these interactions on solvatochromism and as shown in Tables 4.11 and 4.13 non-specific solvent interactions have a major impact on the absorption maxima shifts. The degree of success of Eq. 4.1 and Eq. 4.5 are shown in Fig. 4.8 for all investigated compounds, and excellent linear relationships between the experimental values of  $\nu_{max}$  and the predicted absorption maxima calculated with Eq. 4.1 and Eq. 4.5 are observed.



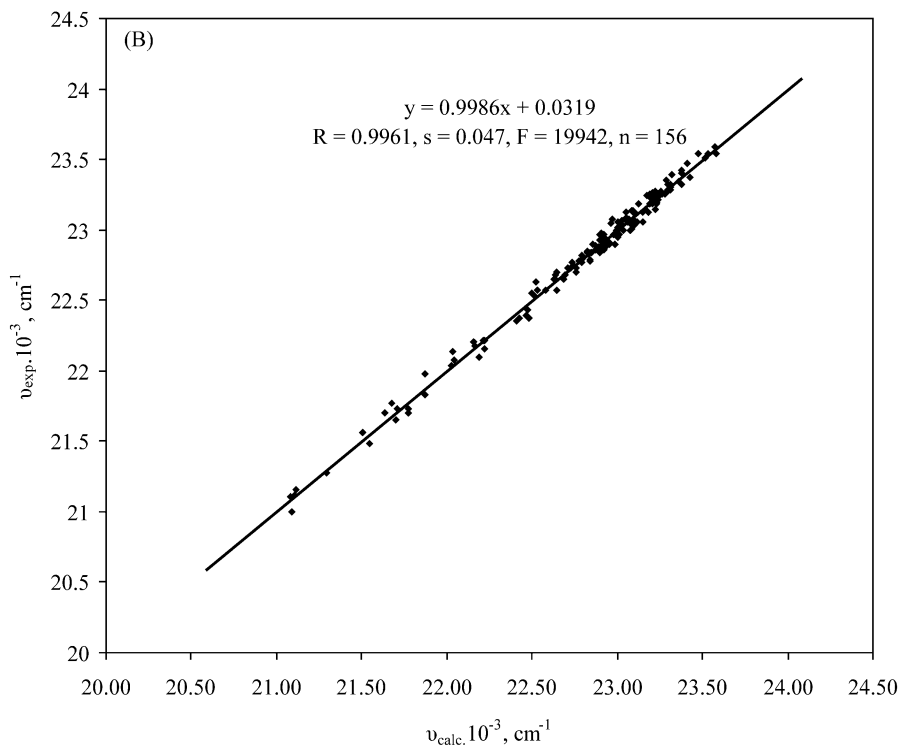


Figure 4.8. Experimental versus calculated values of  $\nu_{\max}$  from Eq. 4.1 (A) and Eq. 4.5 (B).

#### 4.2.6. Substituents effects on the UV-vis absorption spectra

As seen in Table 4.7, the absorption spectra of **A15–A20** dyes were shifted bathochromically in all used solvents when compared to dye **A13**. The absorption spectra of the dyes with electron-accepting substituents were generally shifted hypsochromically in all used solvents (excluding dipolar aprotic solvents) when compared to dye **A13**. It is well known that the absorption maxima of the hydrazone tautomeric form of an azo dyes shift to higher wavelengths when substituents with electron donating characteristics are introduced into the ring of the diazo component. In contrast, electron-accepting substituents generally produce hypsochromic shift. The results presented in Table 4.7 are in agreement with this conclusion and observed relationship strongly suggests that the absorption maxima of the lower energy band of investigated azo dyes originates from hydrazone tautomeric form (Scheme. 4.2, **B**).

The linear free energy relationship (LFER) methodology was applied to the  $\nu_{\max}$  of the studied arylazo pyridone dyes with the aim to get an insight into factors

determining the absorption maxima shifts. The transmission of electronic substituent effects was studied using the Hammett Equation, Eq. 4.2:

$$s = \rho \cdot \sigma + h \quad (4.2)$$

where  $s$  is a substituent-dependent value: absorption frequencies ( $\nu_{\max}$ ),  $\rho$  is the proportionality constant reflecting the sensitivity of the  $\nu_{\max}$  to the substituent effects,  $\sigma$  is the corresponding substituent constant (measure the electronic effect of the substituents), and  $h$  is the intercept (i.e., describes the unsubstituted member of the series).

The plot  $\nu_{\max}$  vs. the  $\sigma_p$  and  $\sigma_{p+}$  substituent constants gave a correlation which showed deviations from the Hammett Equation in all dipolar aprotic solvents. However, a linear Hammett correlation was obtained in protic and non-dipolar aprotic solvents (excluding **A14** and **A19**) (Fig. 4.8). A better correlation of  $\nu_{\max}$  was obtained with the  $\sigma_{p+}$  substituent constants than with the  $\sigma_p$  constants in the solvents used with exception of dipolar aprotic solvents, which indicates extensive delocalization in the azo group ( $-\text{N}=\text{N}-$ ). The existence of these correlations was interpreted as an evidence of significant effect of substituent on azo-hydrazone tautomerism. The azo group ( $-\text{N}=\text{N}-$ ) is an electron-acceptor group and the imino group ( $-\text{NH}-$ ) is an electron-donor, so that azo group is stabilized by the more electron-donating substituents, while an electron-accepting group stabilizes the hydrazone form. Satisfactory linear dependence with positive slope presented in Fig. 4.9 and Eq. 4.6 confirms the presence of a hydrazone form in observed solvent.

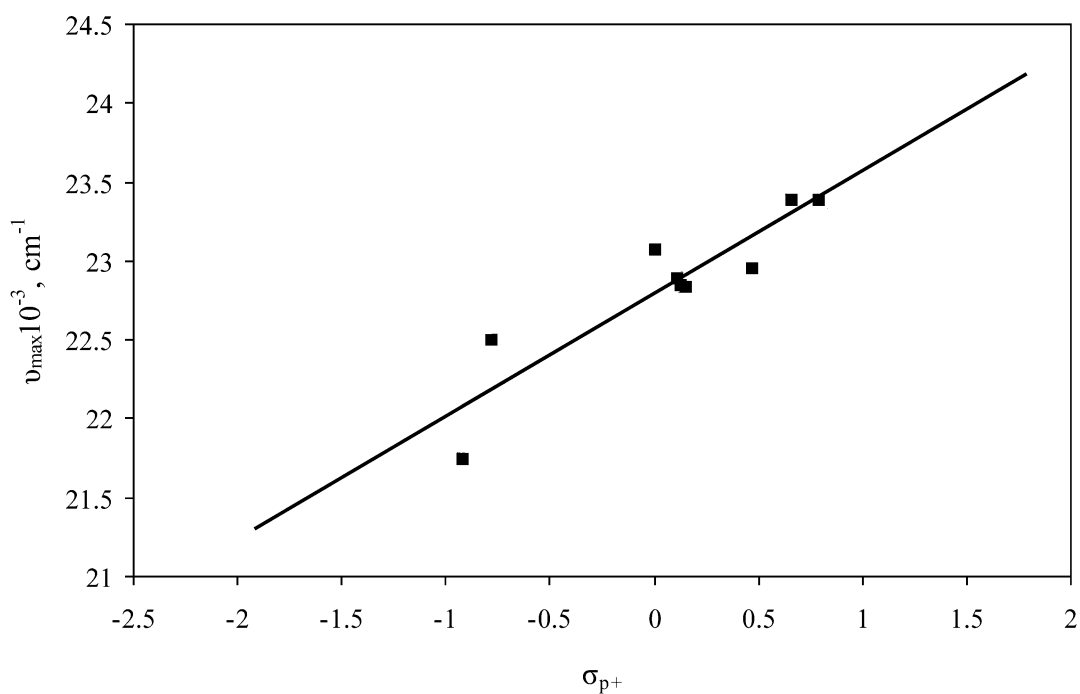


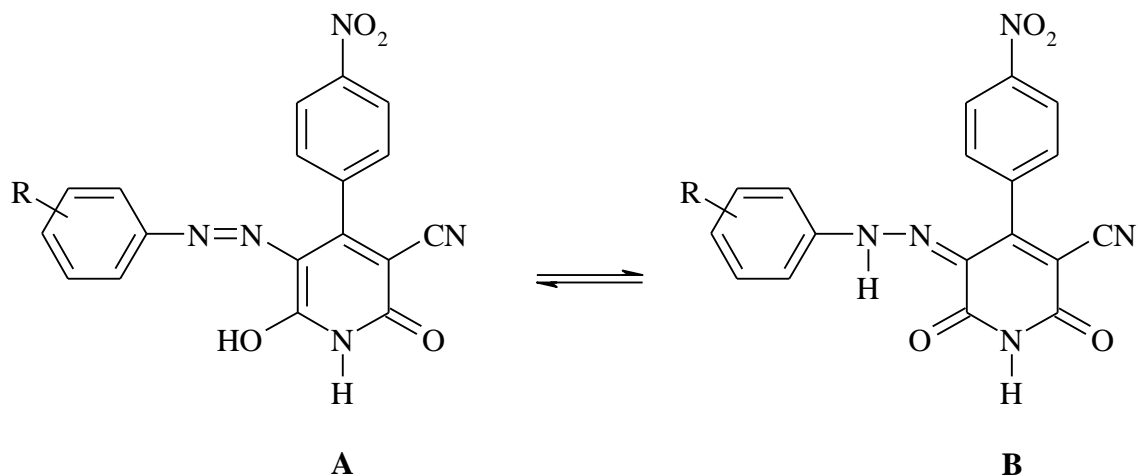
Figure 4.9. Relationship between  $\nu_{max}$  and  $\sigma_{p+}$  for arylazo pyridone dyes in ethanol (excluding **A14** and **A19**).

$$\nu_{max} = 0.776 \sigma_{p+} + 22.794 \quad (4.6)$$

( $r = 0.910$ ,  $s = 0.22$ ,  $F = 33$ ,  $n = 9$ )

### 4.3. Solvent and structural effects on the UV-vis absorption spectra of 5-arylazo-6-hydroxy-4-(4-nitrophenyl)-3-cyano-2-pyridone dyes

In the third part of this thesis ten new 5-arylazo-6-hydroxy-4-(4-nitrophenyl)-3-cyano-2-pyridone dyes (Scheme 4.3) have been synthesized and their solvatochromic properties have been studied in a set of twenty solvents of different properties. In order to describe the spectral changes and the solute - solvent interactions multiparameter Kamlet-Taft and Catalan solvent scales were used. The effects of the solvent and substituent on the azo - hydrazone tautomeric equilibrium were studied and evaluated.



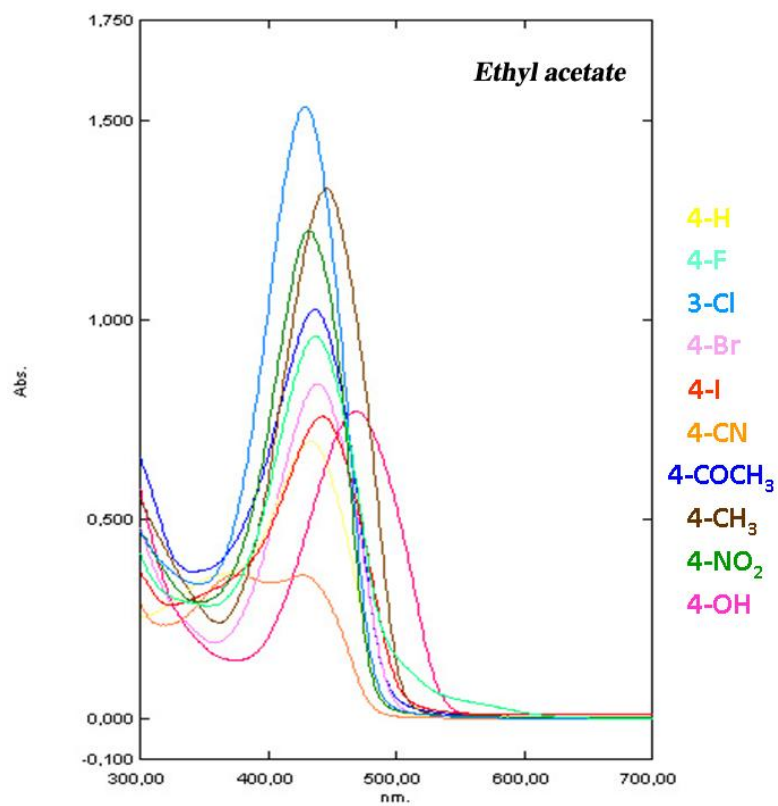
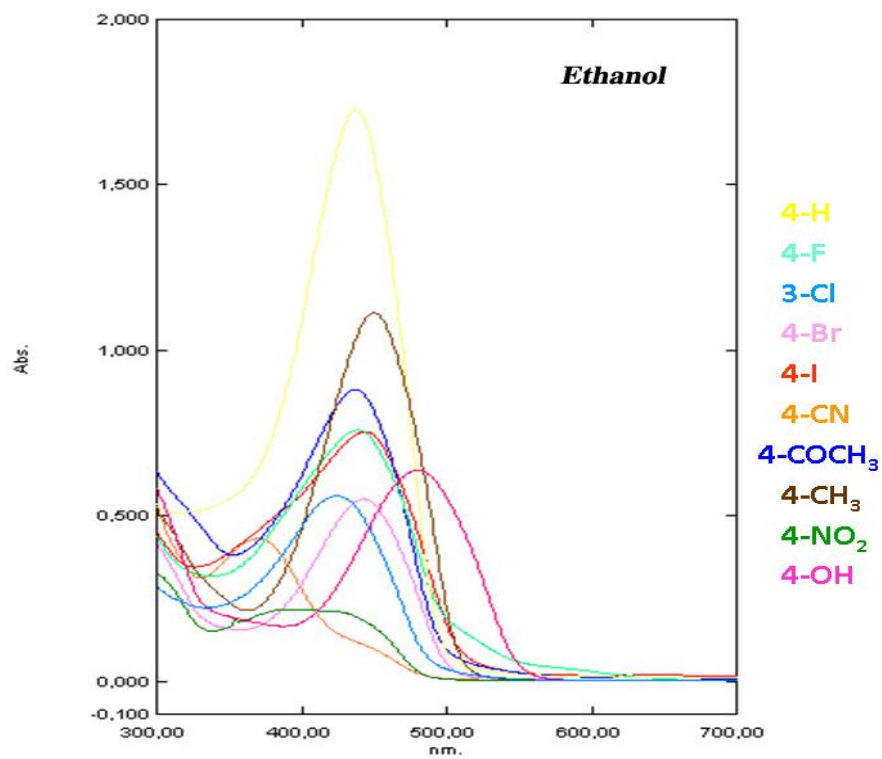
Scheme 4.3. The equilibrium between azo form (**A**) and hydrazone form (**B**) of 5-arylazo-6-hydroxy-4-(4-nitrophenyl)-3-cyano-2-pyridone dyes: R = H (**A24**), 4-F (**A25**), 3-Cl (**A26**), 4-Br (**A27**), 4-I (**A28**), 4-CN (**A29**), 4-COCH<sub>3</sub> (**A30**), 4-CH<sub>3</sub> (**A31**), 4-NO<sub>2</sub> (**A32**), 4-OH (**A33**).

#### 4.3.1. Spectral characteristics and solvatochromism

The infrared spectra of all the synthesized dyes showed two intense carbonyl bands at about 1643 and 1702 cm<sup>-1</sup>, which were assigned to the diketohydrazone form. The FT-IR spectra also showed a band at 3045 – 3268 cm<sup>-1</sup>, assigned to the imino group (N–H) of the heterocyclic (pyridine) ring and a band at 3432–3458 cm<sup>-1</sup> that was assigned to the N–H of hydrazone tautomeric form.

The <sup>1</sup>HNMR spectra of the dyes exhibited a broad signal near 14.38–14.69 ppm. This signal corresponds to the imine N–H proton resonance of the hydrazone form (Scheme 4.3, Structure **B**).

The UV-vis absorption spectra of 5-arylazo-6-hydroxy-4-(4-nitrophenyl)-3-cyano-2-pyridone dyes (**A24–A33**) were measured at room temperature in twenty solvents in the range 300–700 nm and the characteristic spectra in representative solvents are shown in Figure 4.10 (ethanol, ethyl acetate, dimethylformamide).



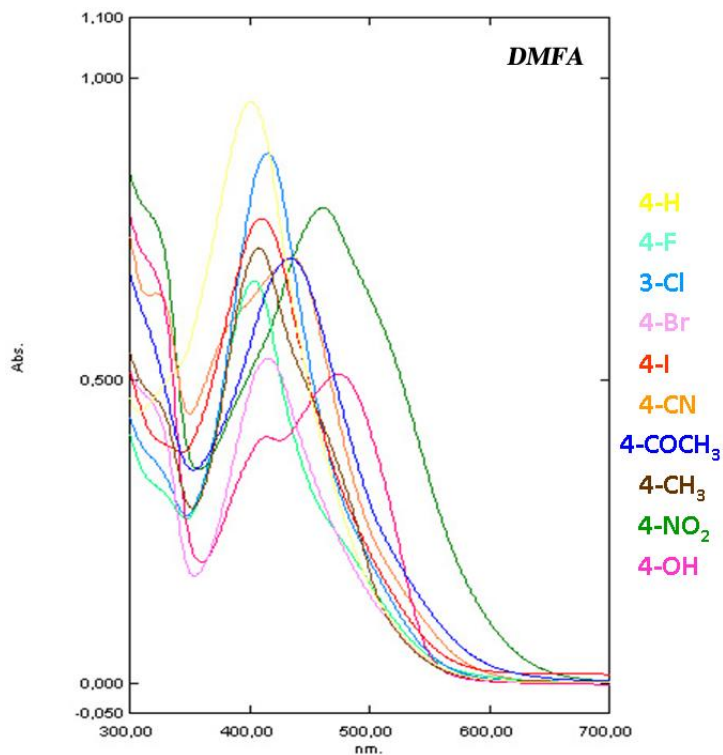


Figure 4.10. UV-vis absorption spectra of azo dyes in different solvents (ethanol, ethyl acetate, dimethylformamide).

The absorption maxima, which correspond to a transition in which electron density is transferred from the hydrazone  $\text{-NH}$  group to the pyridone carbonyl group (lower energy band) are presented in Table 4.14. It was observed that, although slightly positive solvatochromism is evident, the absorption spectra of dyes **A24–A33** did not change significantly in all the employed solvents and the absorption maxima did not correlate with the polarity of the solvent.

Table 4.14. The absorption frequencies of the investigated compounds (A24–A33) in selected solvents.

Solvent / No.	$\nu_{\max} \times 10^{-3} (\text{cm}^{-1})$									
	A24	A25	A26	A27	A28	A29	A30	A31	A32	A33
Methanol	23.20	22.88	23.47	22.73	22.68	23.36	22.94	22.27	23.09	21.01
Ethanol	24.10	23.09	24.51	22.57	22.83	22.94	23.09	22.22	23.53	20.88
Propan-1-ol	23.81	23.26	24.21	22.94	24.33	23.58	22.68	25.00	23.09	20.75
Propan-2-ol	23.42	22.94	23.53	22.57	22.52	22.73	23.15	22.22	23.36	20.70
Butan-1-ol	23.04	22.62	23.26	22.52	22.42	22.78	22.88	22.17	23.26	20.66
2-Methylpropan-1-ol	22.88	22.68	23.09	22.57	22.42	23.09	22.78	22.17	23.26	20.70
2-Methylpropan-2-ol	22.94	22.68	23.09	22.62	22.37	22.73	22.88	22.12	23.26	20.66
Acetonitrile	23.04	22.83	23.20	22.73	22.52	23.26	22.83	22.32	23.04	21.37
Acetone	22.94	22.88	23.31	22.78	22.57	23.36	22.83	22.37	23.09	21.28
1,2-Ethandiol	22.88	22.57	23.81	22.68	22.42	22.57	22.78	21.98	22.94	20.83
Dichloromethane	22.57	22.42	22.83	22.22	22.03	22.88	22.47	21.93	22.83	21.23
1,4-Dioxane	22.68	22.62	22.94	22.42	22.22	23.15	22.62	21.98	22.94	20.75
Tetrahydrofuran	22.99	22.83	24.39	22.73	22.57	23.26	22.83	22.37	23.09	20.66
Diisopropyl ether	22.62	22.99	23.42	22.83	22.68	23.31	23.04	22.52	24.04	21.23
Cyclohexanone	22.83	22.68	23.04	22.62	22.47	23.15	22.73	22.27	22.99	21.05
Ethyl acetate	23.09	22.88	23.36	22.78	22.57	23.36	22.83	22.42	23.20	21.32
Methyl acetate	23.04	22.91	23.31	22.75	22.57	23.39	22.88	22.42	23.20	21.34
Dimethyl sulfoxide	22.70	22.65	23.34	22.45	22.37	22.91	22.57	22.08	22.57	20.77
<i>N,N</i> -Dimethylformamide	25.25	25.19	24.57	24.81	24.88	25.00	23.58	22.03	22.32	21.10
<i>N,N</i> -Dimethylacetamide	23.39	22.88	23.26	22.57	22.60	23.15	22.78	22.25	22.86	20.88

The effect of solvent dipolarity / polarizability and hydrogen bonding on the absorption spectra are interpreted by means of LSER using Kamlet-Taft solvatochromic equation 4.1. The solvent parameters are given in Table 4.3. The correlations of the absorption frequencies  $\nu_{\max}$  for hydrazone tautomer were carried out by means of multiple linear regression analysis. The results are presented in Tables 4.15 and 4.16 and coefficients  $v_0$ ,  $s$ ,  $b$ ,  $a$  fit (Tab 4.15) at the 95% confidence level.

Table 4.15. Regression fits to the solvatochromic parameters (Eq. 4.1).

No.	Substituent	$v_0 \cdot 10^{-3}$ ( $\text{cm}^{-1}$ )	$s \cdot 10^{-3}$ ( $\text{cm}^{-1}$ )	$b \cdot 10^{-3}$ ( $\text{cm}^{-1}$ )	$a \cdot 10^{-3}$ ( $\text{cm}^{-1}$ )	$R^a$	$s^b$	$F^c$	$n^d$
<b>A24</b>	H	19.95 ( $\pm 0.452$ )	3.19 ( $\pm 0.593$ )	3.12 ( $\pm 0.545$ )	-0.89 ( $\pm 0.309$ )	0.928	0.300	19	13
<b>A25</b>	F	20.20 ( $\pm 0.463$ )	2.45 ( $\pm 0.536$ )	3.63 ( $\pm 0.569$ )	-1.83 ( $\pm 0.320$ )	0.920	0.312	16	13
<b>A26</b>	Cl	23.06 ( $\pm 0.180$ )	-0.60 ( $\pm 0.23$ )	1.01 ( $\pm 0.243$ )	0.89 ( $\pm 0.139$ )	0.957	0.160	33	13
<b>A27</b>	Br	19.40 ( $\pm 0.445$ )	4.03 ( $\pm 0.588$ )	2.37 ( $\pm 0.387$ )	-0.93 ( $\pm 0.229$ )	0.932	0.240	24	15
<b>A28</b>	I	18.90 ( $\pm 0.552$ )	4.26 ( $\pm 0.757$ )	2.86 ( $\pm 0.542$ )	-0.93 ( $\pm 0.305$ )	0.929	0.295	19	13
<b>A29</b>	CN	21.39 ( $\pm 0.368$ )	1.86 ( $\pm 0.423$ )	2.38 ( $\pm 0.446$ )	-1.81 ( $\pm 0.241$ )	0.928	0.247	21	14
<b>A30</b>	COCH <sub>3</sub>	22.99 ( $\pm 0.085$ )	-0.69 ( $\pm 0.103$ )	0.45 ( $\pm 0.112$ )	0.14 ( $\pm 0.054$ )	0.939	0.072	25	14
<b>A31</b>	CH <sub>3</sub>	22.89 ( $\pm 0.075$ )	-0.61 ( $\pm 0.076$ )	-0.37 ( $\pm 0.112$ )	-0.10 ( $\pm 0.043$ )	0.950	0.054	34	15
<b>A32</b>	NO <sub>2</sub>	24.88 ( $\pm 0.137$ )	-2.64 ( $\pm 0.171$ )	-0.33 ( $\pm 0.147$ )	-0.04 ( $\pm 0.083$ )	0.982	0.082	81	13
<b>A33</b>	OH	21.90 ( $\pm 0.116$ )	-0.23 ( $\pm 0.116$ )	-1.08 ( $\pm 0.151$ )	-0.21 ( $\pm 0.073$ )	0.953	0.091	39	16

<sup>a</sup> Correlation coefficient.

<sup>b</sup> Standard error of the estimate.

<sup>c</sup> Fisher's test.

<sup>d</sup> Number of solvents included in correlation.

Table 4.16. Percentage contribution of solvatochromic parameters (Eq. 4.1).

No.	Substituent	$P_{\pi^*}$ (%)	$P_{\beta}$ (%)	$P_{\alpha}$ (%)
<b>A24</b>	H	44.31	43.33	12.36
<b>A25</b>	F	30.97	45.89	23.14
<b>A26</b>	Cl	24.00	40.40	35.60
<b>A27</b>	Br	54.98	32.33	12.69
<b>A28</b>	I	52.92	35.53	11.55
<b>A29</b>	CN	30.74	39.34	29.92
<b>A30</b>	COCH <sub>3</sub>	53.91	35.16	10.94
<b>A31</b>	CH <sub>3</sub>	56.48	34.26	9.26
<b>A32</b>	NO <sub>2</sub>	87.71	10.96	1.33
<b>A33</b>	OH	15.13	71.05	13.82

The influence of solvent characteristics on the shift of  $\nu_{\max}$  was additionally analyzed using the linear solvation energy relationship model of Catalan given by Eq. 4.5. The results of the of multiple linear regression analysis are presented in Tables 4.17 and 4.18.

Table 4.17. Regression fits to solvatochromic parameters (Eq. 4.5).

No.	Substituent	$\nu_0 \cdot 10^{-3}$ ( $\text{cm}^{-1}$ )	$d \cdot 10^{-3}$ ( $\text{cm}^{-1}$ )	$c \cdot 10^{-3}$ ( $\text{cm}^{-1}$ )	$b \cdot 10^{-3}$ ( $\text{cm}^{-1}$ )	$a \cdot 10^{-3}$ ( $\text{cm}^{-1}$ )	R <sup>a</sup>	s <sup>b</sup>	F <sup>c</sup>	n <sup>d</sup>
A24	H	24.69 (±0.406)	0.02 (±0.177)	-2.99 (±0.545)	0.59 (±0.242)	1.99 (±0.293)	0.985	0.105	49	11
A25	F	23.69 (±0.218)	0.195 (±0.100)	-2.13 (±0.296)	0.94 (±0.133)	-0.17 (±0.089)	0.957	0.072	28	15
A26	Cl	23.98 (±0.335)	-0.29 (±0.137)	-2.27 (±0.467)	1.23 (±0.185)	1.06 (±0.147)	0.978	0.097	39	12
A27	Br	23.87 (±0.217)	0.25 (±0.091)	-2.40 (±0.314)	0.59 (±0.125)	-1.04 (±0.162)	0.949	0.064	21	14
A28	I	23.19 (±0.196)	0.28 (±0.090)	-1.98 (±0.268)	0.97 (±0.131)	-0.05 (±0.081)	0.963	0.065	29	14
A29	CN	24.33 (±0.341)	-0.05 (±0.143)	-1.10 (±0.460)	-0.54 (±0.218)	-0.88 (±0.150)	0.944	0.104	19	14
A30	COCH <sub>3</sub>	23.75 (±0.187)	-0.04 (±0.109)	-1.75 (±0.266)	0.58 (±0.111)	0.10 (±0.078)	0.960	0.062	27	14
A31	CH <sub>3</sub>	23.59 (±0.158)	-0.40 (±0.096)	-1.12 (±0.234)	-0.37 (±0.109)	-0.22 (±0.066)	0.959	0.051	29	15
A32	NO <sub>2</sub>	27.12 (±0.667)	-1.47 (±0.281)	-4.14 (±0.922)	-0.12 (±0.269)	-0.11 (±0.289)	0.949	0.145	18	13
A33	OH	22.89 (±0.197)	-0.36 (±0.119)	-1.07 (±0.292)	-1.35 (±0.111)	-0.33 (±0.079)	0.977	0.065	59	16

<sup>a</sup> Correlation coefficient.<sup>b</sup> Standard error of the estimate.<sup>c</sup> Fisher's test.<sup>d</sup> Number of solvents included in correlation.

Table 4.18. Percentage contribution of solvatochromic parameters (Eq. 4.5).

No.	Substituent	P <sub>SdP</sub> (%)	P <sub>SP</sub> (%)	P <sub>B</sub> (%)	P <sub>A</sub> (%)
<b>A24</b>	H	0.36	53.49	10.55	35.6
<b>A25</b>	F	5.68	62.01	27.37	4.95
<b>A26</b>	Cl	5.98	46.8	25.36	21.86
<b>A27</b>	Br	5.84	56.07	13.79	24.3
<b>A28</b>	I	8.54	60.37	29.57	1.52
<b>A29</b>	CN	2.01	44.18	21.69	32.13
<b>A30</b>	COCH <sub>3</sub>	1.62	70.85	23.48	4.05
<b>A31</b>	CH <sub>3</sub>	18.96	53.08	17.54	10.43
<b>A32</b>	NO <sub>2</sub>	25.17	70.89	2.05	1.88
<b>A33</b>	OH	11.58	34.41	43.41	10.61

All the results obtained using Kamlet-Taft and Catalan model indicate that the solvent effects on azo–hydrazone equilibrium and UV-vis absorption spectra of the investigated arylazo pyridone dyes are very complex and strongly dependable on the nature of the substituent on the arylazo component. In all cases, the use of Catalan scale gives better regressions than the Kamlet-Taft model. The degree of success of of Eq. 4.1 and Eq. 4.5 are shown in Fig. 4.11 for all investigated compounds, and excellent linear relationships between the experimental values of  $\nu_{\max}$  and the predicted absorption maxima calculated with Eq. 4.1 and Eq. 4.5 are observed. The Catalan solvent scales were found to be more suitable for describing the solvatochromism of investigated arylazo pyridone dyes.

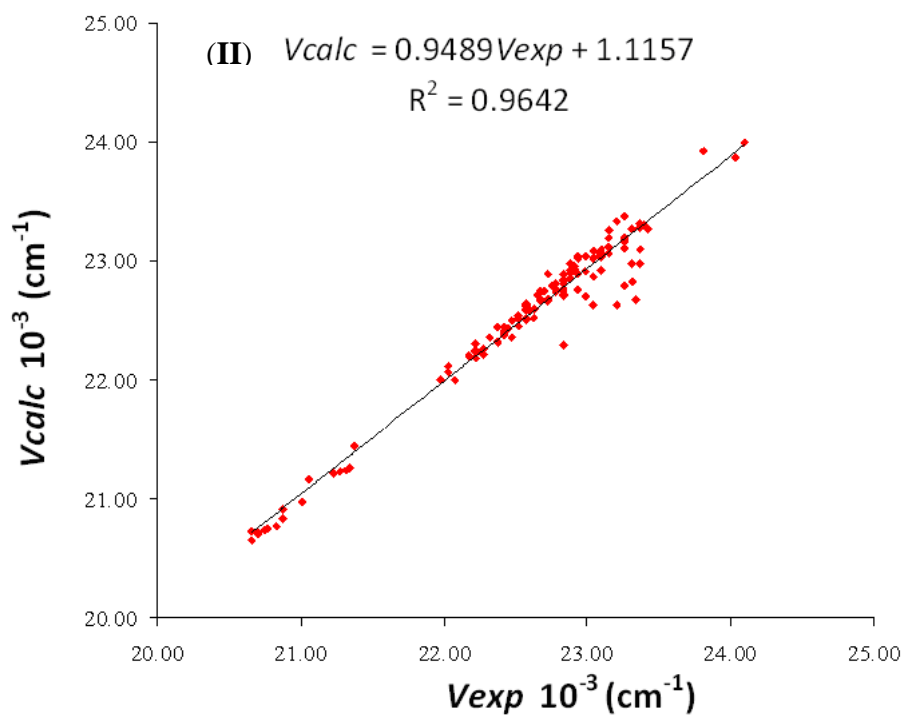
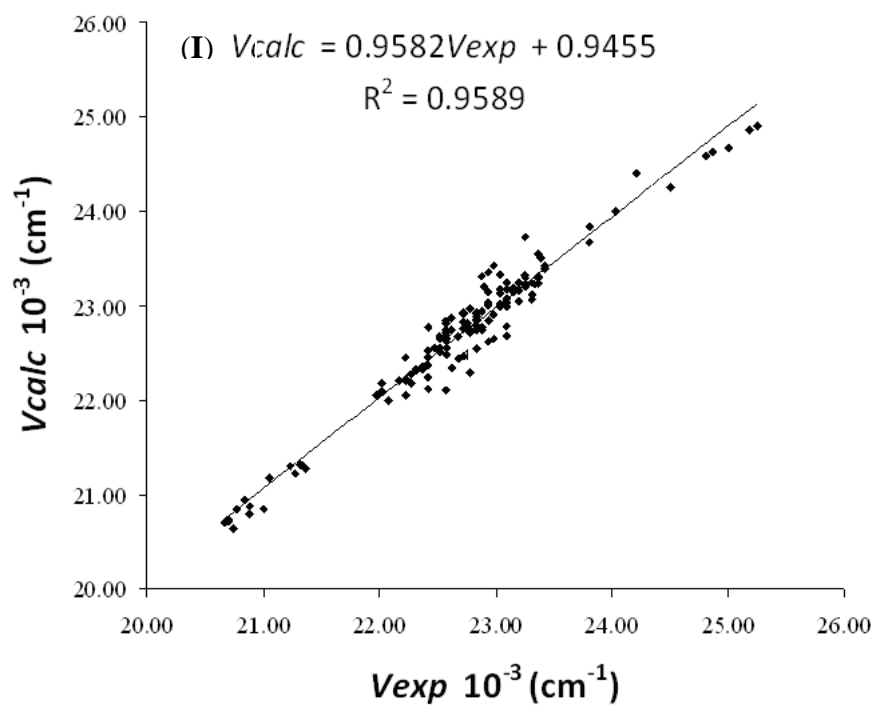


Figure 4.11. The plot of  $\nu_{\max}$  calculated against  $\nu_{\max}$  observed for Kamlet-Taft (I) and Catalan (II) equation in different solvents.

The obtained results show that arylazo dyes with nitro group on the benzene ring in position 4 of pyridone nucleus have stronger bathochromic shifts than other two series of azo dyes. in all used solvents. The percentage of contribution of solvatochromic parameters for all investigated dyes shows that most of the solvatochromism is due to solvent dipolarity / polarizability rather than to the solvent acidity and basicity. These results can be explained by the effect of the positive charge on nitrogen atom in the hydrazone tautomer and stabilization of this form mostly due to the solvent dipolarity / polarizability (non-specific solute-solvent interactions) than due to hydrogen bond donor and hydrogen bond acceptor properties.

## 5. CONCLUSIONS

In this thesis three series of 33 novel arylazo pyridone dyes were synthesized:

- 5-arylazo-6-hydroxy-4-phenyl-3-cyano-2-pyridone dyes;
- 5-arylazo-6-hydroxy-4-(4-methoxyphenyl)-3-cyano-2-pyridone dyes;
- 5-arylazo-6-hydroxy-4-(4-nitrophenyl)-3-cyano-2-pyridone dyes.

The structure of the dyes was confirmed by UV-Vis, FT-IR,  $^1\text{H}$  NMR and  $^{13}\text{C}$  NMR spectroscopy and elemental analysis. Characterization and the absorption ability of the dyes were studied. The results showed that the solvent effect on UV-vis absorption spectra of the investigated arylazo pyridone dyes is very complex and strongly depends on the nature of the substituent on the arylazo component. The introduction of the electron-donating substituents into the arylazo ring results in strong bathochromic shifts in all solvents. These solvatochromic properties are evident for the hydrazone tautomeric form. The introduction of electron-attracting substituents into the arylazo ring produces slight bathochromic or hypsochromic shift. These dyes exist in the hydrazone form in the solid state and in solvent  $\text{DMSO-}d_6$  and there was an equilibrium between hydrazone form and azo form in the different solvents.

The Kamlet-Taft and Catalan parameters were used for describing the solute-solvent interactions and solvatochromic shifts of the visible absorption band. The satisfactory correlation of the ultraviolet absorption frequencies of the investigated pyridone arylazo dyes with equations 4.1. and 4.5. indicates that the correct models were selected. This means that these models give a correct interpretation of the linear solvation energy relationships of the complex system of the azo dyes in the solvents used. In the case, where both solvents and substrates, are hydrogen bond donors and acceptors, it was proven to be quite difficult to untangle solvent dipolarity / polarizability and hydrogen bonding interactions. For these reasons it has been demonstrated that solvatochromic equations 4.1. and 4.5. can be used to evaluate the effects of both types of hydrogen bonding and of solvent dipolarity and polarizability effects. It was found that the solute dipolarity / polarizability (especially polarizability by Catalan equation) play an important role in the description of the pronounced solvatochromism in the studied solutions. The Catalan solvent scales were found to be more suitable for describing the solvatochromic shifts.

On the basis of the results presented in this thesis, it may be concluded that all the synthesized dyes exist in the hydrazone tautomeric form in the solid state. and dyes were predominantly as hydrazones in all the applied solvents. The calculational results of the geometry data using DFT quantum-chemical calculations. were in very good agreement with the experimental data.

The obtained results show that arylazo dyes with nitro group on the benzene ring in position 4 of pyridone nucleus have stronger bathochromic shifts than other two series of azo dyes. in all used solvents. The percentage of contribution of solvatochromic parameters for all investigated dyes shows that most of the solvatochromism is due to solvent dipolarity / polarizability rather than to the solvent acidity and basicity. These results can be explained by the effect of the positive charge on nitrogen atom in the hydrazone tautomer and stabilization of this form mostly due to the solvent dipolarity / polarizability (non-specific solute-solvent interactions) than due to hydrogen bond donor and hydrogen bond acceptor properties.

Based on the results of this thesis, the newly synthesized pyridone arylazo dyes represent promising candidates for application as optical active materials with different technical properties.

## REFERENCES

- [1] R.J. Chudgar. J. Oakes. Dyes. Azo. Kirk-Othmer Encyclopedia of Chemical Technology, 2003.
- [2] A.D. McNaught. A. Wilkinson. IUPAC. Compendium of Chemical Terminology. 2nd ed. (the "Gold Book"). Blackwell Scientific Publications. Oxford. 1997. XML on-line corrected version: <http://goldbook.iupac.org> (2006) created by M. Nic. J. Jirat. B. Kosata; updates compiled by A. Jenkins.
- [3] H.Zollinger. Colour Chemistry. VCH. Weinheim. 1987. pp.85.
- [4] D.Ž. Mijin. M.M. Mišić-Vuković. J. Serb. Chem. Soc., **59** (1994) 969.
- [5] M. Mišić-Vuković. D. Mijin. M. Radojković-Veličković. N. Valentić. V. Krstić. J. Serb. Chem. Soc., **63** (1998) 585.
- [6] D. Mijin. A. Marinković. Synth. Commun., **36** (2006) 193.
- [7] D.Ž. Mijin. B.D. Milić. M.M. Mišić-Vuković. Ind. J. Chem., **45B** (2006) 993.
- [8] G.E.H. Elgemeie. A.M. El-Zanate. A.K. E. Mansour. Bull. Chem. Soc. Jpn., **66** (1993) 555.
- [9] D. Mijin. G. Ušćumlić. N. Perišić-Janjić. I. Trkulja. M. Radetić. P. Jovančić. J. Serb. Chem. Soc., **71** (2006) 435.
- [10] J. Dostanić. N. Valentić. G. Ušćumlić. D. Mijin. J. Serb. Chem. Soc., **76** (2011) 499.
- [11] D.Ž. Mijin. M. Baghbanzadeh. C. Reidlinger. C.O. Kappe. Dyes Pigm., **85** (2010) 73.
- [12] H. Burkhard. F. Mueller. U. Zirngibl. (Sandoz Ltd.). DE 2149137 (1972).
- [13] J. Ribka. E. Heinrich. (Cassella Farbwerke Mainkur A.-G.). DE 2147759 (1973).
- [14] K. Komorowski. (Bayer A.-G.). DE 2340569 (1975).
- [15] (Cassella Farbwerke Mainkur A.-G.). FR 2153417 (1973).
- [16] E. Heinrich. H. Kindler. J. Ribka. (Cassella Farbwerke Mainkur A.-G.). DE 2352858 (1975).
- [17] H. Tappe. K. Hofmann. K. Opitz. M. Schneider. (Cassella A.-G.). DE 3447117 (1986).
- [18] K. Komorowski. K. Ley. P. Kurtz. (Bayer A.-G.). DE 2163378 (1973).

- [19] H. Von Brachel. E. Heinrich. O. Graewinger. K. Hintermeier. H. Kindler. (Cassella Farbwerke Mainkur A.-G.). DE 1817977 (1976).
- [20] E. Heinrich. H. Kindler. J. Ribka. (Cassella Farbwerke Mainkur A.-G.). DE 2523632 (1976).
- [21] G. Wagenblast. H. Reichelt. G. Seybold. G. Kaupp. R.A. Herrmann. (BASF A.-G.). DE 19721619 (1998).
- [22] J. Schaetzer. (CIBA Ltd.. Switz.). EP 776948 (1997).
- [23] K. Gao. M. Li. Y. Zhou. G. Kunyu. L. Mujie. Z. Yingdi. (College of Chemical Engineering. Dalian Univ. of Science & Engineering). CN 1125240 (1996) [C.A. 128/1998 271648].
- [24] G. Gnad. G. Lamm. (BASF A.-G.). DE 2414279 (1975).
- [25] B.R. Fishwick. N. Hughes. R.F. Hyde. (Imperial Chemical Industries Ltd.). DE 2434228 (1975).
- [26] R. Egli. B. Henzi. (Sandoz-Patent-GmbH). DE 19618586 (1996).
- [27] B.R. Fishwick. N. Huges. R.F. Hyde. (Imperial Chemical Industries Ltd.). DE 2323621 (1973).
- [28] K. Anderton. R. Porter. (Imperial Chemical Industries Ltd.). DE 2735376 (1978).
- [29] X. Pan. H. Wang. Y. Wu. Z. Xia. F. Song. (Dalian University of Science and Engineering). CN 1289803 (2001) [C.A.135/2001 332526].
- [30] P. Doswald. R. Wald. (Clariant Finance (BVI) Limited. P. Doswald. R. Wald.). WO 9730125 (1997).
- [31] A. Clement. A. Arquint. U. Lauk. (Ciba Specialty Chemicals Holding Inc.). WO 2004056926 (2004).
- [32] C.C. Chen. I.J. Wang. *Dyes Pigm.*, **15** (1991) 69.
- [33] Z. Bahreini. *Pigm. Resin Technol.*, **38** (2009) 298.
- [34] F.M. Abdelrazek. A.M. Salah El-Din. A.E. Mekky. *Tetrahedron*, **57** (2001) 6787.
- [35] R.W. Sabnis. D.W. Rangnekar. *Dyes Pigm.*, **10** (1989) 295.
- [36] G. Hallas. A. D. Towns. *Dyes Pigm.*, **31** (1996) 273.
- [37] A. Crabtree. (Imperial Chemical Industries Ltd.). DE 1964690 (1970).
- [38] J. Dannheim. (Dystar Textilfarben G.m.b.H. & Co. Deutschland K.-G.). EP 1054041 (2000).

- [39] A.H. Berrie. J.S. Hunter. N. Hughes. (Imperial Chemical Industries Ltd.). GB 1297116 (1972).
- [40] M. Greve. (Sandoz-Patent-G.m.b.H.). DE 2752282 (1978).
- [41] E. Young. (Imperial Chemical Industries Ltd.). DE 2216207 (1972).
- [42] G. Lamm. J. Dehnert. (BASF A.-G.). DE 2917063 (1980).
- [43] D.D. Chapman. J.P. Harmon. (Eastman Kodak Co.). US 4734349 (1988).
- [44] N.A. Tallant. C. Millard. (Avecia Limited). WO 2001021714 (2001).
- [45] A. Tzikas. U. Lauk. R. Dreier. A. Clement. (Ciba Specialty Chemicals Holding Inc.). WO 2002090442 (2002).
- [46] (Clariant International Ltd.). EP 1411089 (2004).
- [47] Y. Matsuzaki. A. Ogiso. Y. Shimokawa. N. Ito. H. Takuma. (Mitsui Toatsu Chemicals). JP 08011443 (1996) [C.A. 124/1996 328495].
- [48] M. Ishida. K. Maeda. Y. Murata. D. Kanazawa. T. Morishima. (Mitsubishi Chemical Industries Ltd.. Mitsubishi Chemical Corp.). JP 2000062327 (2000) [C.A. 132/2000 167668].
- [49] K. Lee. Y. Sonn. S. Um. W. Han. B. Joo. (Hansol Paper Co.. Ltd.). KR 119563 (1997) [C.A. 133/2000 224241].
- [50] J. Mizukami. T. Ozawa. (Mitsubishi Chemical Industries Ltd.). JP 10310583 (1998) [C.A. 130/1999 73892].
- [51] K.T. Lee. Y.S. Son. W.S. Han. B.J. Joo. S.Y. Eom. (Hansol Paper Co.. Ltd.). US 5929218 (1999).
- [52] T. Nagao. R. Fujita. Y. Murata. (Mitsubishi Chemical Industries Ltd.). JP 11334204 (1999) [C.A. 132/2000 28733].
- [53] J.H. Banning. R. Carlini. J.D. Mayo. J.M. Duff. C.W. Jaeger. (Xerox Corporation). US 6590082 (2003).
- [54] J.H. Banning. B. Wu. J.D. Mayo. J.M. Duff. R. Carlini. J.W. Thomas. P.F. Smith. (Xerox Corporation). US 2004007155 (2004).
- [55] O. Kogo. T. Oi. (Mitsui Chemicals Inc.). JP 2004300224 (2004) [C.A. 141/2004 381163].
- [56] K. Araki. T. Aizawa. (Fuji Photo Film Co.. Ltd.). JP 2006124634 (2006) [C.A. 144/2006 477952].

- [57] M. Tanaka. Y. Murai. M. Kato. T. Toyoda. T. Miyazaki. (Canon Kabushiki Kaisha). WO 2008069045 (2008) [C.A. 149/2008 33648].
- [58] T. Miyazawa. Y. Kurose. (Mitsubishi Kagaku Media Co., Ltd.). WO 2006104196 (2006) [C.A. 145/2006 407711].
- [59] I.J. Wang. Y.J. Hsu. J.H. Tian. *Dyes Pigm.*, **16** (1991) 83.
- [60] W. Mueller. P. Lienhard. (Ciba-Geigy A.-G.). CH 72-6615 (1975).
- [61] F. Muzik. J. Ruzicka. J. Marhan. J. Prikryl. F. Vyskocil. CS 258820 (1989).
- [62] J.M. Kanhere. D.W. Rangnekar. *Indian Journal of Textile Research* **13** (1988) 213.
- [63] H. Klier. A. Tzikas. (Ciba Specialty Chemicals Holding Inc.). EP 857762 (1998).
- [64] D.R. Vines. R.P. Pedemonte. (Dystar. L.P.). US 5811529 (1998).
- [65] R. Carlini. J.D. Mayo. J.M. Duff. J.H. Banning. P.F. Smith. G. Liebermann. R.E. Gaynor. (Xerox Corporation). US 6576748 (2003).
- [66] B. Wu. R. Carlini. J.H. Banning. J.M. Duff. J.D. Mayo. J.W. Jr. Thomas. P.F. Smith. M.B. Meinhardt. (Xerox Corporation). US 6663703 (2003).
- [67] R. Carlini. J.H. Banning. J.M. Duff. B. Wu. J.D. Mayo. (Xerox Corporation). EP 1375599 (2004).
- [68] J.D. Mayo. J.M. Duff. R. Carlini. R.E. Gaynor. G. Liebermann. (Xerox Corporation). US 2004006234 (2004).
- [69] R. Carlini. J.M. Duff. J.H. Banning. B. Wu. J.D. Mayo. (Xerox Corporation). US 6646111 (2003).
- [70] B. Wu. R. Carlini. J.M. Duff. J.H. Banning. J.D. Mayo. (Xerox Corporation). US 6673139 (2004).
- [71] A. Tzikas. U. Lauk. R. Dreier. A. Clement. (Ciba Specialty Chemicals Holding Inc.). WO 2002090442 (2002).
- [72] Y. Hattori. N. Furusho. Y. Nakamura. M. Kuroda. (Fuji Electric Co. Ltd.). US 4988594 (1991).
- [73] F. Karci. F. Karci. *Dyes Pigm.*, **76** (2008) 147.
- [74] M. Yamada. T. Higuchi. E. Tanigami. (Yamada Chemical Co., Ltd.). JP 2002302620 (2002) [C.A. 137/2002 312352].
- [75] J. D. Mayo. J.M. Duff. (Xerox Corporation). US 2006117991 (2006).

- [76] M.H. Helal. Synthesis and characterisation of a new series of pyridinone azo dyes for dyeing of synthetic fibers. *Pigm. Resin Technol.*, **33** (2004) 165.
- [77] I.J. Wang. P.Y. Wang. *Text. Res. J.*, **60** (1990) 297.
- [78] P.Y. Wang. I.J. Wang. *Text. Res. J.*, **60** (1990) 519.
- [79] J.M. Dostanić. D.R. Lončarević. P.T. Banković. O.G. Cvetković. D.M. Jovanović. D.Ž. Mijin. . *J. Environ. Sci. Health. Part A: Toxic/Hazard. Subst. Environ. Eng.*, **46** (2011) 70.
- [80] S.D. Kim. E.J. Park. *Fibers Polym.*, **2** (2001) 159.
- [81] M. Matsui. B. Joglekar. Y. Ishigure. K. Shibata. H.Muramatsu. Y.Murata. *Bull. Chem. Soc. Jpn.*, **66** (1993) 1790.
- [82] M. Wang. K. Funabiki. M. Matsui. *Dyes Pigm.*, **57** (2003) 77.
- [83] N. Ertan. P. Gurkan. *Dyes Pigm.*, **33** (1997) 137.
- [84] F. Karcl. *Color. Technol.*, **121** (2005) 275.
- [85] H. Song. K. Chen. H. Tian. *Dyes Pigm.*, **53** (2002) 257.
- [86] H. Junek. G. Uray. A. Kotzent. G. Kastner. *Monatsh. Chem.*, **116** (1985) 1199.
- [87] M.S. Yen. I.J. Wang. *Dyes Pigm.*, **62** (2004) 173.
- [88] M.S. Yen. I.J. Wang. *Dyes Pigm.*, **63** (2004) 1.
- [89] N. Ertan. F. Eyduran. *Dyes Pigm.*, **27** (1995) 313.
- [90] L. Cheng. X. Chen. K. Gao. J. Hu. J. Griffiths. *Dyes Pigm.*, **7** (1986) 373.
- [91] G.S. Ušćumlić. D.Ž. Mijin. N.V. Valentić. V.V. Vajs. B.M. Sušić. *Chem. Phys. Lett.*, **397** (2004) 148.
- [92] W. Jian. L.-b. Cheng. M.-f. Chen. *Ranliao yu Ranse*, **41** (2004) 147-149. 173. [C.A. 142/2005 337760].
- [93] H.F. Qian. H. Wei. *Acta Crystallogr.. Sect. C: Cryst. Struct. Commun.* **C62** (2006) o62-o64. [C.A. 145/2001 177596]
- [94] W. Huang. H. Qian. *Dyes Pigm.* **77** (2008) 446.
- [95] W. Huang. *Dyes Pigm.*, **79** (2008) 69.
- [96] D.Ž. Mijin. G.S. Ušćumlić. N.U. Perišić-Janjić. N.V. Valentić. *Chem. Phys. Lett.*, **418** (2006) 223.
- [97] A.S. Alimmari. A.D. Marinković. D.Ž. Mijin. N.V. Valentić. N. Todorović. G.S. Ušćumlić. *J. Serb. Chem. Soc.*, **75** (2010) 1019.

- [98] N.U. Perišić-Janjić. G.S. Ušćumlić. D.Ž. Mijin. *J. Planar Chrom. Mod. TLC*, **19** (2006) 98.
- [99] Q. Peng. M. Li. K. Gao. L. Cheng. *Dyes Pigm.*, **18** (1992) 271.
- [100] T. Zincke. H. Bindewald. *Chem. Ber.*, **17** (1884) 3026.
- [101] Q. Peng. M. Li. K. Gao. L. Cheng. *Dyes Pigm.*, **14** (1990) 89.
- [102] A. Cee. B. Korakova. A. Lucka. *Dyes Pigm.*, **9** (1988) 357.
- [103] J. Keleman. *Dyes Pigm.*, **2** (1981) 73.
- [104] L. Antonov. S. Kawauchi. M. Satoh. J. Komiyama. *Dyes Pigm.*, **40** (1999) 163.
- [105] L. Onsager. *J. Am. Chem. Soc.*, **58** (1938) 1486.
- [106] A. Becke. *Phys. Rev. (Sect. A)* **38** (1988) 3098.
- [107] C. Lee. W. Yang. R. Part. *Phys. Rev. (Sect. B)* **37** (1988) 785.
- [108] Frisch MJ. Trucks GW. Schlegel HB. Scuseria GE. Robb MA. Cheeseman JR. Montgomery JA Jr. Vreven T. Kudin KN. Burant JC. Millam JM. Iyengar SS. Tomasi J. Barone V. Mennucci B. Cossi M. Scalmani G. Rega N. Petersson GA. Nakatsuji H. Hada M. Ehara M. Toyota K. Fukuda R. Hasegawa J. Ishida M. Nakajima T. Honda Y. Kitao O. Nakai H. *et al.*: *Gaussian 03. Revision C.02*. Wallingford CT: Gaussian Inc; 2004.
- [109] E. V. Anslyn. D. A. Dougherty. *Modern Physical Organic Chemistry*. USA. 2006. chap. 8.
- [110] E. M. Arnett. D. R. McKelvey. *J. Am. Chem. Soc.*, **87** (1965) 1393.
- [111] M. H. Abraham. R. J. Abraham. *J. Chem. Soc. Perkin II* (1974) 74.
- [112] N. S. Isaacs. *Physical Organic Chemistry*. 2<sup>nd</sup> Edition. Longman Scientific & Technical. 1995. chap 4.
- [113] R. A. Y. Jones. *Physical and Mechanistic Organic Chemistry*. Cambridge University Press. 1<sup>st</sup> published 1979.
- [114] F. A. Carey. R. J. Sundberg. *Advanced Organic Chemistry. Part A. Structure and Mechanism*. 3<sup>rd</sup> Edition. Plenum Press. New York. 1990.
- [115] L. P. Hammett. *Chem. Rev.*, **17** (1935) 125.
- [116] L. P. Hammett. *J. Am. Chem. Soc.*, **59** (1937) 96.
- [117] G. N. Burkhardt. W. G. K. Ford. E. Singleton. *J. Chem. Soc.* (1936) 17.

- [118] L. P. Hammett. *Physical Organic Chemistry*. McGraw-Hill. New York. 1940. chap. 7.
- [119] H. H. Jaffe. *Chem. Rev.*, **53** (1953) 191.
- [120] D. H. McDaniel. H. C. Brown. *J. Org. Chem.*, **23** (1958) 420.
- [121] J. Shorter. *Correlation Analysis of Organic Reactivity*. Research Studies Press. England. 1982.
- [122] C. D. Ritchie. W. F. Sager. *Prog. Phys. Org. Chem.*, **2** (1964) 323.
- [123] T. M. Krygowski. B. T. Stepien. *Chem. Rev.*, **105** (2005) 3482.
- [124] S. Ehreson. R. T. Brownlee. R. W. Taft. *Prog. Phys. Org. Chem.*, **10** (1973) 1.
- [125] H. C. Brown. Y. Okamoto. *J. Am. Chem. Soc.*, **80** (1958) 2479.
- [126] H. Van Bekkum. P. E. Verkade. B. M. Wepster. *Red. Trav. Chim. Paysbas.*, **78** (1959) 815.
- [127] W. L. Bright. H. T. Briscoe. *J. Phys. Chem.*, **37** (1933) 787.
- [128] F. J. Dippy. F. R. Williams. *J. Chem. Soc.*, (1934) 161.
- [129] R. W. Taft. I. C. Lewis. *J. Am. Chem. Soc.*, **80** (1958) 2436.
- [130] R. W. Taft. I. C. Lewis. *J. Am. Chem. Soc.*, **81** (1959) 5343.
- [131] R. W. Taft. E. Price. I. R. Fox. I. C. Lewis. K. K. Andersen. G. T. Davis. *J. Am. Chem. Soc.*, **85** (1963) 3146.
- [132] J. Shorter. *Correlation Analysis in Chemistry*. Plenum Press. New York. 1978. 119.
- [133] M. Magat. *Z. Phys. Chem. A.*, 162 (1932) 432.
- [134] M. Berhelot. L. Pean de Saint-Gilles. *Ann. Chin. Et. Phys. 3. Ser.*, **65** (1862) 385.
- [135] N. Menshutkin. *Z. Phys. Chem.*, **1** (1887) 611.
- [136] L. Claisen. *Liebigs Ann. Chem.*, **291** (1896) 25.
- [137] H. Stobbe. *Libigs Ann. Chem.*, **326** (1903) 347.
- [138] O. Dimroth. *Libigs Ann. Chem.*, **377** (1910) 27.
- [139] K. H. Meyer. *Libigs Ann. Chem.*, **380** (1911) 212.
- [140] G. Scheibe. E. Felegr. G. Rößler. *Ber. Dtsch. Chem. Gas.* **45** (1912) 2843.
- [141] F. A. Carey. R. J. Sundberg. *Advanced Organic Chemistry. Part A. Structure and Mechanism*. 3<sup>rd</sup> Edition. Plenum Press. New York. 1990. p 232-239.
- [142] C. Reichardt. *Solvents and Solvent Effects in Organic Chemistry*. VCH. Verlagsgesellschaft mbH. Germany. 2003.

- [143] I. Kol'tsov. G. M. Kheifets. Usp. Khim., **40** (1971) 1646.
- [144] I. Kol'tsov. G. M. Kheifets. Usp. Khim., **41** (1972) 877.
- [145] R. Katrizky. J. M. Lagoeski. *Advances in Heterocyclic Chemistry*. Academic Press. New York. London. 1963. Vol. 1. p. 311.339; Vol. 2. p. 1. 27.
- [146] N. Menshutkin. Z. Phys. Chem., **6** (1890) 41.
- [147] E. Grunwald. S. Winsten. J. Am. Chem. Soc., **70** (1948) 846.
- [148] S. Winsten. A. H. Fainberg. J. Am. Chem. Soc., **78** (1956) 2770.
- [149] A. Koppel. V. A. Palm. *The Influence of the Solvent on Organic Reactivity*. in N. B. Chapman and J. Shorter. *Advances in Linear Free Energy Relationships*. Plenum Press. London. New York. 1972. chap. 5.
- [150] M. J. Kamlet. J. L. M. Abboud. R. W. Taft. Prog. Phys. Org. Chem., **13** (1981) 485.
- [151] Y. Marcus. Chem. Soc. Rev., (1993) 409.
- [152] N. B. Chapman. D. J. Newman. J. Shorter. H. M. Wall. J. Chem. Soc. Perkin Trans. **2** (1976) 847.
- [153] J. Roch. E. Miller. B. Naru. J. Nickl. W. Haarmann. US 260.621 A1 (1981).
- [154] J. M. Bobbit. D. A. Skola. J. Org. Chem., **25** (1960) 560.
- [155] A. Lucka. V. Machacek. Dyes Pigm., **7** (1986) 171.
- [156] H. Bhatti. S. Seshadri. Color Technol., **120** (2004) 151.
- [157] J. Catalan. J. Phys. Chem. B., **113** (2009) 5951.

## 7. APPENDIX

### References based on the thesis

#### Published papers

- [1] A.S. Alimmari, A.D. Marinković, D.Ž. Mijin, N.V. Valentić, N. Todorović, G.S. Ušćumlić, *J. Serb. Chem. Soc.*, **75** (2010) 1019.
- [2] A. Alimmari, D. Mijin, R. Vukićević, B. Božić, N. Valentić, V. Vitnik, Ž. Vitnik, G. Ušćumlić, "Synthesis, Structure and Solvatochromic Properties of Some Novel 5-Arylazo-6-hydroxy-4-phenyl-3-cyano-2-pyridone Dyes", *Chem. Cent. J.* **6** (71) 2012, 1-8, ISSN: 1752-153X, IF (2011) = 3.28.
- [3] A. Alimmari, B. Božić, A. Marinković, D. Mijin, G. Ušćumlić, "Solvent and Structural Effects on the UV-Vis Absorption Spectra of Some 4,6-Disubstituted-3-cyano-2-pyridones" *J. Sol. Chem.* **41** (10) 2012, 1825-1836, ISSN: 0095-9782, IF (2011) = 1.415

#### Proceedings

- [1] B. Božić, A. Alimmari, D. Mijin, G. Ušćumlić, "Synthesis, Structure and Solvatochromic Properties of Novel Dyes Derived from 4-Nitrophenyl-6-hydroxy-3-cyano-2-pyridone", 17<sup>th</sup> ESOC, Hersonissos, Greece 2011, pp. 146.
- [2] A. Alimmari, B. Božić, D. Mijin, G. Ušćumlić, "Solvent and Structural Effects on the Azo-Hydrazone Tautomerism of 5-(4-Substituted Phenylazo)-4-(4-Methoxyphenyl)-6-hydroxy-3-cyano-2-pyridone", 17<sup>th</sup> ESOC, Hersonissos, Greece 2011, pp. 149.
- [3] Adel S. A. Alimmari, Aleksandar D. Marinković, Dušan Ž. Mijin, Nataša V. Valentić and Gordana S. Ušćumlić, "Solvent and substituent effect on the UV-Vis absorption spectra of 5-(3- and 4-substituted phenylazo)-4,6-diphenyl-3-cyano-2-pyridones", 47<sup>th</sup> Meeting of the Serbian Chemical Society, Belgrade, Serbia, March 21<sup>st</sup> 2009., Book of Abstracts pp.136.
- [4] Radovan M. Vukićević, Adel S. A. Alimmari, Dušan Ž. Mijin, Nataša V. Valentić and Gordana S. Ušćumlić, "Solvent and substituent effect on the UV-Vis absorption spectra of 5-(3- and 4-substituted phenylazo)-4-phenyl-6-hydroxy-3-cyano-2-pyridones", 47<sup>th</sup> Meeting of the Serbian Chemical Society, Belgrade, Serbia, March 21<sup>st</sup> 2009., Book of Abstracts, pp. 137.

- [5] Adel S. A. Alimmari, Aleksandar D. Marinković, Nenad Ž. Jovanović, Dušan Ž. Mijin, Nataša V. Valentić and Gordana S. Ušćumlić, "New azo dyes from 4-(4-methoxyphenyl)-6-hydroxy-3-cyano-2-pyridone", 48<sup>th</sup> Meeting of the Serbian Chemical Society, Novi Sad, Serbia, April 17<sup>th</sup>-18<sup>th</sup> 2010., Book of Abstracts, pp. 150.
- [6] Bojan Đ. Božić, Aleksandar D. Marinković, Adel S. A. Alimmari, Jasmina S. Đukanović, Dušan Ž. Mijin and Gordana S. Ušćumlić, "Solvent and substituent effect on the UV-Vis absorption spectra of 4,6-disubstituted pyridones", 48<sup>th</sup> Meeting of the Serbian Chemical Society, Novi Sad, Serbia, April 17<sup>th</sup>-18<sup>th</sup> 2010., Book of Abstracts pp., 189.

# Curriculum vitae

## Personal Information

Name: Adel. S. A. ALIMMARI

Place of birth: G KEAR/ LIBYA

Date of birth: 10/09/ 1972

Address: Perve pruge 3/35 Belgrade 11080

Phone #: +381600912355

## Education

Bachelor degree in Chemistry faculty of Science

Misurata University (1996)

MSc degree in Organic Chemistry Faculty of Technology and Metallurgy

University of Belgrade (2005)

## Professional Experience

1999-2006

The quality control department in liquid fuel plant in the Research center and Development Tripoli, Libya

2006-2008

Department of Chemistry, Faculty of Science University of Al Khums, Libya, Assistant professor



**Izjava o istovetnosti štampane i elektronske  
verzije doktorskog rada**

Ime i prezime autora Adel S. Alimmari

Broj indeksa \_\_\_\_\_

Studijski program \_\_\_\_\_

Naslov rada Synthesis, Structure and Solvatochromism of new 5-(4-substituted phenylazo)-4-(4-substituted phenyl)-6-hydroxy-3-cyano-2-pyridones

Mentor Topgava Yurturmut

Potpisan/a ab

Izjavljujem da je štampana verzija mog doktorskog rada istovetna elektronskoj verziji koju sam predao/la za objavljivanje na portalu **Digitalnog repozitorijuma Univerziteta u Beogradu**.

Dozvoljavam da se objave moji lični podaci vezani za dobijanje akademskog zvanja doktora nauka, kao što su ime i prezime, godina i mesto rođenja i datum odbrane rada.

Ovi lični podaci mogu se objaviti na mrežnim stranicama digitalne biblioteke, u elektronskom katalogu i u publikacijama Univerziteta u Beogradu.

**Potpis doktoranda**

U Beogradu, \_\_\_\_\_

\_\_\_\_\_ ab

## Izjava o korišćenju

Ovlašćujem Univerzitetsku biblioteku „Svetozar Marković“ da u Digitalni repozitorijum Univerziteta u Beogradu unese moju doktorsku disertaciju pod naslovom:

Synthesis, Structure and Solvatochromism of new 5-(4-substituted phenylazo)-  
-4-(4-substituted phenyl)-6-hydroxy-3-cyano-2-pyridones

koja je moje autorsko delo.

Disertaciju sa svim priložima predao/la sam u elektronskom formatu pogodnom za trajno arhiviranje.

Moju doktorsku disertaciju pohranjenu u Digitalni repozitorijum Univerziteta u Beogradu mogu da koriste svi koji poštuju odredbe sadržane u odabranom tipu licence Kreativne zajednice (Creative Commons) za koju sam se odlučio/la.

1. Autorstvo

2. Autorstvo - nekomercijalno
3. Autorstvo – nekomercijalno – bez prerade
4. Autorstvo – nekomercijalno – deliti pod istim uslovima
5. Autorstvo – bez prerade
6. Autorstvo – deliti pod istim uslovima

(Molimo da zaokružite samo jednu od šest ponuđenih licenci, kratak opis licenci dat je na poleđini lista).

**Potpis doktoranda**

U Beogradu, \_\_\_\_\_

\_\_\_\_\_ 

1. Autorstvo - Dozvoljavate umnožavanje, distribuciju i javno saopštavanje dela, i prerade, ako se navede ime autora na način određen od strane autora ili davaoca licence, čak i u komercijalne svrhe. Ovo je najslobodnija od svih licenci.
2. Autorstvo – nekomercijalno. Dozvoljavate umnožavanje, distribuciju i javno saopštavanje dela, i prerade, ako se navede ime autora na način određen od strane autora ili davaoca licence. Ova licenca ne dozvoljava komercijalnu upotrebu dela.
3. Autorstvo - nekomercijalno – bez prerade. Dozvoljavate umnožavanje, distribuciju i javno saopštavanje dela, bez promena, preoblikovanja ili upotrebe dela u svom delu, ako se navede ime autora na način određen od strane autora ili davaoca licence. Ova licenca ne dozvoljava komercijalnu upotrebu dela. U odnosu na sve ostale licence, ovom licencom se ograničava najveći obim prava korišćenja dela.
4. Autorstvo - nekomercijalno – deliti pod istim uslovima. Dozvoljavate umnožavanje, distribuciju i javno saopštavanje dela, i prerade, ako se navede ime autora na način određen od strane autora ili davaoca licence i ako se prerada distribuira pod istom ili sličnom licencom. Ova licenca ne dozvoljava komercijalnu upotrebu dela i prerada.
5. Autorstvo – bez prerade. Dozvoljavate umnožavanje, distribuciju i javno saopštavanje dela, bez promena, preoblikovanja ili upotrebe dela u svom delu, ako se navede ime autora na način određen od strane autora ili davaoca licence. Ova licenca dozvoljava komercijalnu upotrebu dela.
6. Autorstvo - deliti pod istim uslovima. Dozvoljavate umnožavanje, distribuciju i javno saopštavanje dela, i prerade, ako se navede ime autora na način određen od strane autora ili davaoca licence i ako se prerada distribuira pod istom ili sličnom licencom. Ova licenca dozvoljava komercijalnu upotrebu dela i prerada. Slična je softverskim licencama, odnosno licencama otvorenog koda.